

**AFRL-WS-WP-TM-1999-9010**



**PROGRESS REPORT ON METHODS OF  
ANALYSIS APPLICABLE TO  
MONOCOQUE AIRCRAFT STRUCTURES**

**Air Service Information Circular, Volume VIII, No. 713**

**J.S. NEWELL  
J.H. HARRINGTON**

**Air Service  
Engineering Division  
McCook Field  
Dayton OH 45430**

**May 15, 1939**

**Approved for public release; Distribution unlimited.**

**DTIC QUALITY INSPECTED 4**

**AIR FORCE RESEARCH LABORATORY  
AIR FORCE MATERIEL COMMAND  
WRIGHT-PATTERSON AIR FORCE BASE OH 45433**

**19991028 076**

## REPORT DOCUMENTATION PAGE

Form Approved  
OMB No. 0704-0188

Public reporting burden for this collection of information is estimated to average 1 hour per response, including the time for reviewing instructions, searching existing data sources, gathering and maintaining the data needed, and completing and reviewing the collection of information. Send comments regarding this burden estimate or any other aspect of this collection of information, including suggestions for reducing this burden, to Washington Headquarters Services, Directorate for Information Operations and Reports, 1215 Jefferson Davis Highway, Suite 1204, Arlington, VA 22202-4302, and to the Office of Management and Budget, Paperwork Reduction Project (0704-0188), Washington, DC 20503.

1. AGENCY USE ONLY (Leave blank)	2. REPORT DATE	3. REPORT TYPE AND DATES COVERED	
	May 15, 1939	FINAL May 4, 1937	
4. TITLE AND SUBTITLE <b>PROGRESS REPORT ON METHODS OF ANALYSIS APPLICABLE TO MONOCOQUE AIRCRAFT STRUCTURES</b> Air Service Information Circular, Volume VIII, No. 713		5. FUNDING NUMBERS	
6. AUTHOR(S) J.S. NEWELL J.H. HARRINGTON			
7. PERFORMING ORGANIZATION NAME(S) AND ADDRESS(ES) Air Service Engineering Division McCook Field Dayton OH 45430		8. PERFORMING ORGANIZATION REPORT NUMBER	
9. SPONSORING/MONITORING AGENCY NAME(S) AND ADDRESS(ES) Air Service Engineering Division McCook Field Dayton OH 45430		10. SPONSORING/MONITORING AGENCY REPORT NUMBER AFRL-WS-WP-TM-1999-9010	
11. SUPPLEMENTARY NOTES			
12a. DISTRIBUTION AVAILABILITY STATEMENT Approved for public release; Distribution unlimited.		12b. DISTRIBUTION CODE	
13. ABSTRACT (Maximum 200 words) Historical study of methods of analysis applicable to the design of monocoque aircraft structures. Surveys the rational theoretical procedures developed for, and applicable to, stiffened and unstiffened stressed skin structures to see which methods could be used in aircraft design, which could be used if modified by the introduction of empirical coefficients, and which appeared to be inapplicable regardless of how they were changed.			
14. SUBJECT TERMS Shells(Structural forms), Cylindrical bodies, Monocoque aircraft structures, Aircraft design		15. NUMBER OF PAGES 50	
		16. PRICE CODE	
17. SECURITY CLASSIFICATION OF REPORT UNCLASSIFIED	18. SECURITY CLASSIFICATION OF THIS PAGE UNCLASSIFIED	19. SECURITY CLASSIFICATION OF ABSTRACT UNCLASSIFIED	20. LIMITATION OF ABSTRACT SAR

AC2  
# 713

File 629.13/Un3as

AIR CORPS TECHNICAL REPORT No. 4313

# AIR CORPS INFORMATION CIRCULAR

PUBLISHED BY THE CHIEF OF THE AIR CORPS, WASHINGTON, D. C.

Vol. VIII

May 15, 1939

No. 713

## PROGRESS REPORT ON METHODS OF ANALYSIS APPLICABLE TO MONOCOQUE AIRCRAFT STRUCTURES

▽

(AIRCRAFT BRANCH REPORT)



UNITED STATES  
GOVERNMENT PRINTING OFFICE  
WASHINGTON : 1940

## TABLE OF CONTENTS

	Page
Purpose and scope.....	1
Results and conclusions.....	1
Outline of structural problems.....	1
SECTION 1. Critical loads on smooth unstiffened sheet.....	3
2. Isotropic flat rectangular plates—Compressive loads.....	3
3. Isotropic curved rectangular plates—Compressive loads	7
Sechler's Method.....	8
Empirical Method.....	8
Other methods.....	8
4. Stiffener design.....	9
5. Determination of crushing strength—Stiffeners.....	11
6. The stability of open sections.....	16
7. Column strength—Stiffeners.....	17
8. Notes on stiffener design.....	20
9. Stiffened flat plates in compression	20
Empirical methods.....	20
Theoretical methods.....	25
10. Stiffened curved sheets in compression.....	25
Empirical methods.....	25
11. Cylinders in bending.....	27
12. Stiffened cylinders.....	27
13. Isotropic flat rectangular plates—Unstiffened—Shear in plane of sheet.....	34
14. Isotropic flat rectangular plates—Stiffened—Shear in plane of sheet.....	34
15. Isotropic curved rectangular plates—Shear on stiffened sheet.....	37
16. Corrugated sheet—Axial compressive load parallel to corrugations.....	37
17. Corrugated sheet—Column stress.....	39
18. Corrugated sheet—Fixity coefficients.....	40
19. Effect of curving corrugated sheet.....	40
20. Compression on combined flat and corrugated panels.....	40
21. Shear loads parallel and perpendicular to the corrugations.....	41
22. Shear in combined smooth and corrugated panels.....	44
23. Shear on cylinders—Combined smooth and corrugated sheet.....	45

# PROGRESS REPORT ON METHODS OF ANALYSIS APPLICABLE TO MONOCOQUE AIRCRAFT STRUCTURES

(Prepared by J. S. Newell and J. H. Harrington; coordinated by Capt. P. H. Kemmer, A. C., Matériel Division, Air Corps, Wright Field, Dayton, Ohio, May 4, 1937)

## PURPOSE AND SCOPE

The study of methods of analysis applicable to the design of monocoque aircraft structures, the partial results of which are embodied in this report, was initiated for the purpose of surveying the rational theoretical procedures developed for, or applicable to, stiffened and unstiffened stressed skin structures in the light of existing test results to see which methods could be used in aircraft design, which could be used if modified by the introduction of empirical coefficients, and which appeared to be inapplicable regardless of how they were changed.

Efforts have been concentrated on developing rational or empirical procedures for predicting allowable stresses on smooth and corrugated sheet under compressive and shear loads with a view toward preparing a handbook presenting those methods found to be satisfactory. In some cases where procedures have been developed and descriptions of them published, only references have been given. In other cases where the method is of frequent use in design, an attempt has been made to summarize the more important items and to include the more useful curves or data in this report.

## RESULTS AND CONCLUSIONS

In the time available for conducting this study it has been impossible to consider all the problems involved in the design of monocoque structures. An outline was prepared covering the various problems, and studies were then made to determine those on which theory and test data were available and on which theory and tests agreed. In this report methods are given for predicting allowable compressive stresses on corrugated sheets of aluminum alloy or stainless steel and on flat and curved smooth sheet, stiffened and unstiffened. Procedures which are in reasonable accord with test data have been developed for predicting the compressive strength of stiffeners and stiffened sheet and these processes are extended to cover the design of fuselages and wings. Due to the scarcity of data against which to check some of the methods proposed, it is necessary to consider them as possible procedures rather than as established.

Some data are given for the strength of sheets in shear but further tests are needed on corrugated sheet and on curved sheet before satisfactory procedures

may be developed for design. Further investigations of stiffened sheets in shear are necessary to evolve methods for handling this very important problem.

It is concluded that work should be continued on a classification of problems and on investigations of theoretical procedures for solving them. The publication of Timoshenko's "Theory of Elastic Stability" provides an excellent source book for methods applicable to thin sheet structures and it is recommended that more of the procedures described there, and in other publications, be analyzed and checked against test data with a view toward extending the ground covered by this report.

It is believed desirable that later progress reports should include such matters as rivet and spot welding practice, methods for inhibiting corrosion in various types of structures with various materials and, finally, as many weight data on monocoque structures as can be obtained. It is fully appreciated that weight data form part of a manufacturer's engineering investment and, since they affect the estimated performance of his airplane, have a direct bearing on his success with experimental designs, hence constitute one of the items upon which he competes. It is believed, however, that the data may be presented so that it will serve as a guide and check to all, yet divulge specific data on no one design.

## OUTLINE OF STRUCTURAL PROBLEMS

An outline of the basic problems in the analysis of monocoque aircraft follows. Items considered in this report are mentioned with references to the pages involved. Items covered in other publications have references to the articles in question and items upon which few or no data exist are listed in that way. The fact that reference is made to any article or theory does not indicate that the data or methods are approved for use in airplanes submitted to the Air Corps.

In compiling the data in this report no effort has been made to follow the order of the outline but related material has been arranged in what, it is hoped, will prove to be a useful sequence.

In addition to the references in this outline attention should be given those in N. A. C. A. Technical Memorandum No. 785, "Methods and Formulas for Calculating the Strength of Plate and Shell Constructions used in Airplane Design," Heck and Ebner.

**I. FLAT PLATES, RECTANGULAR****A. Isotropic.**

1. Compression in plane of sheet. Stress to produce buckling, p. 3. Stress at maximum load, pp. 3-7.
2. Shear in plane of sheet. Stress to produce buckling, p. 34. Stress at maximum load, p. 34.
3. Load normal to plane of sheet. See Timoshenko's "Strength of Materials," vol. 2, p. 476. Timoshenko's "Theory of Elastic Stability," ch. VI.
4. Combinations of above. See Timoshenko's "Theory of Elastic Stability," pp. 350 and 362. Also Wagner, in W. G. L. Yearbook, 1928, pp. 113-125. Also Stein, in Stahlbau, Bd. 7 (1934) No. 8, pp. 57-60.

**B. Corrugated.**

1. Compression parallel to corrugations. Critical stresses, pp. 37, 38, 39, and 40.
2. Shear in plane of sheet. Critical stresses, pp. 41, 43, 44, and 45.
3. Load normal to plane of sheet. No known data in aircraft sizes.
4. Combinations of above. No known theory or tests.

**C. Stiffened.**

1. Compression parallel to stiffeners. Stress at maximum load, pp. 20-25.
2. Shear in plane of sheet. Stress at buckling, pp. 34-36. Stress at maximum load, pp. 36-37.
3. Loads normal to plane of sheet. See references for isotropic sheet.
4. Combinations of above. No known data.
- D. Combinations of smooth and corrugated sheet, etc.**
1. Compression in plane of sheets. Critical stresses, pp. 40-41.
2. Shear in plane of sheets. Critical stresses, pp. 44-45.
3. Loads normal to plane of sheets. No known data.
4. Combinations of above. No known data.

**II. CURVED PLATES, RECTANGULAR****A. Isotropic.**

1. Compression parallel to generating element. Critical stresses, pp. 7-9. See also Timoshenko, "Theory of Elastic Stability," p. 467.
2. Shear, torsional or transverse. See N. A. C. A. Technical Memorandum 774. Also Timoshenko, "Theory of Elastic Stability," pp. 480-490. Also N. A. C. A. Technical Note No. 343.
3. Loads normal to generating element. See Timoshenko, "Theory of Elastic Stability," pp. 319, 445.
4. Combinations of above. See Timoshenko, "Theory of Elastic Stability," pp. 475, 490.

**B. Corrugated.**

1. Compression parallel to the corrugations. Critical stresses, p. 40.
2. Shear, torsional or transverse. Critical stresses, pp. 45-46.
3. Loads normal to generating element. No known data.

**4. Combinations of above. No known data.****C. Stiffened.**

1. Compression parallel to stiffeners. Critical stresses pp. 25-26.
2. Shear, torsional or transverse. No known data.
3. Loads normal to generating elements. No known data.
4. Combinations of above. No known data.

**III. STIFFENER SECTIONS**

1. Compression parallel to axis. Critical stresses, secs. 4, 5, 6, 7, and 8.
2. Flexural loads. See standard texts on mechanics for analysis of unsymmetrical sections. See Timoshenko, "Strength of Materials," vol. I, p. 192, for analysis of open sections subject to twisting.
3. Shear loads. See standard texts on mechanics.
4. Torsional loads. See standard texts on mechanics and "Theory of Elasticity."
5. Combinations of foregoing. See standard texts.

**IV. MONOCOQUE SECTIONS, UNSTIFFENED****A. Circular sections.**

1. Compression parallel to axis. N. A. C. A. Technical Report 473. Timoshenko, "Theory of Elastic Stability," pp. 419, 439, 453. See also references in N. A. C. A. Technical Memo. 785.
2. Bending. Critical stresses, p. 27. N. A. C. A. Technical Note 479. Timoshenko, "Theory of Elastic Stability," p. 463.
3. Torsion. N. A. C. A. Technical Note 427. N. A. C. A. Technical Report 479.
4. Combinations of above. Compression-Torsion. A. S. M. E. Trans., vol. 56 (1934), No. 11, pp. 795-806. Compression-Bending A. S. M. E. Trans., vol. 56 (1934), No. 8, pp. 569-578.

**B. Noncircular sections.**

Fundamental data on noncircular sections are practically nonexistent.

**V. MONOCOQUE SECTIONS, STIFFENED****A. Circular sections.**

1. Compression parallel to axis. Timoshenko, "Theory of Elastic Stability," p. 470.
2. Bending. Critical stresses, pp. 27-34.
3. Torsion. See N. A. C. A. Technical Memo. 785, p. 38.
4. Combinations of above. No known data.

**B. Noncircular sections.**

Fundamental data on noncircular sections are practically nonexistent.

**VI. CONNECTIONS AND ATTACHMENTS****A. Rivets.****B. Welds, including spot-welds.**

(Not considered in this progress report.)

**VII. CORROSION PREVENTION****A. Ferrous materials.****B. Nonferrous materials.**

(Not considered in this progress report.)

## SECTION 1. CRITICAL LOADS OF SMOOTH, UNSTIFFENED SHEET

The aeronautical structural engineer, in the design of stressed skin or monocoque structures, must choose between proportioning members carrying compression or shear so they will not wrinkle or so they will not collapse until the maximum design load is reached. In some places one criterion serves, and in others the other. Not only must he proportion flat, curved or corrugated sheets to carry the loads desired, but he must also provide stiffening members and other reinforcements to furnish the necessary local stiffness required or to distribute loads which are concentrated locally.

Occasionally the designer is seriously concerned by the stresses causing local buckling or wrinkling of wing or fuselage covering. He may wish to know whether or not the buckling or wrinkling deformations of portions of such structures under normal flying loads will be sufficient to affect adversely the aerodynamic efficiency and handling characteristics, the covering attachment and adjacent structure, or the appearance. To provide for the effects of "shear lag" or to determine when the web of a spar ceases to be shear resistant and starts to act as a tension field, the stress analyst must know the intensity of stress at which buckles form. The first part of the next section of this report deals, therefore, with the stresses which produce wrinkles in smooth sheet.

These buckling stresses depend upon the method of support of the edges of the sheet. A simply supported edge is one that is constrained to remain straight throughout its length, but is free to rotate about the median line of the edge as an axis. Holding the edge in a V- or U-shaped groove or between round rods appears to simulate this condition. A clamped edge is one that is constrained to remain straight throughout its length without rotating. A sheet clamped between heavy plates simulates this condition. A free edge, as the name implies, is not restrained in any way.

## SECTION 2. ISOTROPIC FLAT RECTANGULAR PLATES COMPRESSIVE LOADS

Considering plates subjected to compressive loads, we have those for which buckling is critical and those which are to be stressed beyond the point where they buckle to the absolute maximum they will carry. A summary of formulas applicable to each is given below:

### SECTION I. Conditions to produce buckling.

The general expression for critical compressive stress at the start of buckling is:

$$\sigma_{cr} = \frac{K\pi^2 E}{12(1-\mu^2)} \left(\frac{t}{b}\right)^2 \quad 1$$

where

$\sigma_{cr}$ =intensity of compressive stress (at the start of buckling).

$K$ =theoretical coefficient depending upon sheet dimensions and type of edge support (experimental data are in reasonable accord). See figures 1, 2, 3, and 4 for values of  $K$ .

$E$ =modulus of elasticity of material.

$\mu$ =Poisson's ratio = 0.30 for steel and aluminum alloys.

$t$ =thickness of sheet.  
 $b$ =length of loaded edges.  
 $a$ =length of unloaded edges.

In N. A. C. A. Report No. 382, "The Elastic Instability of Members Having Sections Common in Aircraft Construction," by Trayer and March, an expression is given for the load producing buckling on sheets having one free edge.

It is:

$$P = \left[ \frac{\pi^2}{12(1-\mu^2)} \left( \frac{b}{c} \right)^2 + \frac{1}{2(1+\mu)} \right] E \frac{t^3}{b} \text{ where } c \text{ is the}$$

length of the half wave formed when the sheet buckles. In most cases,  $c$  may be taken as the length of the member, and the first term in the parenthesis becomes negligible, so  $P = 0.385 E \frac{t^3}{b}$  and the stress  $\sigma_{cr} = 0.385 E \left( \frac{t}{b} \right)^2$ . For small ratios of  $\frac{b}{a}$  the value of  $k$  in figure 4 may be taken as 0.456 and when substituted in equation 1 gives  $\sigma_{cr} = 0.412 E \left( \frac{t}{b} \right)^2$  or about 7 percent more than Trayer and March.

The critical loads or stresses given above are those at which buckling due to compression starts. So far as is known no method exists for determining the magnitude of load which will produce stresses in the buckled sheet approaching the yield point of the material and causing the buckles to assume a permanent form. For many purposes it would be desirable to design structures on the basis of stresses just below those causing permanent buckles to form, but this appears impossible at present. For other purposes it is necessary to design to stress intensities which cause failure of the member by crushing or by its collapse due to column action.

Sec. II. Conditions at maximum load, case I, two edges loaded, all four simply supported. von Karman—Sechler Method.

For flat sheets in compression the method described by von Karman, Sechler, and Donnell in their paper of June 1932 in the Transactions of the Applied Mechanics Section, A. S. M. E., appears to be in best agreement with test data. Briefly the method involves solving equation 1 for the width  $b$  at which the critical stress on the simply supported sheet is equal to the yield point of the material. As first described  $K$  was taken as 4, but later developments depend upon a variable  $K$ .

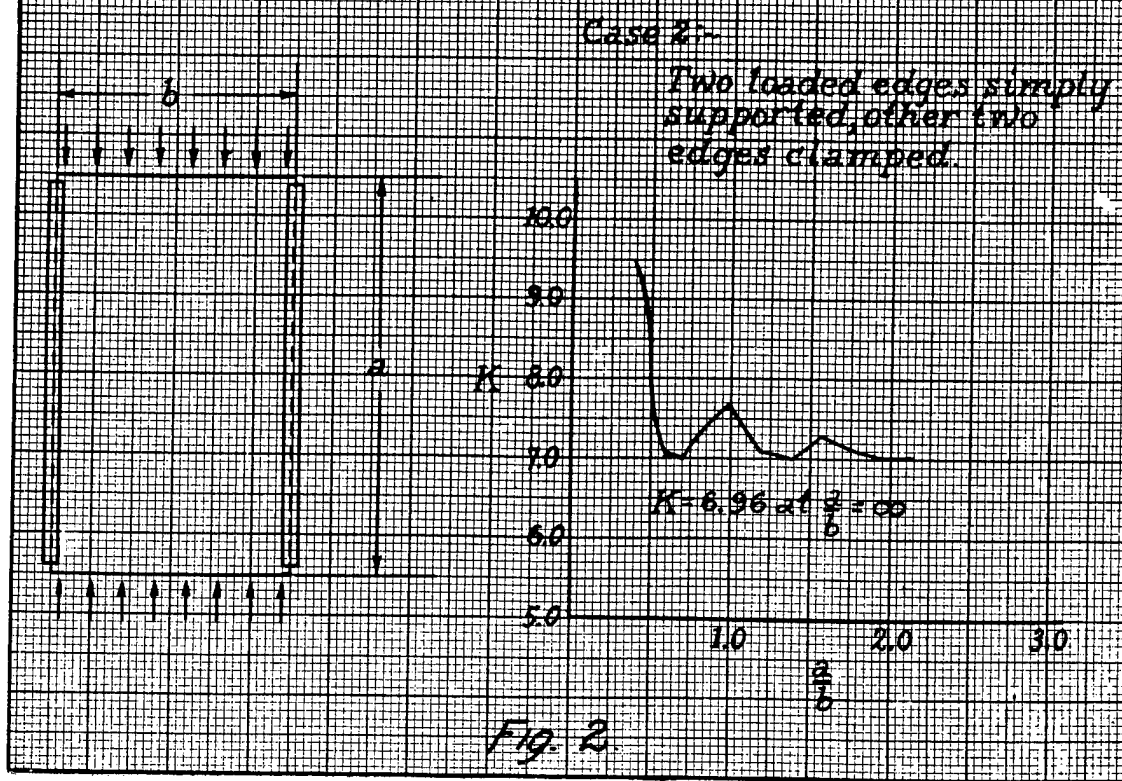
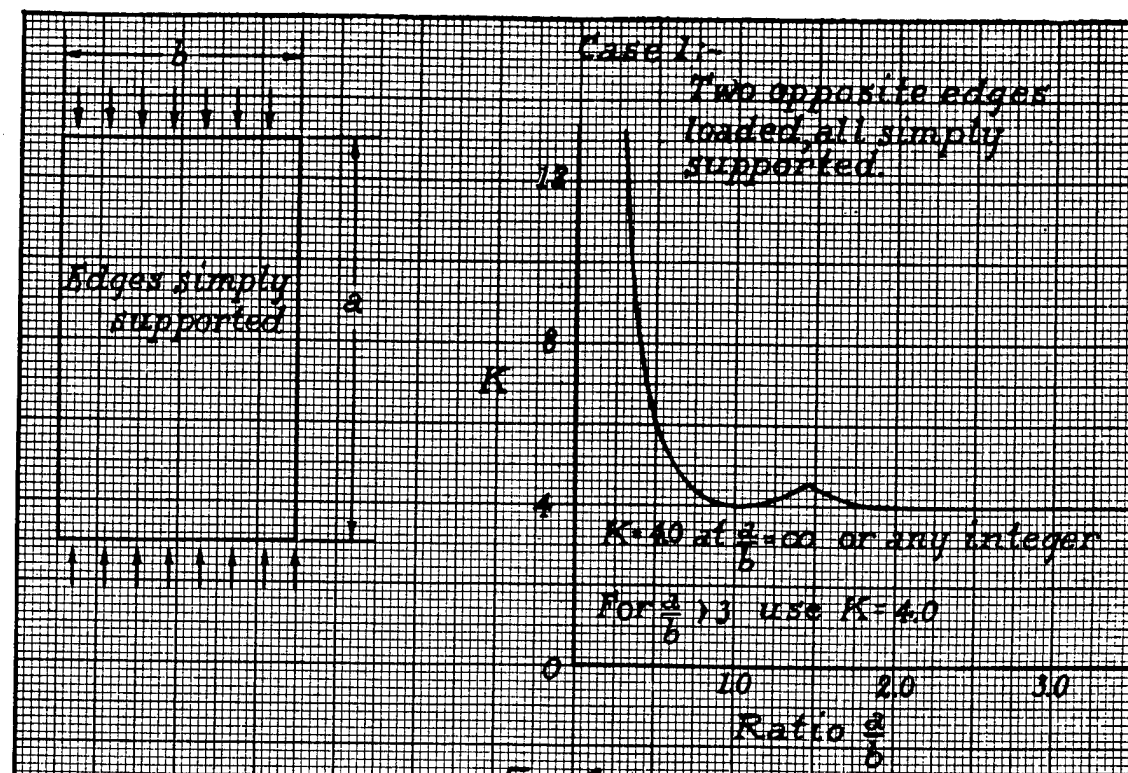
Assuming  $K=4$  we have,  $\sigma_{cr} = \sigma_{vp} = \frac{4\pi^2 E}{12(1-\mu^2)} \left( \frac{t}{b} \right)^2$ , and for aluminum alloy or steel  $\mu=0.30$ , so

$$\sigma_{vp} = 3.61 E \left( \frac{t}{b} \right)^2$$

whence

$$b = 1.90 t \sqrt{\frac{E}{\sigma_{vp}}}$$

Tests made at the Bureau of Standards and recorded in N. A. C. A. Report 356, "Strength of Rectangular Flat Plates under Edge Compression," by Schuman and Back, showed that the load carried by flat sheets with simply supported edges was essentially independent of the width of the sheet, so von Karman and Sechler proposed treating the sheet as though it had an area near each edge which could be stressed to the yield point where the central portion was practically unstressed.



FIGURES 1-2.

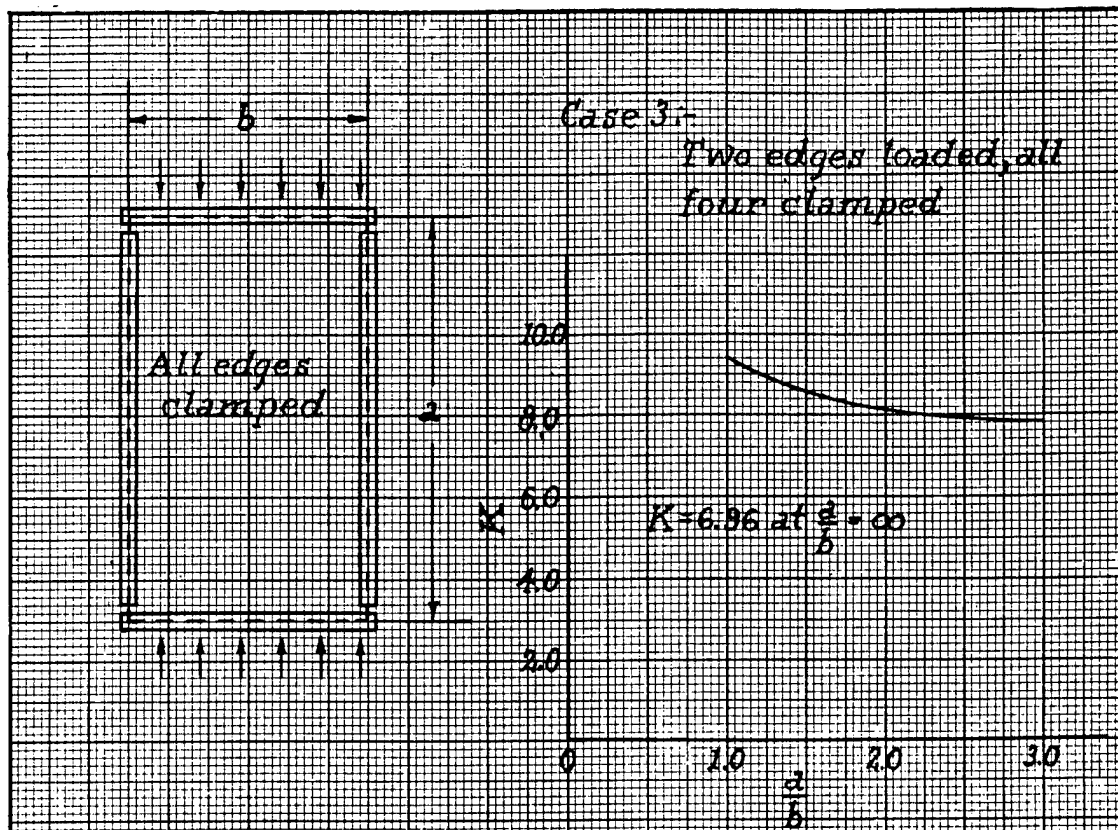


Fig 3

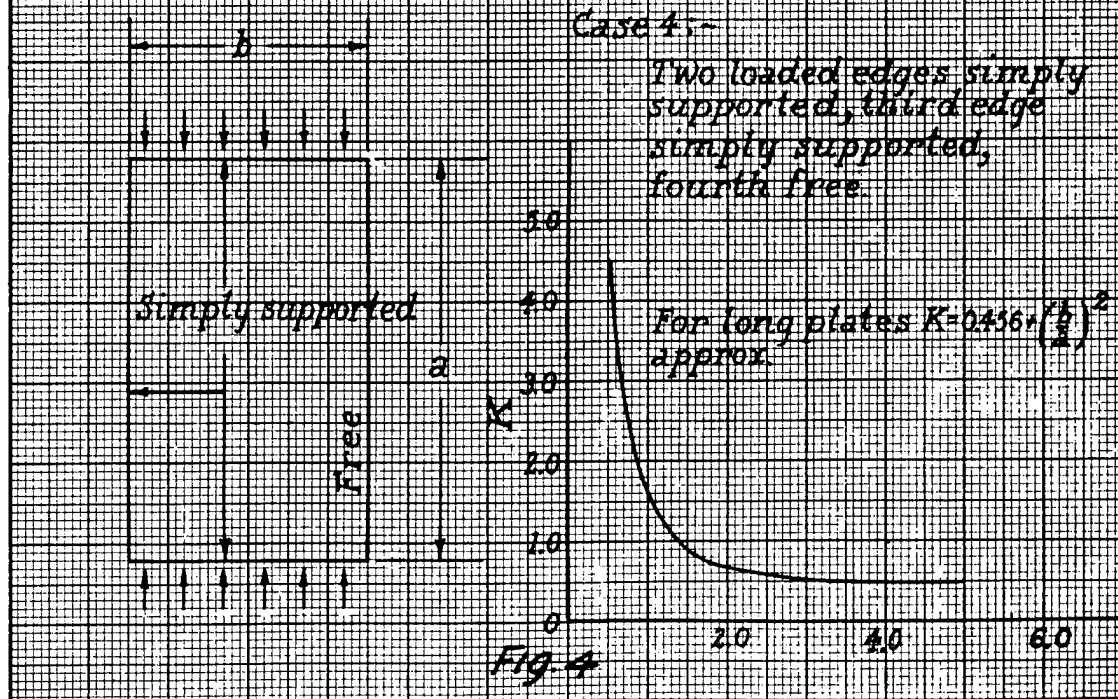


Fig 4

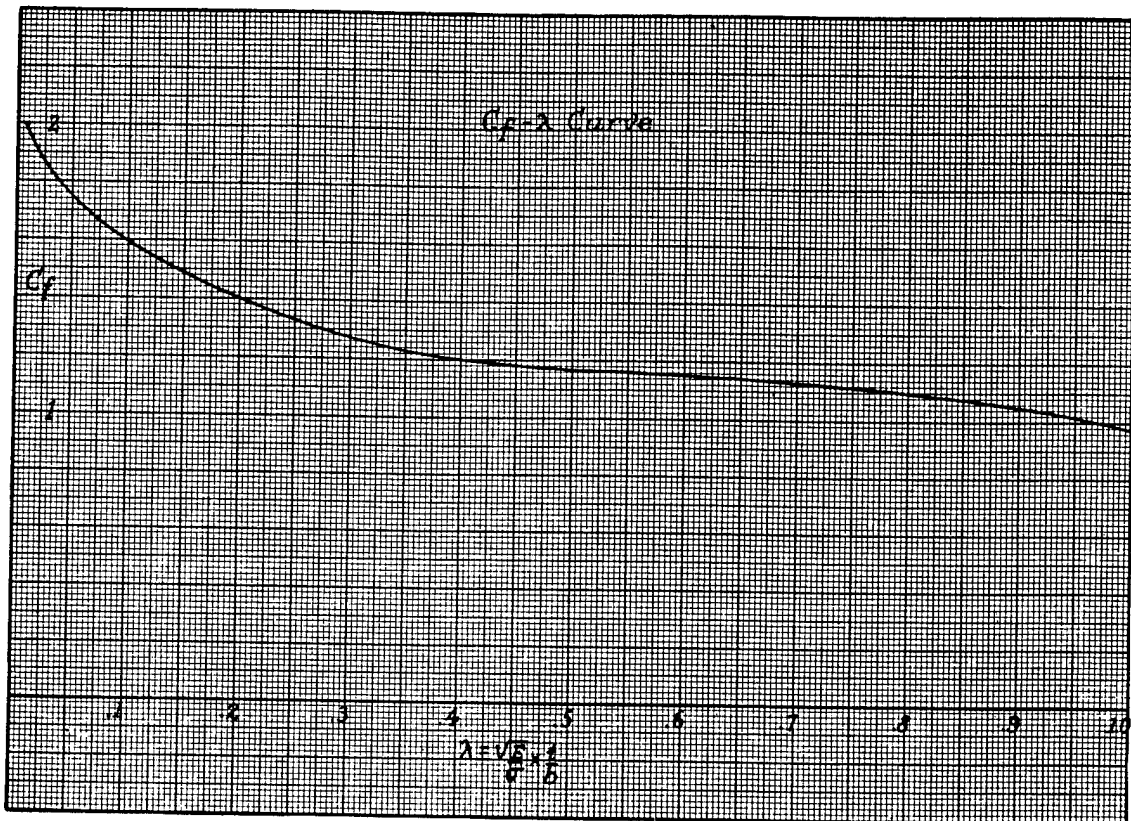


FIGURE 5.

The sum of these two stressed widths, called the "effective width," was then taken as

$$b_e = 2W = 1.90t\sqrt{E/\sigma_{cr}}$$

Tests made at M. I. T., C. I. T., and various other places showed that 1.90 was too high and indicated that it was not a constant. A good average value for sheets of normal size and thickness was found to be 1.73; and 1.7 has been widely used with satisfactory results. Substituting the empirical 1.7 for the more rational 1.9 and assuming that the sheet may act at a stress higher than its yield point if it is attached to a stiffener or otherwise supported, so that it reaches its maximum load when the stiffener is carrying the maximum stress of which it is capable, we have

$$b_e = 1.7t\sqrt{E/\sigma_{cr}}$$

On the basis that the "effective" width,  $b_e$ , carries a stress  $\sigma_{cr}$ , it is obvious that the load on the "effective" area will be  $P = b_e t \sigma_{cr}$ , or  $P = 1.7t^2\sqrt{E\sigma_{cr}}$ .

For normal sizes of sheet the above expressions for "effective" width and total load on simply supported panels are in satisfactory agreement with test results. It has been found that stiffeners provide support, if properly designed, equal to that assumed for the simply supported edge condition.

For investigations requiring more refined computation it is desirable to vary the coefficient 1.7 with  $t\sqrt{E/\sigma_{cr}}$ . The values established by Sechler are shown in figure 5, the coefficient  $C_f$  being plotted against  $\lambda = \frac{t}{b}\sqrt{E/\sigma_{cr}}$ .

The above expressions are summarized below for the case of simply supported edges and for other edge conditions.

Considering cases I to IV as in section I:

**CASE I, TWO SIDES LOADED, ALL FOUR SIMPLY SUPPORTED**

$$\text{Effective width, } b_e = 2W = Ct\sqrt{\frac{E}{\sigma_{cr}}}$$

$$\text{Total load} = P = Ct^2\sqrt{E\sigma_{cr}}$$

$C = 1.90$  by von Karman, theory.

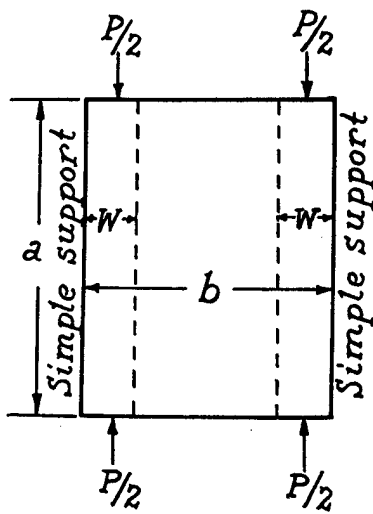


FIGURE 6.

$C=1.70$  by Newell, empirical.

$C$ =value from figure 5 by Sechler.

Cox, R and M 1553 and 1554, gives  $b_e=2W$

$$=C't\sqrt{\frac{E}{\sigma_{cr}}}+Db \text{ where } C'=1.52 \text{ and } D=0.09.$$

CASES II AND III. CLAMPED EDGES

$$\text{Effective width, } b_e=2W=Ct\sqrt{\frac{E}{\sigma_{cr}}}$$

$$\text{Total load, } P=Ct^2\sqrt{E\sigma_{cr}}$$

$C=2.51$  on basis of  $K=6.96$ .

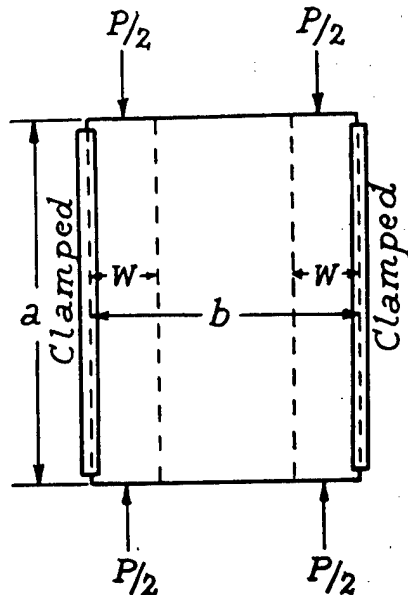


FIGURE 7.

There are no test data to vindicate the above coefficients.

Cox in R and M 1553 and 1554, gives  $b_e=2W$

$$=C't\sqrt{\frac{E}{\sigma_{cr}}}+Db \text{ where } C'=2.18 \text{ and } D=0.14.$$

CASE IV. TWO EDGES LOADED AND SIMPLY SUPPORTED,  
THIRD SIMPLY SUPPORTED, FOURTH FREE

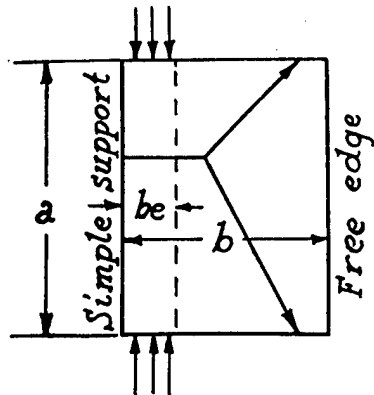


FIGURE 8.

$$\text{Effective width, } b_e=Ct\sqrt{\frac{E}{\sigma_{cr}}}$$

$$\text{Total load, } P=Ct^2\sqrt{E\sigma_{cr}}$$

$C=0.641$ , based on  $K=0.456$  at  $(\frac{b}{a})^2=0$

$C=0.68$  by von Karman.

$C=0.60$  by Lundquist.

$$P=\left[\frac{\pi^2}{12(1-\mu^2)}\frac{b^2}{c^2}+\frac{1}{2(1+\mu)}\right]E\frac{t^3}{b}=\left[0.9\left(\frac{b}{c}\right)^2+0.385\right]$$

$E\frac{t^3}{b}$  for  $\mu=0.3$  and  $\frac{b}{c}$  equal ratio of sheet width to length of half-wave formed. Trayer and March, N. A. C. A. Report 382.

Case I above has been checked against test data on flat sheets of aluminum alloy and stainless steel by several agencies and found to be in satisfactory accord with the tests; so no effort will be made in this report to present data for the purpose of justifying it. The Trayer and March formula of case IV has been checked for isotropic materials and modified for nonisotropic, as recorded in N. A. C. A. Report 382. It appears to give satisfactory results and should be used in preference to the other formulas, since the others do not provide for the reduction in load which occurs as  $b$  increases. It is probable that the maximum load is not entirely independent of the yield point of the material as indicated by the Trayer and March formula, but it is certain that it is not independent of the width.

SECTION 3. ISOTROPIC, CURVED RECTANGULAR PLATES COMPRESSIVE LOADS

The problem of the curved plates in compression is more difficult to treat mathematically, so there are few rational formulas available for the determination of the stress causing buckling or the stress at maximum load on such members. Most of the formulas are modifications of those for complete cylinders, but Timoshenko in "Theory of Elastic Stability," page 467, develops expressions for the critical buckling stress on curved panels and on page 470 states that the resulting equation,  $\sigma_{cr}=0.6E\frac{t}{R}$ , is in satisfactory accord with test data on aluminum alloy panels, provided the axial and circumferential dimensions of the panel are about equal and the central angle subtended by the panel is less than about  $\frac{1}{2}$  radian. As the central angle increases to 2 radians the critical stress diminishes to about half that given above and approaches—

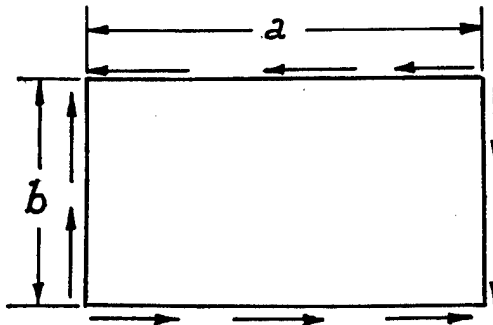


FIGURE 9.

$$\sigma_{ult}=E\frac{0.6\frac{t}{R}-10^{-7}\frac{R}{t}}{1+0.004\frac{E}{\sigma_{yp}}}$$

as developed by Donnell for thin walled tubes in compression.

Where

$t$ =thickness of sheet.

$R$ =radius of curvature.

$\sigma_{ult}$ =ultimate stress in sheet.

$\sigma_{cr}$ =buckling stress.

$\sigma_{vp}$ =stress at yield point.

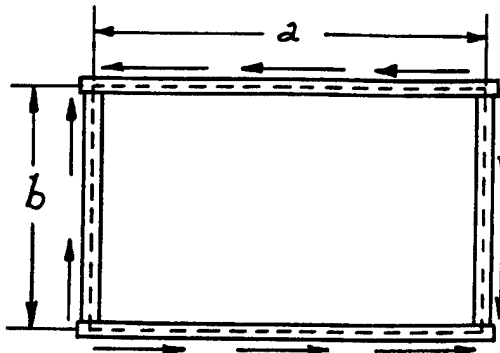


FIGURE 10.

Since airplane structures normally involve dimensions placing some panels in one of the above categories, some in the other and some between, there is little in the above that is of general use to the designer.

#### SECHLER'S METHOD

The adaptation of the von Karman-Sechler formulas for flat plates which was made for curved plates by Sechler appears to be the best all round solution for the stress at ultimate load. Reduced to its simplest terms, Sechler's method amounts to treating a curved panel having simply supported edges as being composed of effective widths, carrying the same stresses and loads as in the case of a flat sheet, plus a central area which works to a stress intensity of  $\sigma = 0.3E \frac{t}{R}$ . The effective width, as in the case of the flat sheet, is found from  $b_e = Ct\sqrt{\frac{E}{\sigma_{cr}}}$  where  $C$  is taken as 1.7 for average values or from figure 5 as the case may be. This width, working to a stress,  $\sigma_{cr}$ , carries a load  $P' = Ct^2\sqrt{E\sigma_{cr}}$  while the area between the effective widths takes  $P'' = t(b - b_e)(0.3E \frac{t}{R})$ . The total load is then  $P' + P'' = Ct^2\sqrt{E\sigma_{cr}} + \left(b - Ct\sqrt{\frac{E}{\sigma_{cr}}}\right)\left(0.3E \frac{t^2}{R}\right)$  which may be simplified to  $P = C_c t^2 \sqrt{E\sigma_{cr}}$ , where

$$C_c = C - 0.3C\lambda\eta + 0.3\eta.$$

$C = 1.7$  or coefficient from figure 5.

$$\lambda = \sqrt{\frac{E}{\sigma_{cr}}} \frac{t}{b}, \eta = \sqrt{\frac{E}{\sigma_{cr}}} \frac{b}{R}$$

The major drawback to this method is that no provision is made for panels of different lengths in computing the load carried by the central area of the sheet. Comparisons of predicted loads with results from tests on curved sheet made at M. I. T. show the method to be slightly conservative for panels 6 inches long, slightly

optimistic for 12-inch lengths and very optimistic, 25 to 50 percent, on panels 18 inches long. Since the load carried by the sheet is normally small in comparison to that in the stiffeners, the errors involved in computing strengths of stiffened panels by this method are usually less than 10 percent, but it should not be forgotten that length has an effect on the strength of curved sheet. As might therefore be expected, the method is in better agreement with test results for sheets having large radii than for those with small radii. It is also better for wide sheets than narrow.

Table 1 shows the agreement between predicted and test loads on curved panels as obtained by this method, the data chosen being representative of that procured on some 150 panels of 17 ST aluminum alloy tested at M. I. T.

In considering the data in table 1 it should be noted that the test data are for most cases the result of a test on a single panel of the dimensions shown and that some of these panels had yield points higher or lower than average, some were thinner or thicker than the nominal dimensions, so it is necessary to make comparisons on the basis of trends rather than on specific values. The agreement between predicted and test values is good and the method simple to apply.

#### EMPIRICAL METHOD

Figures 11 and 12 (figs. showing factors  $K_1$ ,  $K_2$ ) developed empirically from the 17 ST panels tested at M. I. T. give coefficients by which the load computed for a flat sheet may be modified to provide for the effect of radius of curvature, length and width of specimen. That is, the load on a curved sheet is  $P_c = K_1 K_2 P_{flat}$  where the load on the flat sheet is  $P_{flat} = Ct^2\sqrt{E\sigma_{cr}}$  as described above.

The use of figures 11 and 12 gives results whose average error is about the same as that obtained by Sechler's method, but the range of error is greater. However, for determining trial sections it will be found that loads may be found by the use of these figures somewhat more readily than by Sechler's method and with approximately the same results. The curves are included for such purposes.

#### OTHER METHODS

Cox, British R and M 1553 and 1554, and Redshaw, R and M 1565, give formulas for flat and curved sheet. Redshaw's formula, as given in N. A. C. A. Technical Memo 785, is

$$\sigma_{cr} = \frac{E}{6(1-\mu^2)} \left[ \sqrt{12(1-\mu^2) \left(\frac{t}{R}\right)^2 + \left(\frac{\pi t}{b}\right)^2} + \left(\frac{\pi t}{b}\right)^2 \right]$$

It is seen that this expression makes no provision for the effect of length. Applying it to one or two typical panels shows it to be extremely optimistic. It gives

$t$	$R$	$b$	Pre-dicted stress	Test stresses		
				$L=6$	$L=12$	$L=18$
0.020	30	12	4,250	3,900	3,340	2,580
.020	10	12	12,650	7,950	7,710	6,190

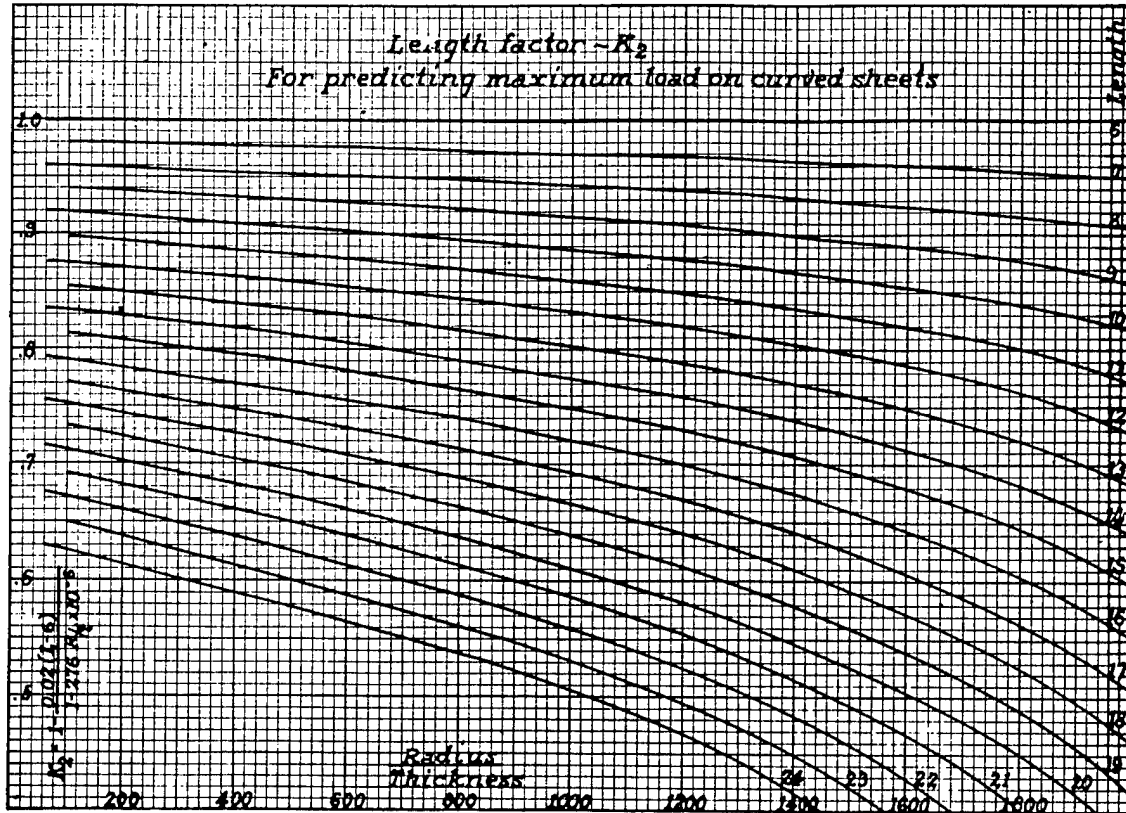


FIGURE 11.

TABLE 1

$t$	$b$	$r$	Pre-dicted load	Test loads		
				$L=6''$	$L=12''$	$L=18''$
0.020	12	30	881	950	800	620
		20	1,110	1,145	1,000	735
		10	1,796	1,910	1,850	1,485
	3	5	3,176	3,200	2,600	2,330
		30	561	540	490	420
		20	630	570	540	440
.020	12	10	834	795	650	525
		5	1,247	1,140	960	740
		30	2,360	2,500	2,100	1,980
	3	20	2,960	3,635	3,370	2,760
		10	4,765	5,580	5,085	5,325
		5	8,375	9,560	9,020	8,570
.033	12	30	1,379	1,210	1,110	1,040
		20	1,491	1,420	1,300	1,180
		10	1,827	1,905	1,725	1,355
	3	5	2,499	2,960	2,585	2,125
		30	5,500	6,750	5,925	5,045
		20	6,880	9,060	8,000	6,815
.051	12	10	11,000	14,900	12,310	13,265
		5	19,240	19,950	19,150	19,300
		30	3,158	2,550	2,160	2,050
	3	20	3,360	3,135	2,765	2,255
		10	3,980	5,000	3,820	2,900
		5	5,160	5,005	5,010	4,190

## SECTION 4. STIFFENER DESIGN

On the basis of the following investigation it is believed that stiffeners made from flat sheet may be approximately proportioned by determining the crushing stress for the cross section and, for members in the short column range, substituting this crushing stress for the yield point in the Johnson parabolic column formula. The crushing stress should be checked by test in any case, but for approximate or preliminary

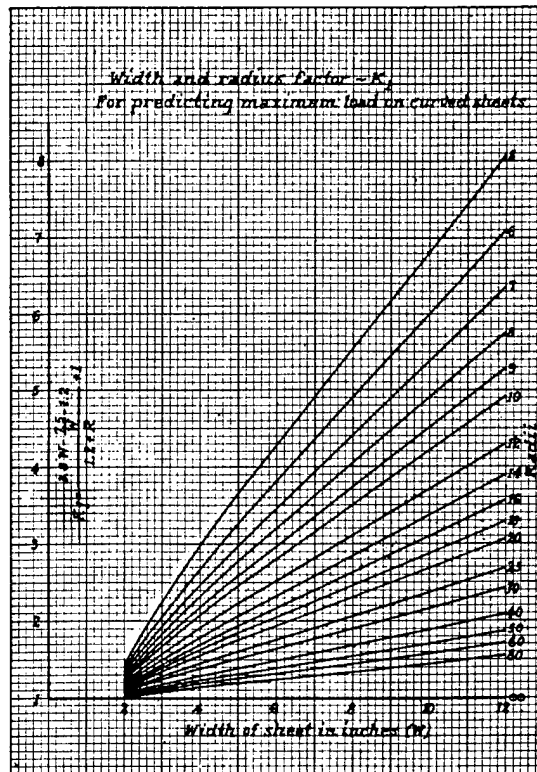


FIGURE 12.

design of members the following analytical procedure is suggested:

1. Assume a section which is composed of a series of flat elements to be made up of flat sheets having elastically restrained or free edges. Where the edge of the sheet is bent 90° around a radius approximately twice the thickness of the sheet, it may in most cases be treated as the equivalent of a simply supported edge which will carry a stress equal to the yield point of the material. Edges having larger radii of curvature and those adjacent to sheets which are wide in proportion to their thickness buckle at stresses less than the yield point and some corrective factor is necessary to provide for this effect. For two types of section sufficient data were available to permit drawing an empirical curve for the coefficient which gives good results. The coefficient is actually a function of the torsional stiffness of the adjacent sheets and edges, hence, should be expected to vary with the radius and angle of bend, the thickness and width of the material adjoining the edge in question, the perfection of the edge formed, and such other factors as may affect the elastic support furnished by the adjacent edges and sides. As will be seen from the tabulated data below, some shapes provide sufficient support so that the effective widths near the edges develop the full yield point of the material before failing, others appear to fail at about 75 percent and some at a much lower fraction of the yield point. It is believed, however, that for any given section a form factor may be developed from tests on relatively few specimens which will represent the conditions of support for the various edges for varying widths of sheet, so that the designer can predict the effect of changes in cross-sectional dimensions with reasonable accuracy.

2. Treat the elements, both edges of which are bent, as simply-supported flat plates which will carry a load of  $P=1.7t^2\sqrt{E \times \sigma_{cr}}$  if their center line width is greater than the effective width found from  $b_e = 1.7t\sqrt{\frac{E}{\sigma_{cr}}}$ ,

where  $\sigma_{cr}$  represents the yield point stress reduced by the appropriate form factor to represent the relative condition of edge support. When the center line width is less than  $b_e$ , the load which the element will carry will be  $P=b \times t \sigma_{cr}$ , where  $b$  represents the center line width.

For elements such as the outstanding legs of channels, one of whose edges is simply supported, the other free, the load may be found from  $P=\left[\frac{\pi^2}{12(1-\mu^2)} \cdot \frac{s^2}{c^2} + \frac{1}{2(1+\mu)}\right]$

$E \cdot \frac{t^3}{s}$  where  $s$  represents the width of the element,  $t$  its thickness,  $c$  the length of half wave formed when it buckles and  $\mu$  = Poisson's ratio. For steel and the aluminum alloys,  $\mu=0.30$  and  $c$  may be taken as the length of the member when such length represents an  $L/\rho$  for the member in the vicinity of 20. In most cases, the first term is negligible and the load may be

represented by  $P=0.385E \frac{t^3}{s}$ . For small values of  $s$ , this expression indicates loads causing stresses beyond  $\sigma_{cr}$ , in which case, the load should be taken as  $P=s \times t \times \sigma_{cr}$ .

An outstanding leg having a small flange or lip rolled on it lies somewhere between a sheet having a simply-supported edge and one having a free edge. As shown by the tabulated data which follows, such a flange, when its length is three or four times its thickness, is usually sufficient to produce a simple support condition.

It is believed that the distance between rivets may be used as the approximate length of half wave in computing the load on the legs of stiffeners attached to sheet, but the data available involve too many other variables to permit establishing this as a fact.

When lightening holes are used, the strength of the element in which they occur should be based on the net area taken through the cut-out. If the holes are flanged, the meager data available indicate that the flange is approximately equivalent to a simply-supported edge and that the strength of the areas to each side of the lightening hole may be determined on that basis. Where the holes are not flanged, the strength of the adjacent material appears to lie between that expected of a free edge and that for a simply-supported edge. The data available are too few to permit the evaluation of the supporting effect in the form of an empirical factor.

Bends of vee or other shape involving sharp edges serve to break a wide, flat element into two narrower elements having approximately simply supported edges. The effectiveness of the "edges" varies, as would be expected, with the size and shape of the groove, but a reasonable approximation can be obtained by assuming the groove to act as a simply-supported edge.

Curved elements, such as that in the  $\text{J-shaped}$  stiffener appear to develop the full yield point stress for the material if their diameter/thickness ratio is 30 or less, and their point of tangency with the flat element appears to act as a simply-supported edge for that element.

Extruded sections having corner fillets have better than simply-supported edges and it appears that the crushing strength of their elements may be based on a condition between simply-supported and clamped edges. For many extruded sections, the crushing stress will be equal to the yield point of the material.

3. Having determined the load which each element of the section will carry, if acting alone under the assumed conditions of edge support, the loads may be summed up for the entire section and divided by the area of the cross-section to obtain an average crushing stress for the section. For stiffening members in the short column range, the average crushing stress based on an assumed length of member sufficient to give an  $L/\rho$  of about 20 may be substituted for  $F$  in Johnson's parabolic column formula,  $P/A=F-\frac{F^2(L/\rho)^2}{4c\pi^2E}$ , and the stress determined for the design  $L/\rho$ . For members in the long column range, the standard Euler formula suffices.

It is assumed for the method outlined above that the stiffeners will be attached to the structure in such a way that they will not fail by combined torsion and bending. Where such failures are possible, the likelihood of their happening should be checked by the method given by H. Wagner and W. Pritschner in N. A. C. A. Technical

Memo No. 784,<sup>1</sup> "Torsion and Buckling of Open Sections." In making tests on stiffener sections to check the predicted crushing stresses given by the above procedure, provision should be made to insure that the failure obtained is a crushing failure and not a torsional one. On members such as simple channels, this can be done by preventing the rotation of the channel during test by attaching a long stick to the specimen near its midlength and applying a small correcting moment when the section starts to twist. Such a device should, of course, be attached so it will not alter the stresses on the specimen and so it will not produce a supporting effect of such character as to reduce the effective length of the member.

### SECTION 5. DETERMINATION OF CRUSHING STRENGTH (STIFFENERS)

The theory of elastic stability may be applied to the buckling of the various elements of a section or it may be applied to the section as a whole. The method outlined below is based on the stability of the separate elements and was proposed by Mr. A. B. Callender and investigated in his thesis, "Elastic Instability of Duralumin Columns in Compression," M. I. T. 1933. It is vindicated by Timoshenko in his "Theory of Elastic Stability," page 333, where he shows the four sides of a square tube to buckle as though each side were a compressed rectangular plate with simply supported edges and on pages 342 to 350 where methods of analysis are developed for various conditions of elastic support of the edges. Due to the complexity of the resulting equations, it is believed that designers will prefer the use of empirical form factors and coefficients to the completely rational method.

The method outlined by Messrs. W. S. Parr and W. M. Beakley of the California Institute of Technology in their paper, "An Investigation of Duralumin Channel Section Struts in Compression," Journal of the Institute of Aero. Sciences, volume 3, September 1935, pages 21-25, is based on the application of the stability equation to the section as a whole rather than to its elements. They establish three types of failure designated Euler, plate and torsional, and express the critical stress as  $\sigma_{cr} = KE(t/s)^2$  where  $K$  is a coefficient which varies with the type of failure. The second condition, or plate failure corresponds with the crushing strength of the section as considered above and the value of  $K$  for that is:

$$K = \frac{2\pi^2 V \left(\frac{s}{b}\right)^2 \left[ (V+1) + 4(1-\mu) V \frac{s}{b} \right]}{12(1-\mu^2)}$$

where  $V = \sqrt{\frac{3}{4}\pi^2 \left(\frac{s}{b}\right)^3 + 3}$

$s$  = length of outstanding leg of the channel.  
 $b$  = width of back of the channel.

It will be noted that  $K$  is a function of  $\frac{s}{b}$  only, so that for channels whose ratios of leg to back are identical,

<sup>1</sup> See also N. A. C. A. Report No. 582, "Theory for Primary Failure of Columns, Lundquist and Fligg."

the critical stress will vary as  $\left(\frac{t}{s}\right)^2$ . A check of this relation against the tests made by Roy A. Miller and recorded in A. C. I. C. No. 598, "Compressive Strength of Duralumin Channels," does not confirm this as fact, but indicates the variation to be more nearly  $\left(\frac{t}{s}\right)^{\frac{1}{2}}$  than  $\left(\frac{t}{s}\right)^2$ . For the series of channels in which the ratio  $\frac{s}{b}$  is 0.5 we have:

Miller's $\sigma_{cr}$	In terms of $t$		Ratio $\frac{t}{s}$	$\left(\frac{t}{s}\right)^2$	$\sqrt{\frac{t}{s}}$
	$b$	$s$			
31,000	24t	12t	0.0833	0.00695	0.288
28,230	28t	14t	0.0714	.00505	.267
25,460	32t	16t	.0625	.00390	.250
22,690	36t	18t	.0555	.00308	.236
19,920	40t	20t	.0500	.00250	.224
17,150	44t	22t	.0454	.00206	.212
14,380	48t	24t	.0416	.00174	.204
13,000	50t	25t	.0400	.00160	.200

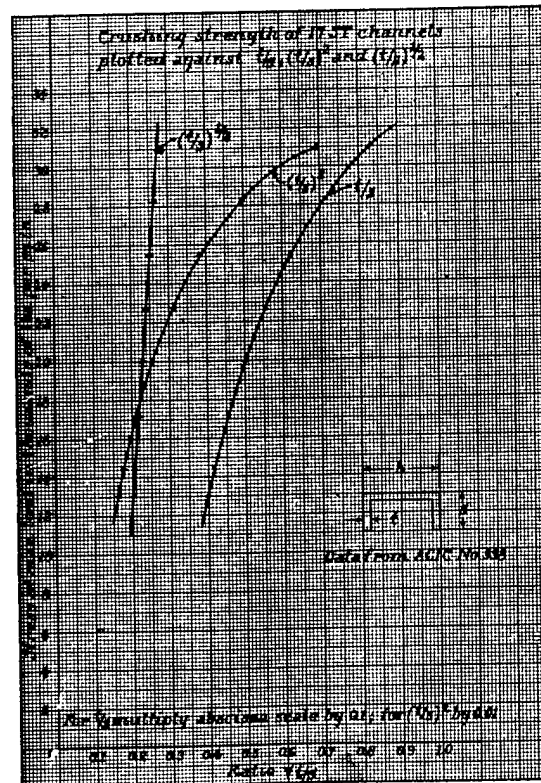


FIGURE 13.

As shown by figure 13 in which  $\sigma_{cr}$  is plotted against  $t/s$ ,  $(t/s)^2$  and  $(t/s)^{\frac{1}{2}}$ , the curve plotted for  $(t/s)^{\frac{1}{2}}$  is practically a straight line where those for  $t/s$  and  $(t/s)^2$  most definitely are not. It must be concluded, therefore, at least in the light of these data, that the method of obtaining crushing stresses from the properties of the entire section instead of its elements is not in suffi-

ciently close accord with standard test data to be accepted for design.

On the basis of these same tests the method of treating each element as a separate entity, as was suggested by Callender, gives the following results when applied in terms of the system of dimensions shown in figure 14.

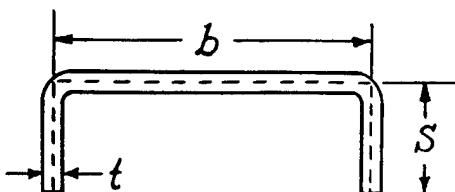


FIGURE 14.

Using  $E=9,730,000$  and  $\sigma_{vp}=37,000$ , the average values given in A. C. I. C. No. 598 and considering a channel having  $b=24t$ ,  $s=12t$  and area approximately  $48t^2$  we have:

$b_e$  for back =  $1.7\sqrt{E/\sigma_{vp}}$   $t=28t$ . The widths of back being less than  $b_e$ ,  $P_b=b\times t\times\sigma_{vp}=24t\times t\times 37,000=888,000t^2$

$$P_s=0.385\times E\times \frac{t^3}{b}=0.385\times 9,730,000\times \frac{t^3}{12t}=312,000t^2$$

$$P_{total}=P_b+2P_s=1,512,000t^2$$

$$\sigma_{crush}=\frac{P_{total}}{\text{Area}}=\frac{1,512,000t^2}{48t^2}=31,500 \text{ lb./in.}^2$$

From tests  $\sigma_{crush}=31,000 \text{ lb./in.}^2$

Table 2 shows this method applied to other sections investigated in A. C. I. C. No. 598.

TABLE 2

Channel size	b/s	Predicted $P_{crushing}$	Test $P_{crushing}$
24t×12t×t	2	31,500	31,000
28t×14t×t	2	28,350	28,230
32t×16t×t	2	23,700	25,460
36t×18t×t	2	20,400	22,690
40t×20t×t	2	17,800	19,920
44t×22t×t	2	15,800	17,150
48t×24t×t	2	14,320	14,380
50t×25t×t	2	13,480	13,000
36t×12t×t	3	28,000	26,650
48t×16t×t	3	19,000	21,900
60t×20t×t	3	14,240	17,150
12t×12t×t	1	29,000	35,400
20t×20t×t	1	18,100	22,700
24t×24t×t	1	16,900	16,400
25t×25t×t	1	16,350	14,800

The agreement between Callender's method and Miller's test results over rather a wide range of sections is sufficiently good to justify further consideration of the proposed procedure.

For some smaller channels of 17ST tested with "flat" ends at M. I. T. the following results were obtained:

For the section:

$$b=0.715 \text{ in.}; 0.75 \text{ in., over all.}$$

$$s=0.484 \text{ in.}; 0.50 \text{ in., over all.}$$

$$t=0.031 \text{ to } 0.033; 0.032 \text{ average.}$$

$$I=0.00146 \text{ in.}^4$$

$$\text{Area}=0.053 \text{ in.}^2$$

$$\rho=0.16 \text{ in.}$$

$$E=10,350,000 \text{ lb./in.}^2 \text{ (average).}$$

$$\sigma_{vp}=39,500 \text{ lb./in.}^2 \text{ (average).}$$

TABLE 3

Length (inches)	$L/p$	Load at failure	
		Predicted	Test
1.00	6.25	1,780	1,740
1.50	9.40	1,610	1,620
2.00	12.50	1,550	1,570
3.00	18.75	1,508	1,400
4.00	25.00	1,494	1,480
6.00	37.50	1,482	1,470

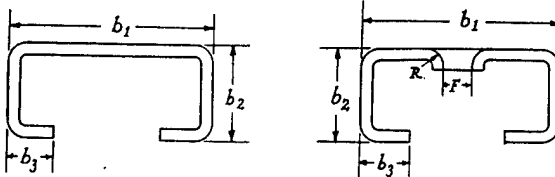
The "predicted" failing load was obtained from  $P_{back}=\sigma_{vp}bt=39500\times 0.75\times 0.032=950 \text{ lb.}$ , the actual width of back being less than the effective.

$$P_{leg}=\left[0.9\left(\frac{0.5}{L}\right)^2+0.385\right] 10,350,000 \times \frac{0.032^3}{0.5}=\left[\frac{0.225}{L^2}+0.385\right] 680$$

These channels were tested with flat ends and the failures were all of the "plate" type, local buckling of the back and legs, so they represented the crushing strength of the section. As is obvious the agreement between predicted and failing load is good although the "predicted" loads were figured from the over-all dimensions of the members. It would seem more rational to have used the center line dimensions as was done in the case of Miller's channels. The agreement with test results is still satisfactory if center line distances are used, the "predicted" loads all being reduced and the method becoming about 5 percent more conservative.

It is apparent from table 3 that the crushing strength of sections having free edges varies considerably with increasing length of section, the difference being about 15 percent in the above case for a range in  $L/p$  from 6.25 to 37.50.

The following data on the crushing strength of lipped channels are based on tests made by the General Aviation Corporation and studied by Walter H. Gale at M. I. T. The pertinent dimensions, based on figure 15, are given in the tables following.



(a)

(b)

Figure 15.

The agreement between predicted and test results is, in general, satisfactory for all specimens having lips 0.75 inch wide. It is fair for the specimens having 0.43-inch lips, being reasonably good for the thicker walled specimens, but not so good for those with thin walls. As the width of the lip decreases, the errors increase and the agreements are poor for the  $1\times 1\times 0.188$  specimens which have not only narrow lips but thin walls as well. It appears, as would be expected, that the less elastic support an edge has due to the thickness and shape of the adjacent material, the lower is the stress at which crushing occurs.

TABLE 4.—Figure 15a type

$b_1$	$b_2$	$b_3$	$t$	$L$	$\sigma_{cr}$	$P_1$	$P_2$	$P_3$	Total load	Crushing stress	
										Predicted	Test
3.23	1.5	0.75	0.0795	6	38,600	6,800	14,600	12,300	20,600	38,300	37,200
3.23	1.5	.75	.050	4	37,000	2,625	2,625	640	9,180	26,600	26,000
2.69	1.5	.75	.050	8	53,000	3,150	3,150	640	10,730	30,400	29,200
2.69	1.5	.75	.050	8	39,500	2,720	2,720	640	9,440	27,600	26,500
2.69	1.5	.75	.050	8	39,500	2,800	2,800	640	9,680	27,800	26,000
2.69	1.5	.75	.050	8	11,700	1,495	1,870	1,440	4,115	12,050	12,600
2.69	1.5	.75	.050	8	14,900	1,670	1,120	1,660	5,030	14,300	11,700
2.69	1.5	.75	.081	4	38,600	7,075	14,700	2,350	21,175	36,000	35,000
2.69	1.5	.75	.041	4	42,500	1,875	1,875	350	6,325	23,500	21,800
2.69	1.5	.75	.049	3	46,000	2,820	2,820	605	9,660	30,500	23,900
2.375	1.25	.406	.0513	6	36,000	2,740	1,200	1,750	8,840	33,300	26,400
2.375	1.25	.430	.0208	5	38,500	465	465	81	1,557	13,550	10,870
2.375	1.25	.4375	.0529	6	37,400	3,235	2,475	865	9,915	36,800	27,100
2.375	1.313	.4375	.0613	5	31,700	3,650	2,550	1,860	10,450	32,000	29,800
1.53	1.47	.375	.0625	5	37,000	3,540	1,400	870	12,000	42,000	37,400
1.375	1.0	.3125	.039	6	36,500	1,600	1,425	1,445	4,895	35,600	32,000
1.375	1.0	.3125	.025	6	40,000	875	675	200	2,425	28,200	19,600
1.0	1.0	.188	.0208	8	36,000	450	450	1,141	1,630	24,700	15,600
1.0	1.0	.188	.0241	4	36,000	607	607	1,183	2,150	28,000	21,500
1.0	1.0	.188	.0153	6	36,000	245	245	73	880	17,800	14,600

<sup>1</sup> Load on area indicated is  $\sigma_{cr} \times b \times t$ .

Assuming this to be a fact and considering the U and  $\square$  sections tested by the Ford Motor Co., the data for which are given on pages 22 and 23 of A. C. I. C. No. 685, "An Investigation of Available Information on the Strength Properties of Reinforced Skin Construction," it is possible to develop curves showing the effect on the critical stress of this variation in elastic support. Figure 16, for instance, presents curves obtained empirically, which show the variation in the critical stress for different ratios of width to thickness of the back of the channel. They are in the nature of form factor curves applying to the particular shapes and sizes covered by Ford's U and  $\square$  sections. One interesting thing which they show is that the variation in the form factor for each type is roughly linear so that each could have been established from tests on two or three sections and the strengths of channels of intermediate gages or dimensions could have been predicted with sufficient accuracy for preliminary estimates and design without the need for

an elaborate series of tests. Where adequate data are available, more accurate results become possible. While the development of such curves for each shape of stiffener proposed is admittedly a task, it is not a difficult one and it is believed that enough can be learned by comparing the curves for several typical stiffeners to show which features are advantageous and which deleterious.

It would appear from figure 16 that it is an advantage to turn the flanges of channels outward instead of inward since the critical stress will not drop off so rapidly with increasing ratios of back width to thickness, nor will it drop so low in the range of normal sizes of section. Applying the coefficients of figure 16 to the sections, Ford R and U series of sections, the dimensions for which are indicated in figure 17, gives the predicted load values shown in table 5 which, when compared with the test loads, are seen to be in reasonable accord. All are based on  $E=10,000,000$   $\sigma_{cr}=40,000$  lb./in.<sup>2</sup>

TABLE 5

Section	$b_1$	$b_2$	$b_3$	$b_4$	$t$	$P_1$	$P_2$	$P_3$	$P_4$	Crushing load	
										Predicted	Test
U	1	1	1	1	-----	0.020	320	320	106	1,172	1,215
U	1	1	1	1	-----	.028	754	754	208	2,678	2,820
U	1	1	1	1	-----	.035	All elements work to $\sigma_{cr}=40,000$ lb./in. <sup>2</sup>	568	568	1,860	1,680
U	2	2	2	2	-----	.035	All elements work to $\sigma_{cr}=14,000$ , test stress=13,500.	568	568	-----	-----
U	2	2	2	2	-----	.049	All elements work to $\sigma_{cr}=20,000$ , test stress=20,000.	60	60	-----	-----
U	2	2	2	2	-----	.065	All elements work to $\sigma_{cr}=28,000$ , test stress=28,000.	-----	-----	-----	-----
U	2	2	2	2	-----	.083	All elements work to $\sigma_{cr}=40,000$ lb./in. <sup>2</sup>	-----	-----	-----	-----
U	2	2	2	2	-----	.095	All elements work to $\sigma_{cr}=40,000$ lb./in. <sup>2</sup>	1,410	1,155	3,912	3,670
U	2	2	2	2	-----	.065	3,040	2,260	255	8,070	7,450
U	2	2	2	2	-----	.083	5,960	4,130	450	15,120	14,300
U	2	2	2	2	-----	.095	All elements work to $\sigma_{cr}=34,000$ , test stress=33,500.	-----	-----	-----	-----
R	1	2	2	2	-----	.020	360	360	100	2,000	1,980
R	1	2	2	2	-----	.035	1,080	1,175	700	5,230	5,350
R	2	2	2	2	-----	.035	1,120	1,120	525	4,690	4,600
R	2	2	2	2	-----	.049	2,185	2,185	885	8,785	8,800
R	2	2	2	2	-----	.065	All elements work to $\sigma_{cr}=32,000$ , test stress=32,500.	-----	-----	-----	-----
R	2	2	2	2	-----	.049	1,000	2,000	1,030	8,580	8,650
R	2	2	2	2	-----	.065	3,810	3,520	1,590	14,830	14,550
R	2	2	2	2	-----	.0208	320	320	70	1,100	1,030
U	1	1	1	1	-----	.0241	510	510	115	1,750	1,640
U	1	1	1	1	-----	.0153	160	160	45	570	720

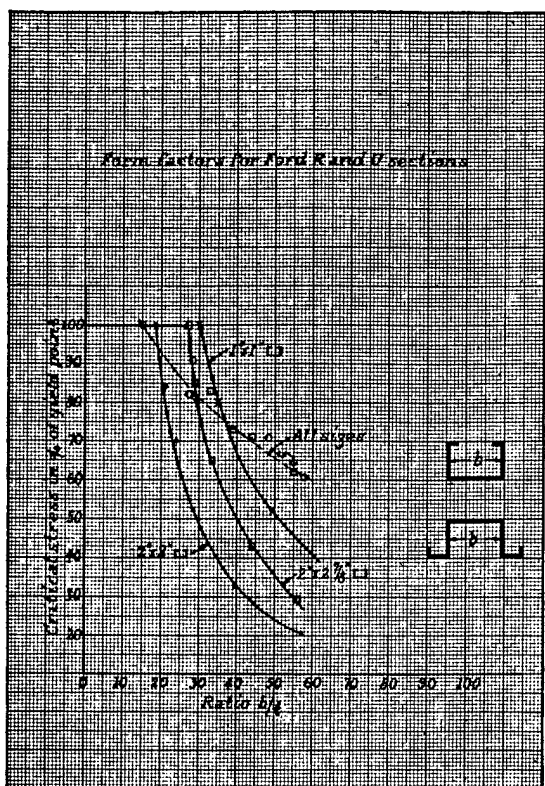


FIGURE 16.

The agreement between predicted and test loads in table 5 is excellent as might be expected because the form factor curves were developed to fit the above tests. However, the data do show what can be done with the proposed method of predicting crushing stresses when a few tests on short lengths of specimens of the desired shape are available.

Returning to a consideration of the channels having flanged lightening holes, figure 15b, and treating them as having no form factor because of their properties, the following results are obtained:

The net area of the back is assumed to carry a stress equal to the yield point of the material because the widths between the flanged hole and the outstanding legs are less than the "effective" widths for the thickness of material used. This appears to be a reasonable approximation and is the equivalent, so far as crushing goes, of assuming a flanged slot running the length of

the channel instead of a series of flanged holes; hence, we conclude that the area between lightening holes carries little compression, but serves primarily to make the two sides of the section act as a unit. The outstanding legs are treated as flat plates with simply-supported edges and the lips as having one supported edge, one free. See figure 15.

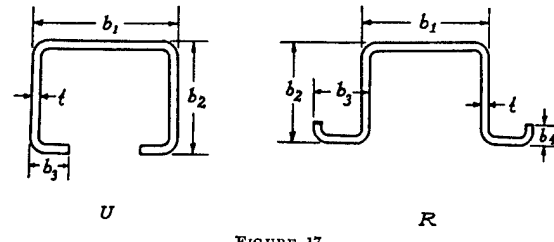


FIGURE 17.

The proposed method of analysis has been applied to sections having shapes as shown in figure 18 with errors of 10 percent or less. The stiffener shown at A was analyzed as three flat plates having simply supported edges plus two plates having one edge simply supported, one free. Due to the flanged edges on stiffener B, it was treated as five plates having simply supported edges while C, for the same reason, was treated as three. There are not enough data to permit the determination of the length of flange required to provide the equivalent of a simply supported edge, but it would appear to be small.

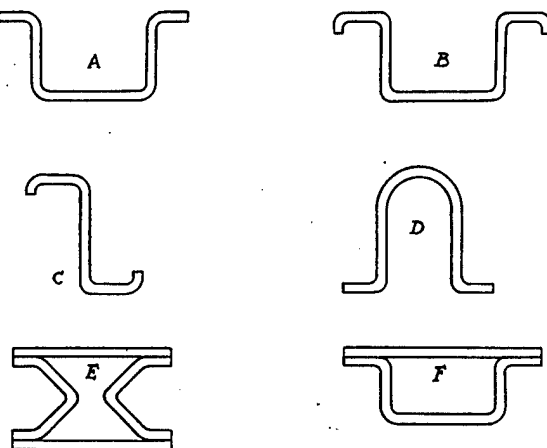


FIGURE 18.

TABLE 6

$b_1$	$b_2$	$b_3$	$F$	$t$	$\sigma_{yp}$	$P_1$	$P_2$	$P_3$	Total load	Crushing stress	
										Predicted	Test
3.23	1.5	0.75	2.5	0.080	38,600	2,240	4,600	2,300	16,040	38,600	{ 45,000
3.23	1.5	.75	2.5	.0465	37,000	1,720	2,625	640	8,200	21,400	{ 44,000
2.69	1.5	.75	1.31	.0408	42,500	1,875	1,875	350	6,325	28,400	{ 32,700
2.69	1.5	.75	1.31	.080	38,600	4,950	4,625	2,320	18,840	38,400	{ 29,600
											{ 27,300
											{ 40,600
											{ 35,000

The agreement between predicted and test results is good with the exception of the first specimen for which the yield point stress given in the test data is undoubtedly in error.

Stiffeners of type D were analyzed on the basis of being a half tube plus two angles but the results were unsatisfactory. They were then regarded as a curved element which would carry a stress equal to the yield point of the material for normal ratios of diameter to thickness, two flat sheets having simply supported edges and two having one edge simply supported, one free. It may not appear reasonable to assume the edge of tangency between curve and flat as the equivalent of simple support, but the agreement between predicted crushing stress and test data was good, a representative case studied by Sousa and Greenwood in their thesis, M. I. T., 1934, having shown an error of 6 percent.

Aluminum alloy stiffeners similar to A were attached to sheet as shown by F in figure 18, and tested by the Boeing Aircraft Co. For sections having the dimensions shown in figure 19, table 7 gives a comparison between predicted and test loads. In obtaining the "predicted" values, the outstanding leg of the stiffener was treated as a sheet having one edge simply supported, one free, even though it was attached to the skin because the rivet pitch used, from 1 to 1.5 inches, appears to have been sufficient to permit buckling of that edge between rivets. The skin was treated as a simply supported sheet and, due to its being attached by two rows of rivets, was assumed to carry a stress equal to  $\sigma_{cr}$  for the section if its width were less than the effective width. Since the test report gave no values for  $E$  or the yield point,  $E$  was assumed to be 10,000,000 and the yield point was taken as 36,000. The latter value was modified by a form factor of 75 percent and  $\sigma_{cr}$  taken at 27,000. This gave good results in three cases: Fair in one and poor in one, the unfavorable results occurring with the thin-walled sections, or with those having a high  $b/t$ . A greater reduction in  $\sigma_{cr}$  should apparently have been made in both cases to provide for the low edge supporting effect of the elements of these sections.

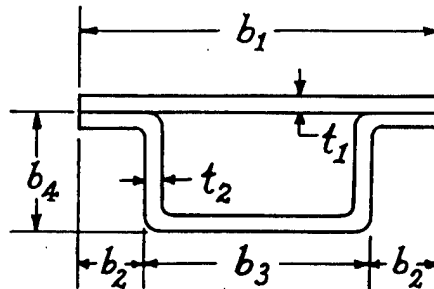


FIGURE 19.

Stainless steel stiffeners of type E were treated as a series of flat plate elements but with a greatly reduced

TABLE 7.

$b_1$	$b_2$	$b_3$	$b_4$	$t_1$	$t_2$	Crushing loads	
						Predicted	Tests
1 $\frac{1}{16}$	3 $\frac{1}{16}$	3 $\frac{1}{16}$	3 $\frac{1}{16}$	0.020	0.025	1,580	1,730
1 $\frac{1}{8}$	3 $\frac{1}{16}$	3 $\frac{1}{16}$	3 $\frac{1}{16}$	.020	.020	1,380	1,075
1 $\frac{1}{8}$	1 $\frac{1}{16}$	2 $\frac{1}{16}$	2 $\frac{1}{16}$	.020	.025	1,720	1,700, 1,727
1 $\frac{1}{8}$	1 $\frac{1}{16}$	2 $\frac{1}{16}$	2 $\frac{1}{16}$	.025	.020	1,940	1,860, 1,830
1 $\frac{1}{16}$	1 $\frac{1}{16}$	3 $\frac{1}{16}$	3 $\frac{1}{16}$	.025	.020	2,375	1,690, 1,740

value of  $E$ , 16,000,000 having been found to give good results for the cases tried. This was, of course, the equivalent of using a form factor to provide for the elastic conditions at the edges and in the grooves, but too few specimens were available to permit constructing a set of curves similar to those of figure 16. However, representative results show predicted loads of 13,000, 12,450, 15,100, and 14,000 compared with crushing loads of 12,485, 12,080, 14,320, and 14,010 pounds, respectively, obtained from tests.

Data obtained from one manufacturer on square 17ST tubes having  $E=10,000,000$   $\sigma_{vp}=46,000$  lb./in.<sup>2</sup> follow. The tubes were analyzed as four simply supported flat plates.

TABLE 8

$t$	Width of side, $b$	Test, <sup>1</sup> $P$		Predicted, $P$
		Inches	Test, <sup>1</sup> $P$	
0.040	4		8,000	7,400
.040	3		7,750	7,400
.041	2		7,600	7,780
.040	1		7,300	7,360

<sup>1</sup> Each value is the average of 3 tests.

$$b_e = 1.7 \sqrt{\frac{E}{\sigma_{vp}}} \quad t = 25.5t = 1.02'' \text{ for } t = 0.040, 1.045'' \text{ for } t = 0.041.$$

$$P \text{ for each side} = 1.7\sqrt{E\sigma_{vp}} \quad t^2 = 1,850 \text{ for } t = 0.040, 1935 \text{ for } t = 0.041$$

Since the one-inch sides are less than the effective width,  $P = 1 \times t^2 \times 46,000$  or 1,840 pounds for each, giving the predicted  $P$  for the one-inch square tube as 7,360.

Similar tests made at M. I. T. on small square tube,  $\frac{1}{16}$ - $\frac{1}{8}$ - $\frac{1}{4}$ - $\frac{1}{2}$ -inch sides, gave higher crushing stresses in most cases where the width of side,  $b$ , was less than  $b_e$ , than the yield point and in some cases higher than the tensile strength of the material as determined from strips cut from the sides of the tube. For such sections it would appear conservative to compute the crushing stress as the product of the area times the yield point of the material in the sides. It is believed that the work done on the material in forming the corners of the tubes increases its strength properties considerably so that the corners actually withstand crushing stresses equivalent to the tensile strength of the flat faces. Tests made by Boeing and recorded in reports of tests Nos. 14575 and 13889 show similar effects on tubes whose sides were less than  $b_e$  in width.

For the wider tubes, in terms of  $b/t$ , we have from the M. I. T. tests on 17ST tubes having  $E=10^7$  lb./in.<sup>2</sup>

TABLE 9

Width of tube, $b$	Wall thickness, $t$	$L/\rho$	$b_e = \sqrt{\frac{E}{\sigma_{vp}}} t$	Load per side $1.7 t^2 \sqrt{E\sigma_{vp}}$	Predicted <sup>1</sup> crushing stress	Test crushing stress
0.9375	0.031	21.7	0.79	1,075	35,000	42,250
.8125	.016	18.6	.40	288	22,000	22,200
.6875	.016	21.8	.40	288	25,300	24,000
.5625	.016	17.9	.40	288	32,000	32,200

<sup>1</sup>  $\sigma_{vp}$  based on averaged value obtained from tests of strips from sides of tubes = 44,000 lb./in.<sup>2</sup>

For rectangular tubes of 24SRT aluminum alloy Boeing test report 14575 gives, with  $E = 10.5 \times 10^6$  lb./in.<sup>2</sup>

TABLE 10

Outside dimensions of tube	Wall thickness, $t$	$b_s$	Load on wide sides, each	Load on narrow sides	Based on yield point	Crushing load	
						Predicted	Test
$2\frac{3}{4} \times 1\frac{1}{4} \times \frac{1}{8}$	0.0495	22.5 $t$	3,300	2,260	60,000	11,120	11,800
$2\frac{1}{4} \times 1\frac{1}{4} \times \frac{3}{32}$	.098	21.6 $t$	13,300	13,000	65,000	52,600	53,100

<sup>1</sup>  $\sigma_{vp}$ , based on tests of strips from sides of similar tubes varying between 60,000 and 66,500 lb./in.<sup>2</sup>.

For "barrel" sections of 24SRT, the same Boeing report gives—

TABLE 11

Outside dimensions	Wall thickness	$b_s$	Load on flat sides	Load on curved sides	Y. P.	Crushing load	
						Predicted	Test
$2\frac{3}{4} \times 2\frac{3}{4} \times \frac{1}{2}$	0.050	21.7 $t$	3,490	4,815	64,300	16,610	21,400
$2\frac{1}{4} \times 1\frac{1}{4} \times \frac{1}{2}$	.0585	21.6 $t$	4,800	6,750	65,000	23,100	25,500
$2\frac{1}{4} \times 1\frac{1}{4} \times \frac{3}{16}$	.0565	23.1 $t$	4,200	5,950	57,000	20,300	25,600
$2\frac{1}{4} \times 1\frac{1}{4} \times \frac{3}{8}$	.065	23.2 $t$	5,530	6,470	56,500	24,000	33,200

The loads on the flat sides of the barrel tubes were computed as though they were flat sheets,  $P = 1.7 t^2 \sqrt{E \sigma_{vp}}$ , and the load on the curved sides was taken as the area times the yield point, it having been assumed that the curvature was sufficient to cause the material to work to the yield point of the material. The predicted results are low by approximately 25 percent. However, if the entire tube area be multiplied by the yield point of the material, a good agreement is obtained between predicted and test values. Hence, it may be that by cambering opposite sides of a rectangular tube, the stability of the entire section is so altered that crushing does not occur until the average stress on the cross section reaches the yield point or it may again be that the strength of the corners exceeds that of the faces so that the average strength of the complete tube exceeds the value expected from the properties obtained on strips from the sides.

## SECTION 6. THE STABILITY OF OPEN SECTIONS

As the stress on a column approaches its ultimate strength the cross section usually undergoes distortions which may be local or may extend over the length of the member. Such distortion of the section causes a shift of the axis of resistance of the member from the axis of loading so moments are created by the eccentricity of the axial load and these moments cause the member to deflect with the result that a shear is developed on the affected sections whose magnitude is  $P \sin i$  where  $i$  represents the slope of the bent section,  $P$  the axial load on the column. Such shear stresses produce forces on the elements of an open section which may cause it to rotate as a whole or which may aggravate the bending of the deflected elements. Where a stiffener is fastened to a sheet these forces are normally insufficient to cause the combination of sheet and stiff-

ener to rotate about the center of twist of the stiffener but they may suffice to bend the elements of the stiffener itself and cause it to fail in a combination of bending and twisting.

Figure 20 shows representative shapes of stiffeners and the direction of the shear forces acting on their elements when the axial load is applied eccentrically.

A study of figure 20 shows why sections such as channels sometimes fail by the legs bowing inward or outward if they do not fail by twisting as a whole. When bending subjects one leg to compression; the other to tension, the section tends to twist as a whole as shown at (a). When the eccentricity is along the other axis the tendency is to fail by bending the outstanding portions inward or outward due to the shear forces, as shown in (b) to (f), the direction depending on whether the point of loading is one side or the other of the centroid and on whether such flanges as may be used, bend inward or outward. Sketches (e) and (f) do not present a true picture of the shear forces acting since they are unsymmetrical sections. They would tend to deflect about both of the axes shown due to a moment in the plane of either, the axes not being principal axes for these sections.

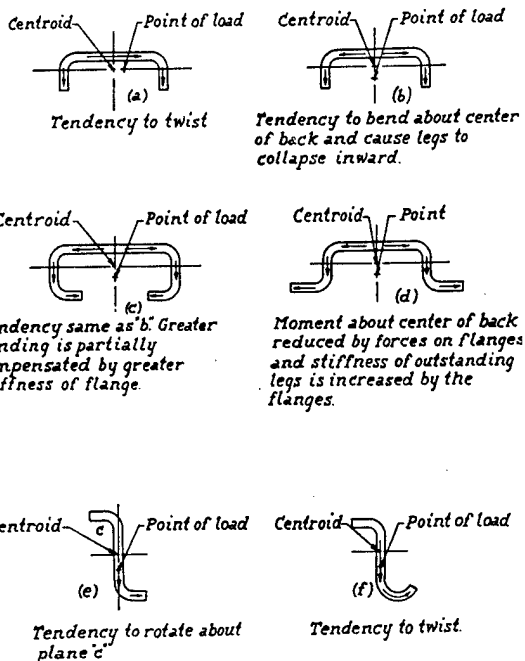


FIGURE 20.

It is seen, therefore, that open section stiffeners may fail due to secondary moments and shears induced in them by eccentricity of the loading or by bending of the stiffener and the material to which it is attached. Due to the fact that the least radius of gyration occurs about one of the principal axes rather than the axis parallel to the sheet some stiffeners tend to fail as columns by buckling about a principal axis. The skin reduces this tendency so the effective  $L/p$  is greater than the minimum, but the exact effect has not been evaluated. It should also be noted that tests of certain sheet-stiffener combinations made on flat panels will

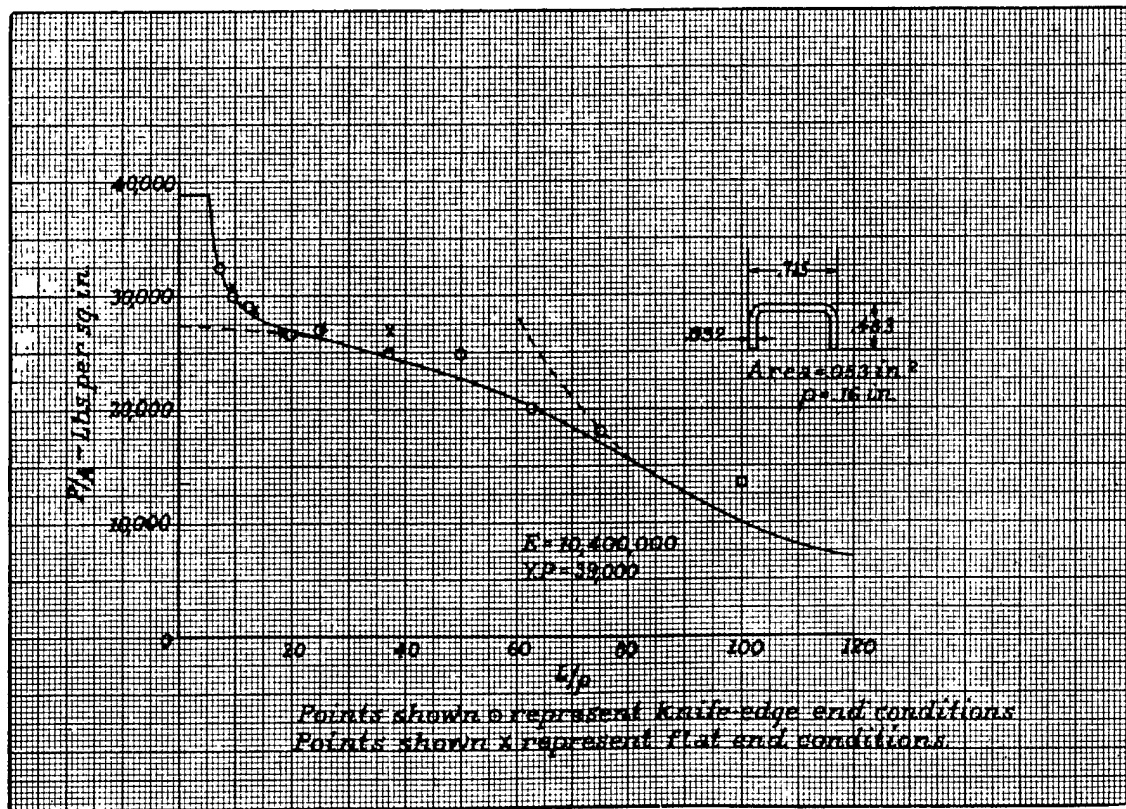
not indicate the true strength of such combinations in a wing or fuselage where bending of the structure produces a curvature in the panel which with unsymmetrical sections causes them to rotate and produce secondary bending and torsional effects, causing them to fail at stresses which may be materially below those obtained on the flat panel. In developing shapes of stiffeners this feature should be considered since it is impossible to predict the magnitudes of the secondary shears and moments developed by such accidental but unavoidable eccentricities; hence it is impossible to determine the stresses produced in the stiffener by them. Effort should be made to avoid unstable shapes where possible.

#### SECTION 7. COLUMN STRENGTH (STIFFENERS)

The foregoing procedure for computing crushing stresses, while not conclusive because of the limited test data against which to check it, gives a close enough approximation to the crushing strength for channels, square and rectangular tubes to warrant further consideration, especially since it has been found that for many shapes a good approximation to the column strength can be obtained by use of the Johnson-Euler curves, the yield point as normally used in the Johnson formula being replaced by the crushing stress for the section. When making such use of the column formulas it is necessary to select a reasonable value for the fixity coefficient to provide for knife-edge or pin-end conditions, "flat" ends, and similar conditions.

Figure 21 shows the results of a series of tests on channels of the same size as those considered in table 3. The points indicated by circles represent tests made between knife edges to insure a fixity coefficient of 1.0. The data from table 3 have been added as crosses and it is apparent that for the very short lengths there is no difference between the channels having "flat" ends and those having pinned-end conditions. The difference begins to show up at an  $L/\rho$  of 25 or 30. At an  $L/\rho$  of 20 or thereabout the failing stress is so near the crushing stress for the section that a Johnson parabola of the form  $\sigma_c = \sigma_{cr} - \frac{(\sigma_{cr})^2(L/\rho)^2}{4c\pi^2 E}$ , where  $\sigma_c$  is the stress the member will carry as a column and  $\sigma_{cr}$  its crushing stress, is in very good accord with the test data. The members of high  $L/\rho$  lie near the Euler curve as would be expected. Figures 22, 23, 24, 25, will facilitate the use of these formulas.

It is believed, therefore, that a reasonable approximation to the strength of open section or other shapes of stiffeners may be obtained by determining the crushing strength of a section whose  $L/\rho$  is about 20 by test or by the analytical method suggested above, and by using this crushing stress in the Johnson column formula for obtaining the allowable stress for other slenderness ratios. It is further believed that the stress so computed represents the critical conditions for stiffeners attached to sheet and that the condition of torsion and buckling contemplated by Wagner and Pretschner in N. A. C. A. Technical Memo 784 need



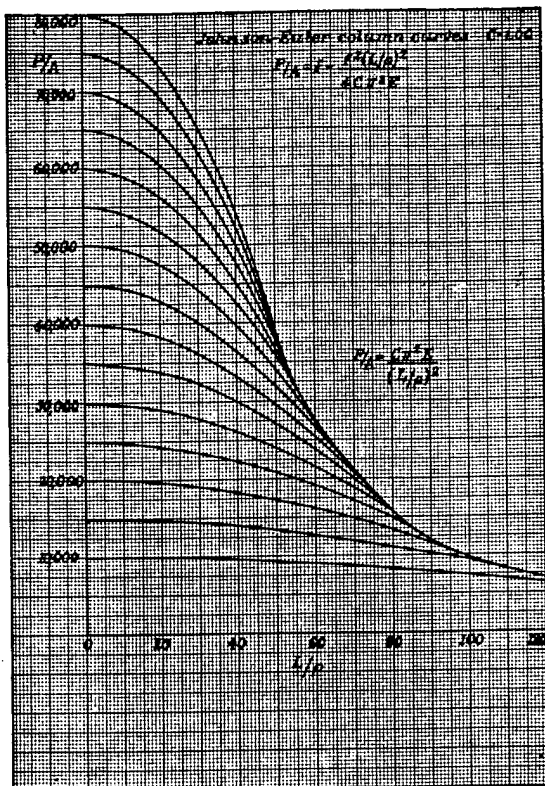


FIGURE 22.

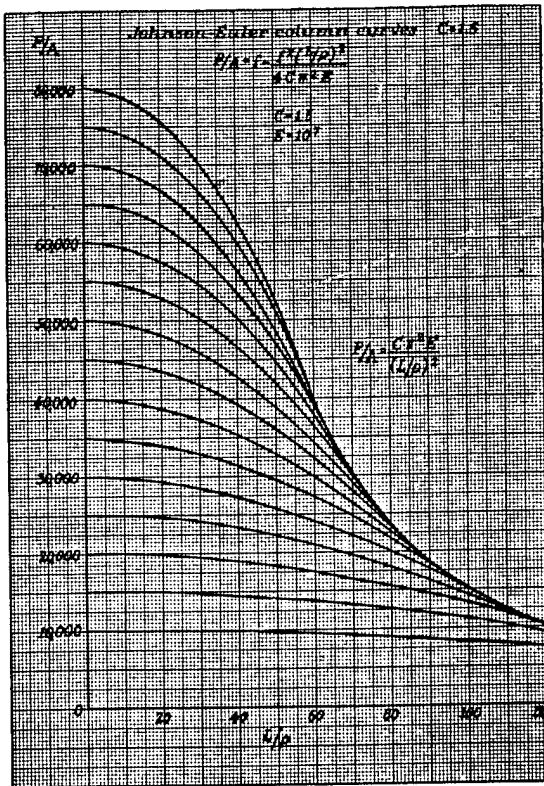


FIGURE 23.

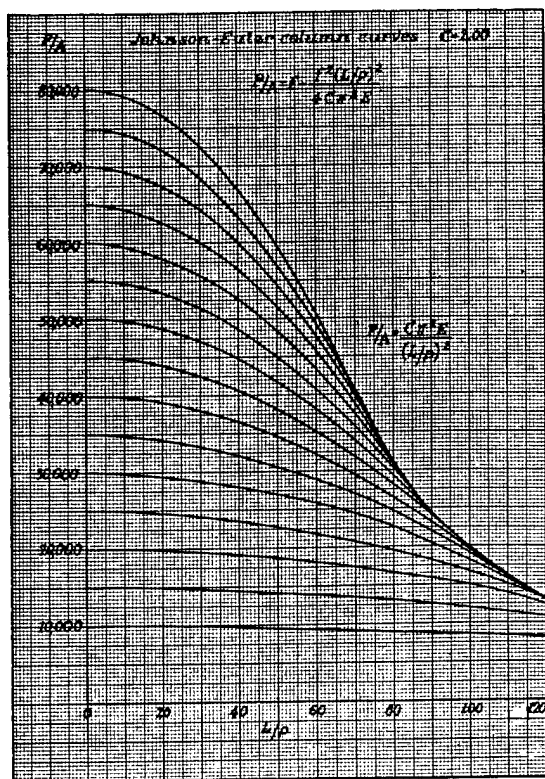


FIGURE 24.

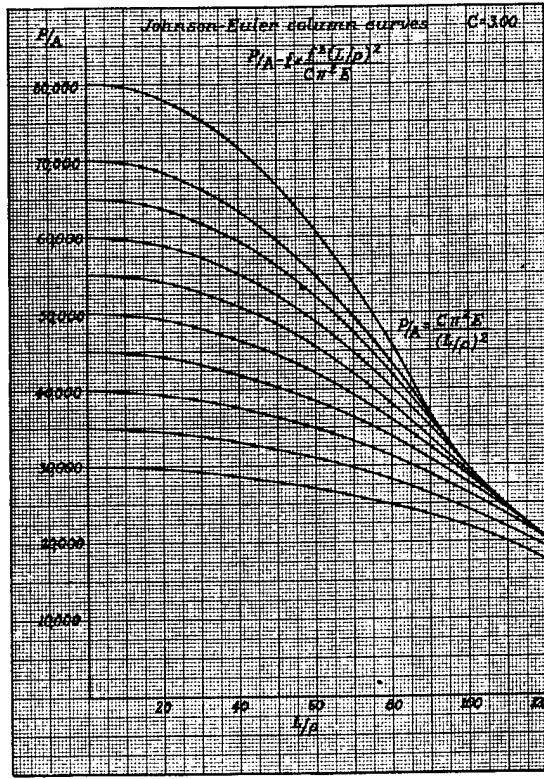


FIGURE 25.

not be considered with normal stiffeners normally attached.

To verify the procedure proposed for determining column strengths from crushing stresses the following tables are offered:

Considering square tubes first, taking those from Boeing test report 13889, whose walls are so thick in comparison to their widths that the crushing stress is equal to the yield point of the material.

TABLE 12

Tube size	Material	Crush- ing stress	$L/\rho$	C	Failing column stress	
					Predicted	Test
$2\frac{1}{16} \times 2\frac{3}{16} \times 0.094$	H. T. steel.	151,000	53.6	1	94,000	84,000
$2\frac{1}{16} \times 2\frac{3}{16} \times 0.097$	do	160,000	39.1	1	128,000	117,000
$2\frac{1}{16} \times 2\frac{3}{16} \times 0.140$	do	181,000	37.0	1	141,000	140,000
$2\frac{1}{16} \times 2\frac{3}{16} \times 0.142$	do	182,000	54.7	1	97,500	113,000
$2\frac{1}{16} \times 2\frac{1}{16} \times 0.240$	17SRT	75,500	54.5	1	33,000	32,000
$2\frac{1}{16} \times 2\frac{1}{16} \times 0.240$	17SRT	75,500	25.0	1	66,000	63,000

Taking the 24SRT rectangular and "barrel" sections of Boeing report No. 14575 whose crushing strengths were considered in tables 10, 11, we obtain:

TABLE 13

Tube size	Shape	Crush- ing stress	$L/\rho$	C	Failing column stress	
					Predicted	Test
$2\frac{1}{16} \times 1\frac{1}{16} \times 0.0495$	Rectangular	140,500	24.7	1	37,000	39,200
$2\frac{1}{16} \times 1\frac{1}{16} \times 0.0495$	do	142,300	31.5	1	37,500	35,800
$2\frac{1}{16} \times 1\frac{1}{16} \times 0.0495$	do	141,300	45.2	1	32,000	29,900
$2\frac{1}{16} \times 2\frac{1}{16} \times 0.098$	do	162,600	20.6	1	58,000	65,600
$2\frac{1}{16} \times 2\frac{1}{16} \times 0.098$	do	162,600	33.3	1	51,500	53,400
$2\frac{1}{16} \times 2\frac{1}{16} \times 0.098$	do	162,600	46.0	1	42,000	42,300
$2\frac{1}{16} \times 2\frac{1}{16} \times 0.0585$	Barrel	62,400	20.4	1	58,000	63,300
$2\frac{1}{16} \times 1\frac{1}{16} \times 0.0585$	do	62,400	30.4	1	53,500	56,600
$2\frac{1}{16} \times 2\frac{1}{16} \times 0.0585$	do	62,400	40.5	1	46,250	48,900
$2\frac{1}{16} \times 2\frac{1}{16} \times 0.0585$	do	59,000	20.8	1	55,000	57,600
$2\frac{1}{16} \times 2\frac{1}{16} \times 0.0585$	do	59,000	29.0	1	51,000	52,300
$2\frac{1}{16} \times 2\frac{1}{16} \times 0.0585$	do	59,000	45.5	1	40,500	41,200

<sup>1</sup> Based on predicted loads from tables 10 and 11.

<sup>2</sup> Test value.

For the channel sections of A. C. I. C. 598 Miller recommended the substitution of the crushing stress for the yield point in the Johnson column formula as has been suggested above, since that gave the best agreement with test data.

Two other series of channels of 17ST alloy whose back width is recorded as  $b$ , leg width as  $s$ , and thickness as  $t$ , gave the results shown in table 15. No form factor was used with either series.

For the lipped channels as tested by General Aviation we have results as tabulated below:

For this series of tests the short and long members are in good agreement, but there are large discrepancies in the middle range. The data for yield points were not obtained for each specimen but were average values, hence may not have been correct for some of the specimens. The predicted crushing stress from which the column stress was determined was based on the full value of the yield point whereas, as has been noted above, a better approximation for some sections has

TABLE 14.—For channels of fig. 15a

$b_1$	$b_2$	$b_3$	$t$	$L/\rho$	Predicted crush- ing stress	Stress of ultime- tate load	
						Predicted	Test
3.23	1.5	.75	0.0795	6	38,300	38,100	{ 36,200
3.23	1.5	.75	.0795	10.25	38,300	37,900	39,100
3.23	1.5	.75	.0795	16	38,300	37,350	33,500
3.23	1.5	.75	.0795	25	38,300	36,000	34,100
3.23	1.5	.75	.080	34	38,600	34,300	31,200
3.23	1.5	.75	.0795	58	38,300	25,800	29,650
3.23	1.5	.75	.0795	82.3	38,300	13,100	29,850
							26,800
							25,750
							23,900
							13,700

been obtained by using a reduced yield point to provide for the elasticity of the edge supports. Had the crushing stress been based on a yield point modified by a suitable form factor, the agreement with column tests would have been improved.

TABLE 15

Length	$b$	$s$	$t$	$L/\rho$	Pre-dict- ed crush- ing stress	Stress at ultime- tate load	
						Predicted	Test
2.80	0.65	0.70	0.053	31,300	13.3	30,850	31,600
4.00	.70	.72	.052	29,600	17.9	28,900	30,800
6.30	.72	.73	.052	28,800	27.5	27,100	28,490
8.00	.70	.72	.052	29,610	35.8	26,750	27,530
10.62	.72	.75	.052	28,600	43.7	24,200	23,720
12.73	.70	.72	.052	29,610	57.0	21,950	21,730
14.62	.70	.72	.052	29,610	65.4	20,000	17,930
4.08	1.75	.84	.053	24,000	15.5	23,750	28,300
6.90	1.72	.88	.053	22,600	24.5	21,750	24,480
9.80	1.75	.93	.053	22,200	32.5	21,000	23,250
15.15	1.72	.97	.052	20,600	47.2	18,000	21,960
17.95	1.76	.92	.052	21,450	60.7	17,180	17,510
20.68	1.75	.91	.052	22,000	70.2	15,850	16,480
23.45	1.74	.92	.051	20,000	80.2	13,250	14,170

For the channels of figure 15b, we have:

TABLE 16

$b_1$	$b_2$	$b_3$	$F$	$t$	$L/\rho$	Pre-dict- ed crush- ing stress	Stress at maxi- mum load	
							Predicted	Test
3.23	1.5	.75	2.5	0.05	6	31,400	31,300	{ 32,700
3.23	1.5	.75	2.5	.05	10	31,400	31,140	29,600
3.23	1.5	.75	2.5	.05	16	31,400	30,760	30,400
3.23	1.5	.75	2.5	.05	25	31,400	29,840	28,500
3.23	1.5	.75	2.5	.05	34	31,400	28,520	27,300
								24,900

The above table shows a reasonable agreement between predicted and test results though the crushing stress for the section was based on the full yield point.

The stainless steel stiffeners, type E of figure 18, when checked for other values of  $L/\rho$  than those used for determining the crushing stress gave the following results as recorded in the thesis, "A Design Procedure

for Thin Stainless Steel Sheets in Compression," Stark and Seary, M. I. T. 1935.

TABLE 17

Length	Thickness of sheet	$L/\rho$	Maximum loads		Fixity coefficient
			Predicted	Test	
3.48	.019	15.6	13,000	12,485	1
4.49	.019	20.1	12,450	12,080	1
7.54	.021	33.5	10,450	10,240	1
10.70	.019	47.9	7,300	7,500	1
15.32	.021	68.1	4,750	4,630	1
19.97	.019	89.4	3,000	2,765	1
.97	.021	4.3	15,100	14,320	2
1.46	.021	6.5	14,900	13,800	2
6.00	.021	26.7	13,200	13,400	2
9.23	.019	41.3	11,150	10,860	2
13.81	.019	61.5	9,750	9,040	2
18.47	.019	82.6	6,900	8,480	2

The critical stress was taken as 145,500 lb./in.<sup>2</sup> in predicting the above loads. The first series was tested with pin ends giving a fixity coefficient of one and the second series with flat ends. The agreement between predicted and test loads is good with the fixity coefficient assumed to be two.

#### SECTION 8. NOTES ON STIFFENER DESIGN

From the foregoing discussion it appears that the crushing strength of a formed section may be predicted with fair accuracy by considering the stability of each of the elements of the section having due regard for the conditions of elastic support at the edges of each such element contributed by the adjacent sides and edges. In the present state of the art it seems desirable to use empirical coefficients in the way of "form factors" to account for the varying degrees of support obtained rather than deal with the complex equations provided by theory. In the future it may be possible to develop charts empirical or theoretical which will evaluate the contribution of various shapes of section to the stability of each edge so that critical crushing stresses may be predicted accurately. In any case, it seems desirable to use as sharp corners as possible without damaging the material and to keep the ratio of width to thickness of each element as low as possible so that it will stabilize adjacent elements and withstand high stresses before failure.

The latter condition, however, is opposed to the requirements established for sections which fail due to column action rather than crushing. For such sections it is desirable that the material be spread out so the radius of gyration is as great as possible. A compromise must therefore be effected between the requirements that both crushing stress and radius of gyration have their maximum values. For thin walled, or lightly loaded shapes this may require the use of grooves to stiffen wide, thin areas or lightening holes to reduce their weight. Where grooves are used it appears desirable to have them sharp cornered so that they will provide a stiff edge and cause the element in which they are made to work to a high stress intensity. Where lightening holes are used, it seems advisable to flange them and to have them of sufficiently small diameter that they do not cut out any of the effective width of

the material. Of the two methods for increasing strength or reducing weight, it is believed that the use of grooves with thin sheets is more satisfactory than the use of a heavier sheet and lightening holes. This item would provide a field for research, but does not appear to be of sufficient importance to demand immediate action.

The use of curved elements instead of all flat ones appears to stabilize some shapes of stiffeners and cause them to develop high crushing stresses. It is probable that they restrict the buckling of the flat sheet to one direction, that is, it must buckle so that its tendency is to reduce the radius of the contiguous curved sheet but not to increase it, hence cause it to develop higher stress intensities before failure.

Closed stiffener sections offer distinct advantages over open sections because of their increased stability at high loads or when they are bent due to the distortion of the sheet or structure to which they are attached. It is appreciated that such sections are liable to corrosion from the inside out and that they are difficult to attach, but from the standpoint of strength they are superior to the open section which, when once deflected, develops internal shear or compressive forces tending to twist it or to deflect it still further.

Designers should consider these effects in determining the allowable stresses to be used with such sections, since tests made on the stiffener alone may give appreciably lower strength properties due to the instability of the elements of the section than will be developed when the stiffener is attached to the structure, assuming, of course, that the method of attachment tends to stabilize the critical elements. On the other hand, stiffener sections which are unsymmetrical may be expected to fail at lower stresses in an actual structure than in a test. As normally used they are constrained by the material to which they are attached to bend in a plane which does not contain one of the principal axes of the section so they are forced to bend in a direction normal to that plane as well. Such stiffeners roll over readily and may not develop as high loads when deformed as part of a structure as when tested on a panel under a direct compressive load.

#### SECTION 9. STIFFENED FLAT PLATES IN COMPRESSION

##### EMPIRICAL METHODS

###### Approximate Method.

Mr. H. W. Gall, in 1930, found from tests of stiffened aluminum alloy panels that he could make a very good approximation to the load obtained in test by assuming the stiffeners acted to break the panel up into a series of simply supported sheets, each of which carried a load equal to that found by Schuman and Back in N. A. C. A. Report No. 356. By adding the load carried by the stiffeners to that carried by the sheets, assuming the two to act independently, a good agreement was obtained between predicted and test values.

For preliminary design a modification of Gall's original method which requires a minimum of computation will be found very useful in obtaining approximate sizes of members. To the load on a simply supported

sheet, found from  $P = Ct^2\sqrt{E\sigma_{cr}}$ , add the column load for the given length stiffener on the basis of  $C=1$  for pin-end condition,  $C=2$  for flat ends,  $\sigma_{cr}$  being the stress at which the stiffener would fail if tested as a simple column, that is, without the sheet. The sum of these two loads divided by the area of sheet and stiffener will give an average stress at maximum load for the combination which is in close accord with test data. The strength of the stiffener may be obtained by the analytical method described in articles 4 to 8 of this report or from a column test. The following example will serve to illustrate the procedure.

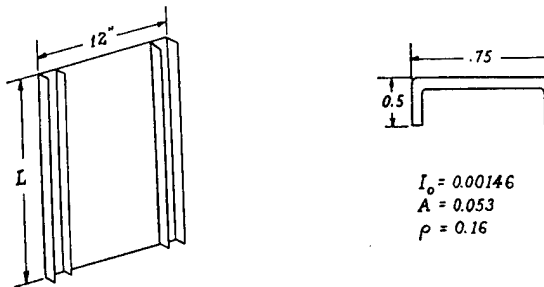


FIGURE 26.

Assuming  $L=6$  inches the load at failure for the above stiffeners is 1,482 pounds as predicted in table 3,  $\sigma_{cr} = 1,482/0.053 = 28,000$  lb./in.<sup>2</sup>. For an 0.019 sheet of 17ST,  $P = 1.7 \times 0.019^2 \sqrt{10^7 \times 28,000} = 325$  pounds, if the panel width is greater than  $b_e$ , as it is here. This panel would be predicted to carry  $2 \times 1,482 + 325 = 3,289$  pounds. A test on this size panel gave 3,300 pounds.

A third stiffener added to the above panel half way between the two shown would result in a predicted load of  $3 \times 1,482 + 2 \times 325 = 5,096$  pounds. When tested such a panel carried 5,300 pounds.

A similar panel, 18 inches long, having an 0.033-inch sheet and four stiffeners of the above type spaced equally across the sheet, carried 5,600 pounds. The crushing stress for a length of this stiffener having an  $L/\rho = 20$  is approximately 28,000 lb./sq. in.,  $\frac{1,500}{0.053} = 28,300$ , and by using this as the critical stress, we have for  $C=2$ ,  $L/\rho = \frac{18}{0.16} = 112.5$ , an allowable of 15,500 lb./sq. in., a load of  $15,500 \times 0.053$  or 820 pounds. At this stress intensity the sheet would carry a load,  $P = 1.7 \times 0.033^2 \sqrt{10^7 \times 15,500} = 730$  lb., so the panel would have been predicted as failing at  $4 \times 820 + 3 \times 730 = 5,470$  lb. instead of the 5,600 pounds shown by test.

This procedure has been checked against a number of tests with very satisfactory results. It is based on Gall's and Lundquist's procedures, Gall having been the pioneer and having assumed the sheet to carry a stress approximately equal to the yield point of the material, Lundquist having assumed the stiffener and effective sheet width to act as an independent column. Lundquist's method is described more completely below.

It appears from the foregoing that stiffeners should be proportioned to develop as high a stress as possible over the length for which they are to be used so that the sheets to which they are attached will also carry a high stress on their effective widths. When a stiffener fails at low stress intensities it may in effect be considered as

less than the equivalent of a simply supported edge for the sheet so the panel will carry less load than is expected of it.

Anything which improves the effectiveness of the "edges" of the sheets or increases the stress at which the sheet stops taking load, naturally improves the strength-to-weight ratio of a stiffened panel. Anything which weakens the edge support, such as insufficient rivets connecting sheet and stiffener, reduces the strength of the panel.

For joints in which all elements carry compressive stresses of the same, or approximately the same, magnitude failure is liable to occur by buckling of the outside elements between rivets. Tests indicate that when such buckling occurs the element which buckles behaves very nearly the same as a fixed-ended column so that Euler's formula may be written for the "effective" column lying between rivets  $L$  inches apart. The formula is

$$\frac{f = C\pi^2 E}{\left(\frac{L}{\rho}\right)}$$

in which  $C=4$  for fixed ends and  $\rho^2 = t^2/12$  for a sheet of thickness  $t$ . Making these substitutions and re-writing, the expression gives

$$L = 1.814t\sqrt{E/f}$$

This equation is identical with that developed by Mr. W. L. Howland in his paper "Effect of Rivet Spacing on Stiffened Thin Sheet in Compression" published in the October 1936 Journal of the Aeronautical Sciences. Since it depends upon Euler's formula it cannot be expected to hold when  $f$  exceeds one-half the yield point stress of the material in hand unless the modulus of elasticity of the material be reduced so that the value of  $f$  given by Euler's formula is the same as that given by Johnson's parabola, the straight-line or other standard formula for short columns.

Figure 27 represents the conditions when  $L$  is determined for various aluminum alloys on the basis of  $E = 10,000,000$  lb. per sq. in. for stress intensities below 20,000 lb. per sq. in. and where it is reduced to accord with the Johnson parabola for stresses between 20,000 and the yield point. In using the figure enter at the left with the desired compressive stress and proceed horizontally to the curve representing the yield point of the material in hand, thence vertically to the line representing the sheet thickness. A horizontal line from that point to the scale at the right gives the rivet pitch, the distance between the centers of adjacent rivet holes, required to prevent the sheet from buckling under the design compressive stress.

There are no known data to corroborate this figure when the design stress exceeds 20,000 lb. per sq. in., but it gives results in reasonable accord with past experience and current practice and is believed to be dependable. Mr. Howland's tests appear to check the curve for stresses of 20,000 lb. per sq. in. and various tests appear to agree with the results which it gives for stresses lower than that. Until further data are available to vindicate or disprove the basic relations used in drawing figure 27, it should be looked upon as giving reasonable results and used with discretion.

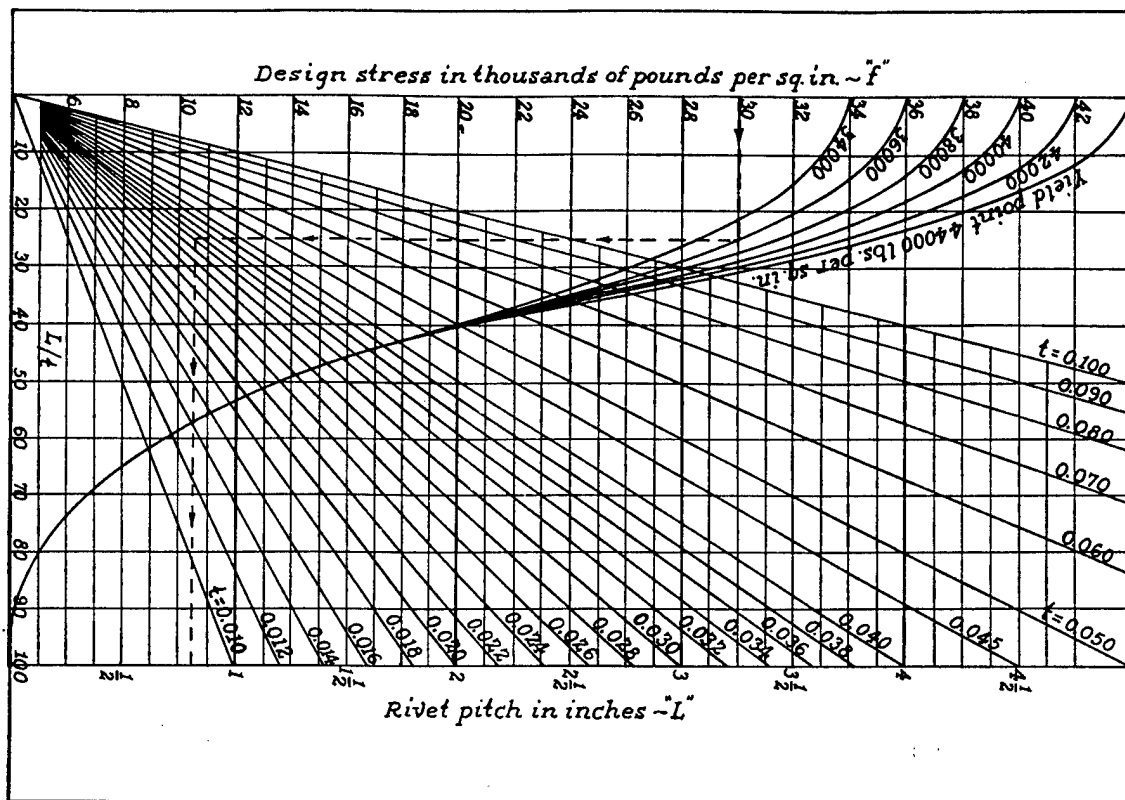


FIGURE 27.

Application of the foregoing approximate method to representative panels tested by Consolidated Aircraft Corporation and recorded in their report No. 27Z117 gives the following results based on an average yield point of 42,000,  $E=10,000,000$ . See table 18.

The load on the stiffeners which are of the type shown in figure 30 was determined analytically and the average stress on a short length used as the crushing stress which was then reduced for column effects. The stress computed for the given  $L/p$  of the stiffener was then employed in determining the effective width of sheet and the load it carried. Where the actual width was less than the computed effective width as in the case of the edge stiffeners, the actual width was of course the value used. It was assumed that each row of rivets developed the equivalent of a simply supported edge so that each stiffener would have, except for overlapping areas and discontinuities, two effective widths of sheet acting in conjunction with it.

The normal rivet pitch used on these specimens was three-fourths inch, but several had 1 inch and a few  $1\frac{1}{2}$  inches, staggered. Some reduction in panel load is to be seen as the pitch is increased, but the results are not sufficiently uniform to permit definite conclusions. The differences might be attributed to variations in thickness of material or in strength properties as well as to changes in rivet pitch. Since few of the specimens failed by buckling between rivets, the only conclusion which can be reached is that the stresses developed were not critical for the pitches used, so the sheets did not fail between rivets although their strength

was affected to some extent by the rivet pitch, possibly as a variation in the elastic support provided the effective widths of sheet.

TABLE 18

Specimen No.	Stiffener gage	Sheet gage	Edge sheet <sup>1</sup> and stiffener take	Intermediate sheet and stiffener take	Number of stiffeners	Load at failure	
						Predicted <sup>1</sup>	Test
240	0.0908	0.0745	16, 530	17, 560	3	51, 620	52, 700
202	0.0895	.075	16, 530	17, 560	3	51, 620	52, 095
241	.0904	.0735	16, 530	17, 560	3	51, 620	51, 090
242	.0707	.072	14, 420	15, 450	4	59, 740	58, 450
183	.0713	.0765	14, 420	15, 450	3	44, 290	47, 895
198	.0710	.072	14, 420	15, 450	3	44, 290	46, 025
243	.0702	.0745	14, 420	15, 450	3	44, 290	43, 755
304	.0888	.0615	14, 570	15, 450	3	44, 590	47, 850
204	.0780	.0620	14, 570	15, 450	3	44, 590	47, 630
205	.0875	.0625	14, 570	15, 450	3	44, 590	45, 780
246	.0705	.0635	12, 460	13, 340	4	51, 600	53, 980
247	.0712	.0652	12, 460	13, 340	3	38, 260	41, 170
301	.0712	.0651	12, 460	13, 340	3	38, 260	41, 720
184	.0647	.063	11, 700	12, 580	4	48, 560	52, 700
199	.0626	.0625	11, 700	12, 580	3	35, 980	38, 800
302	.0634	.0640	11, 700	12, 580	3	35, 980	35, 140
297	.0206	.0195	2, 006	2, 006	4	8, 024	7, 980
298	.199	.0197	2, 006	2, 006	3	6, 018	5, 860
299	.210	.0194	2, 006	2, 006	3	6, 018	6, 355

<sup>1</sup> Based on nominal gages of sheet and stiffener, 0.090, 0.072, 0.064, 0.050, etc.

#### Lundquist's Method.

In N. A. C. A. Technical Note No. 455, Mr. E. E. Lundquist proposes the determination of the load on stiffened sheet by the following procedure:

- Determine the intensity of stress at which the given length of stiffener will fail assuming it to act as a simple

column with C-1 for pin-end conditions, C-2 if the panel is tested with flat ends.

2. Reduce this stress 2 to 5 percent and compute the effective width of sheet which would carry this reduced stress if its edges were simply supported.

3. Assume this effective width to act with the stiffener as a column and determine the location of the centroid and the values of  $A$ ,  $I$ , and  $\rho$  about an axis through that centroid and parallel to the plane of the sheet. Since  $A$  will normally increase more rapidly than  $I$ , the  $\rho$  of the combination of sheet and stiffener is generally less than that of the stiffener alone.

4. Having the  $L/\rho$  of the combination of stiffener and its effective width of sheet determine the stress at which it will fail as a column, having due regard to the fixity coefficient. If this stress is in close agreement with that computed under 2, the load may be computed by multiplying the stress by the area of stiffener and effective sheet. If it is not in close accord, repeat 2, 3, and 4 until it is. Normally, two or three trials are required.

A formula for determining the variation of stress and reducing the number of trials has been developed by Mr. R. J. White at C. I. T. and is presented in appendix A of Mr. Sechler's thesis, "The Ultimate Compressive Strength of Thin Sheet Metal Panels," C. I. T. 1935. It is,

$$\frac{\sigma}{\sigma_o} = 1 + \left[ 1 + \frac{S^2}{\rho_o} \right] \frac{lt}{A_o}$$

$$(1 + \frac{lt}{A_o})^2$$

$\sigma$  = stress for stiffener and sheet.

$\sigma_o$  = stress for stiffener alone.

$S$  = distance from center of sheet to centroid of stiffener.

$\rho_o$  = radius of gyration of stiffener alone.

$l$  = effective width of sheet acting with stiffener.

$t$  = thickness of sheet.

$A_o$  = area of stiffener.

As has been indicated in the section on stiffeners, the addition of a sheet to some stiffener shapes will alter their crushing strengths materially, hence will modify the allowable stress for the combination column considered under the foregoing paragraph (4). When such an effect occurs allowance should be made for it, although because its effect is normally to increase the crushing strengths of the sections, it is generally conservative to disregard it.

Table 19 gives some comparative results obtained by applying Gall's original method and Lundquist's method to panels having stiffeners as shown in figure 26. As may be seen from the table both methods give satisfactory results for the thin sheet or for the shorter lengths of panels for the thicker sheet. While Gall's original method is definitely poor when applied to the longer panels of heavy sheet, Lundquist's method is seen to be in good agreement with tests. The approximate method described above yields results essentially the same as Lundquist's, although comparative data are not included in this table. The test data are from panels tested at M. I. T. as given in the Report on Aircraft Materials Testing for 1931-32. They were tested with flat ends, were 17ST, and had average values

of  $E=10,000,000$  and yield point = 36,000 lb./in.<sup>2</sup>. All were 12 inches wide.

As an illustration of Lundquist's method, let it be applied to the 12-inch panels having 0.032-inch sheet in table 19, the stiffeners being similar to those investigated in table 3 except that they are 0.035-inch thick instead of 0.032. For  $E=10,000,000$  and  $\sigma_{vp}=36,000$ , the effective width of an 0.035-sheet is 0.99 inch which exceeds the width of back of the channel. Hence, the back works to the yield point of the material and carries  $0.715 \times 0.035 \times 36,000 = 900$  pounds, while each leg carries  $0.385 \times 10^7 \times \frac{0.035^3}{0.484} = 342$  pounds. The predicted load for this channel is then  $900 + 2 \times 342 = 1,584$  pounds and the crushing stress  $1,584/0.0566 = 28,000$  lb./in.<sup>2</sup>. Substituting this in Johnson's formula, with  $L=12$  inch,  $L/\rho=12/0.16=75$ , and  $C=2$ , gives 22,300 lb./in. as the allowable stress for the stiffener.

TABLE 19

Sheet thickness	Length	Number of stiffeners	Predicted loads		Test loads	
			Gall's method A	Lundquist's method B	A	B
0.019-0.020	6	2	3,480	3,620	3,300	3,100
.019-.020	6	3	5,410	5,480	5,000	5,300
.019-.020	6	4	7,340	7,340	6,500	7,100
.019-.020	12	2	2,980	3,060	2,890	2,060
.019-.020	12	3	4,660	4,630	4,500	3,900
.019-.020	12	4	6,400	6,200	6,390	6,470
.019-.020	18	2	2,140	2,120	2,450	2,300
.019-.020	18	3	3,400	3,210	3,280	3,270
.019-.020	18	4	4,660	4,300	4,700	4,200
.032-.033	6	2	4,250	4,760	4,400	4,600
.032-.033	6	3	6,900	7,260	6,300	7,020
.032-.033	6	4	9,650	9,760	9,080	9,500
.032-.033	12	2	3,680	3,770	4,100	4,030
.032-.033	12	3	6,060	5,700	6,110	6,025
.032-.033	12	4	8,440	7,810	8,450	7,570
.032-.033	18	2	2,910	2,640	2,200	2,700
.032-.033	18	3	4,940	4,050	4,300	3,830
.032-.033	18	4	6,970	5,460	5,900	5,300
.051-.052	6	2	5,915	6,500	7,300	6,950
.051-.052	6	3	10,170	10,640	11,200	11,150
.051-.052	6	4	14,780	14,380	14,000	15,000
.051-.052	12	2	5,460	5,340	5,250	5,320
.051-.052	12	3	9,620	8,510	9,720	9,950
.051-.052	12	4	13,780	11,600	12,500	13,200
.051-.052	18	2	4,620	3,300	3,350	2,920
.051-.052	18	3	8,360	5,090	4,650	4,800
.051-.052	18	4	11,960	6,880	6,580	6,660

Assuming this reduced to 22,000 lb./sq. in. by the addition of the effective width of sheet, this effective width is found to be,

$b_e = 1.7 \times 0.032 \sqrt{\frac{10^7}{22 \times 10^3}} = 1.16$  inch. This width may work with the intermediate stiffeners so they become "effective" columns as shown in figure 28.

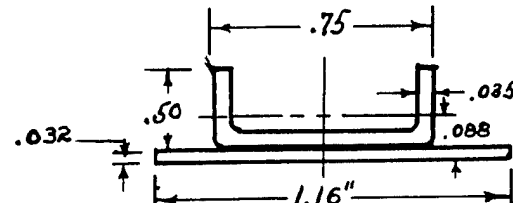


FIGURE 28.

$I=0.00211$ .  
 $A=0.0566+0.0372=0.0938 \text{ in.}^2$   
 $\rho=0.15$ .  
 $L/\rho=12/0.15=80$  and the allowable stress is  $21,500 \text{ lb./in.}^2$ . Then the effective width of sheet is  $1.7 \times 0.032$   
 $\sqrt{\frac{10^7}{21,500}}=1.17$  inch which is near enough the assumed width, so that  $\rho$  will not be changed, hence  $21,500 \text{ lb./in.}^2$  can be considered as the ultimate stress for the "effective" column. Its area is  $0.0566+1.17 \times 0.032=0.0941 \text{ inch}^2$  so it will carry 2,020 pounds.

Since one side of each edge stiffener is at the edge of the sheet, the entire 1.17 inches of effective width cannot be assumed to act with the edge stiffeners. Moreover, the edge of the plate is free to buckle away from the stiffener, so it will carry  $0.385 \times 10^7 \times \frac{0.032^3}{0.375}=336$  pounds or  $0.375 \times 0.032 \times 22,000=264$ , whichever is the smaller; the latter is, so we conclude that the 0.375-inch on one side of the rivet line and the  $\frac{1.16}{2}=0.58$  inch on the other carry the same stress as the channel. They form a column having  $\rho=0.152$ ,  $L/\rho=79$  and the allowable stress is  $21,600 \text{ lb./in.}^2$ . The edge stiffeners each carry  $21,600 [0.0566+[(0.375+0.58)0.32]]=1,885$  pounds.

The panel with the two stiffeners would then be assumed to take  $2 \times 1,885=3,770$  pounds, that with one intermediate and two edge stiffeners  $2 \times 1,885+2,020=5,790$  pounds, and that with four stiffeners,  $2 \times 1,885+2 \times 2,020=7,810$  pounds.

It will be noted that the foregoing, completely rational procedure is in reasonable accord with the test results, being some 8 to 10 percent on the safe side. At  $21,500 \text{ lb./in.}^2$  the stiffener is computed to carry about 1,220 pounds, whereas, tests of several such stiffeners show an average load of 1,300 pounds for a 12-inch length. Had this been used as the basis of allowable stress values for the effective columns, it would have indicated 23,000 instead of  $21,500 \text{ lb./in.}^2$  and improved the agreement between predicted and test results. As data accumulate it is believed satisfactory agreement can be obtained between predicted and test results for any normal sheet-stiffener combination, so that the number of test panels required with any new construction can be reduced, eventually, to one or two and possibly eliminated entirely.

A comparison of predicted and test results on panels made by the Northrop Corporation, as recorded in their report No. 146, gives for the extruded stiffener section shown in figure 29.

Area = 0.185,

$E=10,000,000$ ;  $y. p.=42,000$ .

Panel No.	Length	Predicted loads	Test loads
XS-12166	18	14,880	14,400, 14,000.
XS-12166-30	22.5	13,800	13,250, 13,200, 13,100.
268756	18	23,010	24,950, 26,200, 23,930.
268756-1	22.5	21,390	25,600, 23,540, 24,750.

Panels XS-12166 and XS-12166-30 were assumed to act as two stiffeners plus the effective area of 0.025 sheet expected to act at a stress of  $36,700 \text{ lb./in.}^2$  for the 18-inch specimens, 34,000 for the 22.5-inch specimens. The other two panels had three stiffeners each with its effective sheet area and, since the edges were supported, another effective width of sheet due to the support at the edges.

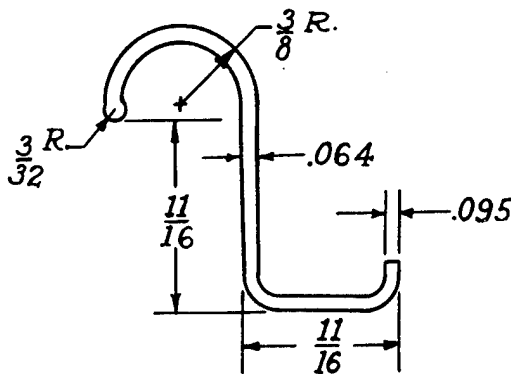


FIGURE 29.

A further application of Lundquist's procedure to the Consolidated Aircraft panels from table 18 will now be made. Both stiffeners and sheet were 24ST having  $E=10,000,000$  and an average yield point of  $42,000 \text{ lb./in.}^2$ . Due to variations in gage of sheet and stiffener the computations are based on nominal dimensions, 0.072 inches for the stiffener, 0.075 for the sheet. The actual specimens used in the comparison had somewhat thinner material and should have failed at loads below the predicted. They failed at somewhat higher loads, however.

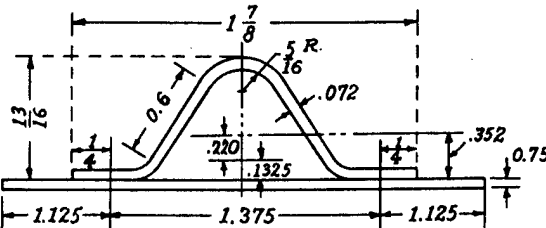


FIGURE 30.

Stiffener 3M005.

Area = 0.2105 sq. in.

$\rho=0.310 \text{ in.}$

On the basis of critical stress being equal to the yield point of the material, the effective width,  $b_e=1.7 \times t \sqrt{\frac{10^7}{42 \times 10^3}}=26.2$ . For the stiffener,  $b_e=26.2 \times 0.072=1.885$  which exceeds the width of any flat side, hence, the crushing stress for a short length section is equal to the yield point.

$\rho=0.310$  for the stiffener alone and for  $L=20''$ ,  $L/\rho=64.5$ .

Assuming  $C=2$ , the allowable stress at an  $L/\rho$  of 64.5 is  $32,500 \text{ lb./in.}^2$  by Johnson's formula.

For the effective width of sheet, assuming allowable stress on sheet and stiffener reduced to 32,000,  $b_e = 1.7 \times 0.075 \sqrt{\frac{10^7}{32 \times 10^3}} = 2.25$  inches. There should be 2.25 inches effective, 1.125 each side of each line of rivets, but there is only 1.375 between rivet lines so the total effective width of sheet  $1.375 + 2 (1.1250) = 3.625$  on intermediate stiffeners.

The c. g. of the center stiffener is:

$$\frac{0.2105 \times 0.352 - 3.625 \times 0.075 \times 0.0375}{0.2105 + 3.625 \times 0.075} \\ = \frac{0.064}{0.4825} = 0.1325$$

$$I = 0.0201 + 0.2105 \times 0.220^2 + 0.272 \times 0.17^2 = 0.0382.$$

$$A = 0.4825, \rho = \sqrt{\frac{0.0382}{0.4825}} = 0.282.$$

$$L/\rho = \frac{20}{0.282} = 71.0 \quad \sigma_{allow} = 30,500 \text{ lb./in.}^2$$

This is less than the stress assumed in computing  $b_e$  so the effective width of sheet must be revised. It is

$1.7 \times 0.075 \sqrt{\frac{10^7}{30 \times 10^3}} = 2.325$  instead of 2.25. This increases the total effective width to 3.70, but makes no appreciable change in  $\rho$  or  $\sigma_{allow}$ .

An intermediate stiffener will therefore carry 30,500  $(0.2105 + 3.70 \times 0.075) = 14,900$  pounds.

Since the sheet does not protrude beyond one edge of the edge stiffeners, the effective width for an edge stiffener on the basis of  $\sigma_{allow} = 30,500$  is  $0.25 + 1.375 + 1.16 = 2.79$  inches.

c. g. of edge stiffener is:

$$\frac{0.2105 \times 0.352 - 2.79 \times 0.075 \times 0.0375}{0.2105 + 2.79 \times 0.075} = \frac{0.0664}{0.4195} = 0.158 \\ I = 0.0201 + 0.2105 \times 0.194^2 + 0.209 \times 0.196^2 \\ = 0.03605$$

$$A = 0.4195, \rho = \sqrt{\frac{0.03605}{0.4195}} = 0.293.$$

$$L/\rho = 20/0.293 = 68.3, \sigma_{allow} = 31,100 \text{ lb./in.}^2$$

$b_e = 1.7 \times 0.075 \times \sqrt{\frac{10^7}{31.1 \times 10^3}} = 2.28$ . Total active width is, then  $0.25 + 1.375 + 1.14 = 2.77$  inches, which will not change  $\rho$  or  $\sigma_{allow}$ . Load per edge stiffener and sheet is then  $31,100(2.77 \times 0.075 + 0.2105) = 31,100 \times 0.4180 = 13,000$  pounds.

A specimen having two edge and one intermediate stiffeners should therefore take  $2 \times 13,000 + 14,900 = 40,900$  pounds. Consolidated specimen No. 243 took 43,755 pounds. A specimen having two edge and two intermediate stiffeners should take  $2 \times 13,000 + 2 \times 14,900 = 55,800$  pounds, whereas specimen No. 242 carried 58,450 pounds in test.

The agreement between predicted and test values in the above cases is good and indicates what can be done toward establishing a rational method for predicting strengths of panels composed of flat sheets and stiffeners. Combinations of corrugated and flat sheet may be treated in the same manner when subjected to compression parallel to the corrugations. With adequate rivets in the connection between the two, each line of rivets becomes the equivalent of a simply supported edge and permits an effective width of flat sheet to work

to the same stress as the corrugated. There is some evidence that the frequency of support provided by the corrugated sheet causes a width greater than  $b_e = 1.7t\sqrt{\frac{E}{\sigma_{cr}}}$  to function, in some cases the entire flat sheet seems to be effective, but the data available are inadequate to establish form factors or similar coefficients facilitate the evaluation of the elastic support afforded.

In all of the above applications the areas of sheet between the edges of the effective widths have been assumed to carry no load. It has been suggested that these areas might be considered to work at the stress intensity causing buckling, that is,  $\sigma = \frac{K\pi^2 E}{12(1-\mu^2)} \left(\frac{t}{b}\right)^2$  where  $K$  has the values for a simply supported sheet. Some test results justify this procedure, but the load is generally very small and, it is believed, is best neglected.

#### THEORETICAL METHODS

For a completely rational procedure, the designer is referred to Timoshenko's "Theory of Elastic Stability," article 70, page 371. Due to the complexity of the procedure it will not be presented here. Where the stiffeners are equally stiff and equally spaced, the method may be simplified by replacing the actual sheet and stiffeners with an orthotropic plate as is discussed by Timoshenko on page 380. The procedure is particularly well adapted to corrugated sheets and is discussed in this report under that heading.

#### SECTION 10. STIFFENED CURVED SHEETS IN COMPRESSION

##### EMPIRICAL METHODS

Curved sheets with stiffeners may be analyzed by methods similar to those described for flat sheet, it being assumed that the effective width of curved sheet acting with a stiffener is identical with that of a flat sheet. This assumption is reasonable since the tendency is for the flat sheet to bend near each stiffener when the load approaches the ultimate, whereas the less effective part of the sheet between stiffeners buckles under the load. Hence, by treating the effective width of curved sheet as though it were flat and computing the properties of the "effective" column on that basis, it is possible to obtain the load on the stiffeners and adjacent sheet by the Approximate method or by Lundquist's method.

When the radius of curvature is small the load carried by the areas of sheet between effective widths is appreciable and should be added to that taken by the stiffeners. The most satisfactory method for evaluating these loads is that developed by Sechler and described above in the section on compressive loads in curved plates. Sechler recommends the stress on the areas between effective widths be taken as  $\sigma = 0.3E \frac{t}{R}$  and that the load on these areas be added to that computed for the effective widths. Comparisons with test data show this procedure to be in good agreement with test data.

For preliminary determination of sizes, figures 11 and 12 are useful in obtaining the loads carried by the sheet on the assumption that it acts independently of the stiffener. In using these curves, it is assumed that the stiffeners suffice to give the equivalent of a simply supported edge at each point of connection to the sheet so the width to be used in determining the coefficients is the width between stiffeners. The curves were obtained on the basis of tests made on simply supported curved sheets of 17ST aluminum alloy and are in good agreement with the test data. However, due to the fact that the elastic support of a stiffener having high  $L/\rho$  is not the equivalent of a simply supported edge since the stiffener fails before the effective width of sheet reaches the yield point stress for the material, these curves indicate higher loads than can be carried on sheets braced by long or slender stiffeners. For thin sheets or sheets braced by stiff members, the agreement is good between loads predicted by adding stiffener strength to sheet strength and loads obtained by test. In any case the procedure being simple and easy to apply will be found helpful in determining approximate sizes for trial designs.

Since data are available on a series of curved panels of 17ST similar to the flat panels represented in table 19, they will be used to show the degree of approximation involved in the above methods.

Applying Lundquist's method first we have from page 23 the loads on 12-inch stiffeners and effective widths of sheet as 2,020 pounds on an intermediate stiffener, 1,885 pounds on each edge, the effective width of 0.032 sheet being 1.17 inches. For the panel having two stiffeners and a 30-inch radius of curvature, the width of panel between edges of "effective" widths would be  $12 - (2 \times \frac{1}{3} + 1.17) = 10.08$  inches and the allowable stress on that area,  $\sigma = 0.3 \times 10^7 \times \frac{0.032}{30} = 3,200 \text{ lb./in.}^2$ . The intermediate section would therefore carry a load of  $10.08 \times 0.032 \times 3,200 = 1,030$  pounds, so the total for two-edge stiffeners and this section should have been  $2 \times 1,885 + 1,030 = 4,800$  pounds, whereas the test panel carried 4,300. For a 10-inch radius we would expect the intermediate section to carry a stress of 9,600 lb./in.<sup>2</sup>, or a load of 3,090 pounds, while the edge stiffeners would carry the same 1,885 pounds each. The predicted load would be 6,860, but the panel carried only 5,420 pounds in test.

Considering similar panels with two edge and one intermediate stiffener the width of each intermediate

area of sheet would be  $\frac{12 - (2 \times \frac{1}{3} + 2 \times 1.17)}{2} = 4.46$  inches and the load on that with the 30-inch radius would be  $4.46 \times 0.032 \times 3,200 = 457$ , so the total predicted on the panel would be  $2 \times 1,885 + 2,020 + 2 \times 457 = 6,704$  pounds. The test panel carried 5,700 pounds. With the 10-inch radius the load on the intermediate areas would be 1,371 pounds each, so the panel should have taken  $2 \times 1,885 + 2,020 + 2 \times 1,371 = 8,532$ , whereas, the test panel failed at 7,400 pounds.

For the panels having two edge and two intermediate stiffeners, the agreement is considerably better, the predicted load for the 30-inch radius being 8,602 pounds, the test 8,800, while that predicted for the 10-inch radius is 10,186 and the test 11,100 pounds.

As is obvious the Lundquist-Sechler method is not in perfect accord with test results, although the errors involved in the above comparison are larger than normally occur. Since there is an improvement in the case where the stiffeners are close together, it is believed that part of the discrepancy between predicted and test results is due to the stiffeners not contributing elastic support to the sheet equivalent to simply supported edges.

Further studies should be made on this problem to develop a method in closer accord with test results. Pending such studies it is probably advisable to neglect the loads on the intermediate widths of sheet and assume that only the stiffener and its effective width of sheet carry load.

Table 20 gives a comparison between the approximate method and test results for the panels just investigated by the Lundquist-Sechler procedure. The stiffener is rated at 1,300 pounds on the basis of tests made on several 12-inch specimens and the sheet loads are based on that taken by a flat sheet of the same thickness times the coefficient  $K_1$  and  $K_2$  obtained from figures 11 and 12 to provide for the effect of width, length, and radius/thickness ratio.

It is to be noted that the errors involved in this approximate method are somewhat, but not much greater than those for the Lundquist-Sechler system. Neither method is completely satisfactory for design purposes, but they appear to be the best available at present. It is probable that the Lundquist-Sechler method may be used for stainless steel and other materials, but comparisons made between loads predicted by the approximate method and those obtained in test indicate too large discrepancies to permit its application to the design of members other than aluminum alloy.

TABLE 20

Number of stiffeners	Load on stiffeners	Skin thickness	Radius of curvature (inches)	Load on flat sheet	Width between rivet rows	$K_1$	$K_2$	Load on curved sheet	Loads at failure	
									Predicted	Test
2	2,600	0.0335	30	1,190	11.25	2.310	0.830	2,310	4,910	4,300
3	3,900	.0320	30	1,080	5.63	1.610	.836	2,905	6,805	5,700
4	5,200	.0320	30	1,080	3.75	1.350	.836	3,660	8,860	8,800
2	2,600	.0335	10	1,190	11.25	4.650	.870	4,815	7,415	5,420
3	3,900	.0320	10	1,080	5.63	2.675	.869	5,020	8,920	7,400
4	5,200	.0320	10	1,080	3.75	1.975	.869	5,560	10,760	11,100

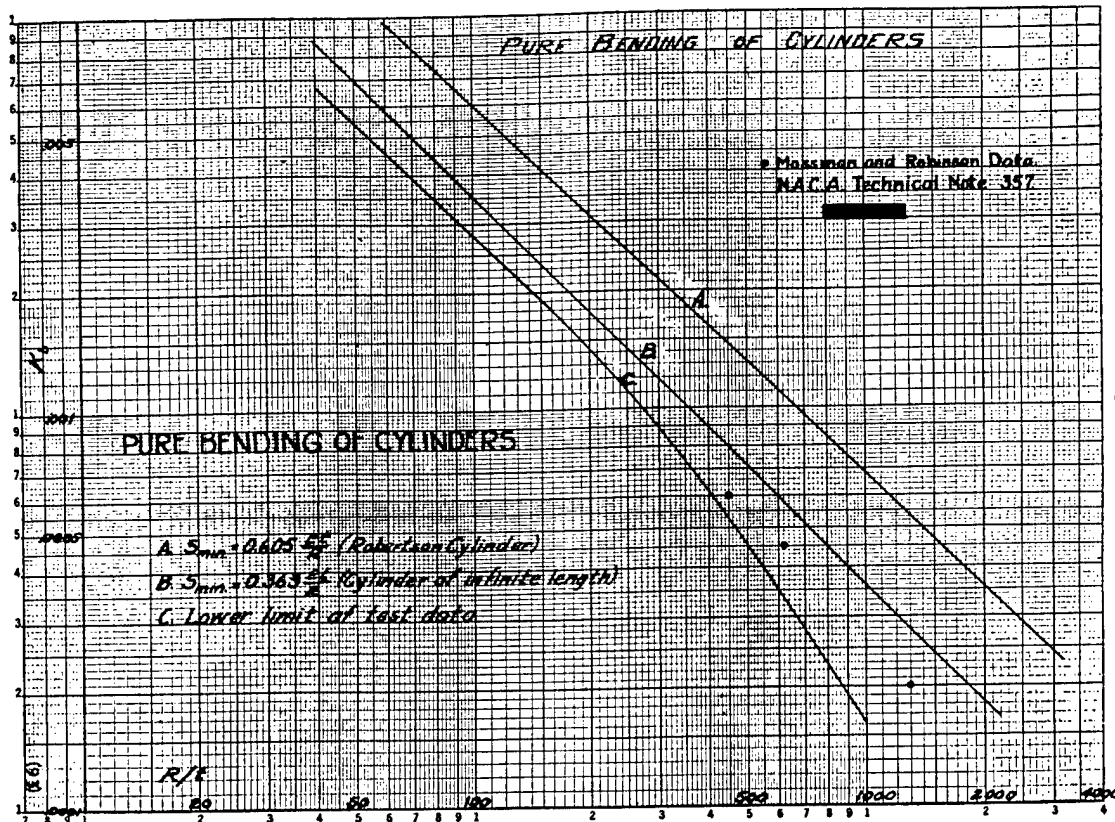


FIGURE 31.

### SECTION 11. CYLINDERS IN BENDING UNSTIFFENED CYLINDERS

Lundquist, in N. A. C. A. Technical Note No. 479, gives the critical stress on the extreme fiber of a cylinder subjected to pure bending as  $\sigma_b = K_b E$  where  $K_b$  is a coefficient depending on the dimensions and imperfections of the given cylinder.  $K_b$ , plotted against  $R/t$  is given in figure 31, curve A being based on Robertson's theory for cylinders, curve B on Southwell's theory and curve C representing the lower limit of test data. For design purposes, it is desirable to use the lower, more conservative coefficients based on curve C.

The points plotted between curves B and C were obtained by Mossman and Robinson in their cylinder tests at Stanford University. They lie approximately on a curve whose equation is  $\sigma = 0.3E \frac{t}{R}$ , the expression suggested by Sechler as representing the stress on the intermediate areas of simply supported curved panels.

In N. A. C. A. Technical Note No. 523, Lundquist presents diagrams showing the effect of shear on the allowable stress in bending on a thin walled cylinder. Figure 32 presents curves giving the percent of the allowable stress in pure bending developed for various ratios of  $M/RV$  where  $M$  is the moment,  $V$  the shear at the critical section of radius  $R$ . The curves are given for different ratios of bending stress at the extreme fiber to shear stress at the neutral axis by being plotted

against  $\frac{M}{RV} = \frac{\sigma_b}{\sigma}$ , where  $\sigma_b = \frac{M}{\pi R^2 t}$  and  $\sigma = \frac{V}{\pi R t}$  and for various ratios of allowable stress in bending,  $S_b$ , to allowable stress in shear,  $S_s$ , between 0.25 and 10.0.  $S_b$  may be taken as the allowable stress in pure bending on a cylinder of the same dimensions while  $S_b = 1.25 S_s$  where  $S_s$  represents the allowable shear stress on a cylinder subjected to torsion.

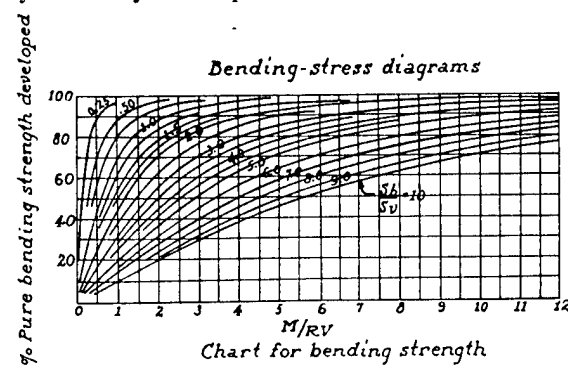


FIGURE 32.

### SECTION 12. STIFFENED CYLINDERS

Fuselage structures are normally built with stiffeners running longitudinally and with bulkheads or frames transversely. Many wings have similar structures, the stiffeners running spanwise and the ribs furnishing the

transverse stiffness. The average fuselage is so nearly circular that it may be treated as a cylinder but the normal wing covering is of such large radius of curvature that it is generally analyzed as a flat sheet. Both structures are subjected to bending moments and shear and each involves problems concerning the allowable stresses in compression and shear on stiffened sheet. It is the purpose of this section of this report to investigate static test and other data with a view toward determining whether or not the failing strength of complete wing or fuselage structures may be computed by the methods used in previous sections on flat and curved panels if such methods be modified by the use of empirical fixity coefficients, arbitrary panel widths, and similar devices.

Stress distribution studies on stiffened circular cylinders made at M. I. T. and, on fuselages tested at Wright Field (see A. C. I. C. 684, An Investigation of the Stress Distribution Due to Bending and Torque in the Boeing XP-9 Semi-Monocoque Fuselage) show that the maximum stress does not occur at the fiber most distant from the neutral axis unless the transverse stiffeners are sufficiently close together to prevent any distortion of the cross section under load. A series of four circular cylinders, 40 inches in diameter by 10 to 15 feet long, was tested at M. I. T., one having no transverse frames except at the support and load points, the others having bulkheads spaced 18, 12, and 6 inches, respectively. These bulkheads were  $\frac{3}{8}$ -inch fir plywood with 20-inch diameter access holes through them so there was a 10-inch expanse of plywood in a radial direction to stiffen the skin at any point. These bulkheads approximated infinite stiffness for the 0.032 and 0.020 skin used.

Each cylinder had 16 channel-shaped stiffeners running longitudinally, the spacing being uniform at  $22.5^\circ$  7.85-inch intervals around the circumference. Strain gage measurements made at each stiffener by 8-inch Berry gages and 1-inch Huggenbergers showed that the most stressed elements on the compression side of the cylinder having no transverse bulkheads were at the stiffeners at the ends of the  $45^\circ$  radii instead of at the fiber most distant from the neutral axis, the stress being about 2,850 lb./in.<sup>2</sup> at the  $45^\circ$  stiffener, as compared with 1,900 at the extreme fiber, for a ratio of  $M/I=107.5$ . With the 18-inch bulkhead spacing and the same  $M/I$  ratio, the maximum stress still occurred at the  $45^\circ$  stiffener, but was practically the same as that at the  $22.5^\circ$  and extreme fiber stiffeners, the variation being between 2,000 and 1,900 lb./in.<sup>2</sup>. With the 12-inch spacing of bulkheads the stress at the  $22.5^\circ$  and extreme fiber stiffeners was practically the same, about 2,300 lb./in.<sup>2</sup>, the distribution across the rest of the cylinder approximating that from the beam theory. In the case of the 6-inch spacing the cylinder did not distort appreciably from its circular section and the stress distribution was very nearly that from the beam theory, the maximum variation being about 8 percent at the  $22.5^\circ$  stiffener. The theory indicated 2,100 lb./in.<sup>2</sup> at the extreme fiber and the test showed 2,200 for the  $M/I$  ratio used. At higher  $M/I$  ratios the discrepancy between measured stress and beam theory became larger.

The conclusion is reached, then, that the methods of analyzing ordinary structures in bending are not directly applicable to stressed-skin fuselages unless the internal stiffening provided is adequate to prevent distortion of the cross section. This is difficult to do in the average structure, although recent tests appear to show that it is less difficult than it has been previously considered.

A second series of three cylinders recently tested at M. I. T. showed that very flexible rings, when used as intermediate transverse frames, sufficed to maintain the circular cross section in the plane of the ring, although they permitted the cylinder to distort between frames. These cylinders were identical with the series mentioned above except that the stiffness of the transverse frames was varied and that the longitudinal stiffeners were placed on the outside of the cylinder to obviate cutting the frames. The frames were spaced at 12-inch intervals so that, with the cylinder of the first series having plywood bulkheads at 12-inch spacing, there are four cylinders available for comparison. The pertinent data are summarized in table 21.

TABLE 21

Type of transverse frame	$I$ of frame section about its centroid	Moment at maximum load on cylinder in inch-pounds
$\frac{3}{8}$ -inch plywood.....	Infinite	350,000
$1\frac{1}{2}$ -inch hat.....	0.0217	332,000
$\frac{1}{2}$ -inch hat.....	.00491	329,000
$2\frac{1}{8} \times 1\frac{1}{2}$ inch angles.....	.000977	337,000

It appears from the above tests that the stiffness of the transverse frames has little effect upon the ultimate strength of a circular cylinder carrying bending loads. The cylinder having a very rigid plywood bulkhead carried but 5 percent more load than one having very flexible frames made of two angles,  $\frac{3}{8} \times \frac{1}{2}$  inch spaced 1 inch apart and having the  $\frac{1}{2}$ -inch legs outstanding. The  $1\frac{1}{2}$ - and  $\frac{1}{2}$ -inch hat-shaped frame members were of the square or "high-hat" section, having  $\frac{3}{8}$ -inch legs, spaced 1 inch apart, attached to the skin of the cylinder. The heights of the "hats" were  $1\frac{1}{2}$  and  $\frac{1}{2}$  inch respectively.

On the basis of these tests, which are too few in number to be conclusive, it would seem more desirable structurally to use a number of light, transverse frames at frequent intervals to maintain the cross-sectional shape rather than a few heavy sections spaced far apart. It would also appear that sections stiff enough to withstand handling or accidental loads would suffice for intermediate members which carry no external or concentrated loads.

In discussing these results with Mr. E. E. Lundquist of the N. A. C. A., he suggested that a tentative criterion, based on an approximate theoretical analysis, for the relative strengths of longitudinal and transverse stiffening members might be taken as

$$\frac{I_T}{D_L} > \frac{I_L}{D_T}$$

where  $I_T$  represents the moment of inertia of the

transverse stiffener section,  $I_L$ , that of the longitudinals; where  $D_L$  is the distance along the transverse stiffeners between longitudinals and where  $D_T$  is the distance along the longitudinals between transverse stiffeners. Some criterion of this sort is desirable for use in design and this is suggested for consideration and for modification as subsequent data confirm it or show it to be incorrect.

The tests on the last series of cylinders showed a considerable shift of the neutral axis below the horizontal diameter and indicated that the effective section modulus,  $I/y$ , on the compression side of these cylinders as they approached ultimate load was about half that of the cylinder based on the properties computed for the neutral axis at the horizontal diameter. Such a phenomenon would be expected in view of the reduced effectiveness of the skin once it had buckled and, as the buckling is progressive as the load increases, it is obvious that there will be a change in the neutral axis with change in load.

This leads us to the following procedure, modified from a method developed by Walter H. Gale, former Research Assistant at the M. I. T., which is in fair agreement with the strength of these cylinders. It is rational and should be applicable to structures of other shapes but requires further checking to establish the degree of error involved in its use.

1. For the first approximation assume the longitudinal stiffeners and the entire skin effective in carry-

ing stress, except that portions adjacent to cut-outs or other discontinuities should be omitted when determining the locus of the neutral axis and the moment of inertia of the section.

2. Determine the stress at each stiffener point and at the midpoints of the panels of skin between stiffeners by use of the ordinary beam formula  $f = \frac{My}{I}$ .

3. Assuming that some of the skin on the compression side of the section will buckle under these stresses, and so change the location of the neutral axis and the values of  $I$  and  $y$ , multiply the stresses determined under (2) by a suitable coefficient for the section considered. (A limited experience in the application of this method shows that two is a reasonable factor for circular sections.)

4. Determine the effective widths of skin acting with each stiffener on the basis of these modified stresses and compute "efficiency factors" for the panels of skin between these effective widths. The "efficiency factor" is the ratio of the compressive stress, causing the panel to buckle,  $\sigma = 0.3E_R^t$ , to the stress computed at the midpoint of the panel under (3).

5. Determine the area of each stiffener with its effective width of sheet and assume it to act at the centroid of the stiffener. Determine the area of the panels of skin between the effective widths of sheet acting with the stiffeners, multiply these areas by the "effi-

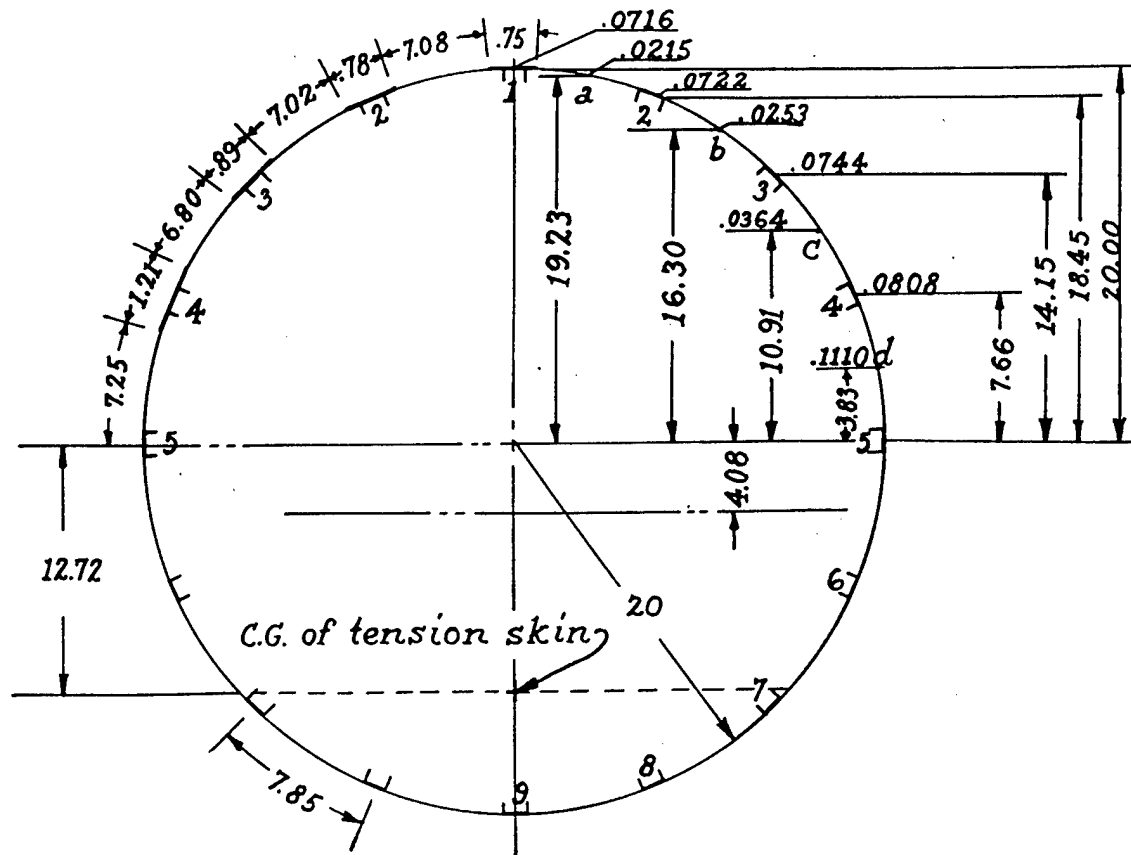


FIGURE 33.

ciency factor" computed for the panels under (4) and assume the resultant effective areas to act as though concentrated at the midpoints of the panels. This operation is the equivalent of saying that the skin between stiffeners acts to carry its normal buckling stress in compression, but no more.

6. Determine the locus of the neutral axis and recompute the properties of the section on the basis of the effective areas carrying stress in compression, the whole area in tension.

7. Determine the stress intensities at the extreme fiber and at any other points which might be critical and compare them with the allowable stresses at these points.

8. The allowable compressive stress on the combination of stiffener and effective sheet area may be obtained as in the case of stiffened panels, using a fixity coefficient of 1.0 to 1.5 on the stiffener and a column length equal to the distance between transverse stiffeners or bulkheads. It would seem reasonable that the column length assumed might be greater than the distance between transverse members when such members are flexible but the data in hand do not appear to justify such an assumption, the very flexible transverse rings in conjunction with an 0.020-inch skin having been adequate to provide the longitudinal stiffeners the support necessary to develop a fixity coefficient greater than 1.0. The allowable tensile stress is, of course, tensile strength of the material.

9. The compressive stresses computed under (7) should not exceed the allowables determined under (8). If they do, the overstressed parts should be assumed to buckle and the section properties be recomputed on the basis of these parts being only partially effective. While it is sometimes possible to show a condition of equilibrium to exist with one or two stiffening members buckled and out of action, it is believed that such structures are unsafe and that they should not be used in aircraft.

An application of the method will now be made to one of the 40-inch diameter cylinders discussed above. The one having a 12-inch spacing between transverse frames is chosen because it is representative of the spacing used in cylinders of this diameter. The section and pertinent dimensions are shown in figures 33 and 34.

$$M = 350,000 \text{ in.-lb.}$$

The moment of inertia of the entire cross section is:

$$I = \frac{2\pi(0.020)(20)^3}{2} + \frac{16(0.0566)(20)^2}{2} = 502 + 181 = 683 \text{ in.}^4$$

$$y = 20 \text{ in.} \quad I/y = 34.15$$

On the assumption that the entire cross section carries stress:

$$f_1 = \frac{350,000 \times 20}{683} = 10,250$$

$$f_2 = \frac{350,000 \times 18.45}{683} = 9,450$$

$$f_3 = \frac{350,000 \times 14.15}{683} = 7,250$$

$$f_4 = \frac{350,000 \times 7.66}{683} = 3,930$$

$$f_5 = 0$$

$$f_A = \frac{350,000 \times 19.23}{683} = 9,860$$

$$f_B = \frac{350,000 \times 16.30}{683} = 8,350$$

$$f_C = \frac{350,000 \times 10.91}{683} = 5,600$$

$$f_D = \frac{350,000 \times 3.83}{683} = 1,965$$

For the 0.020 skin the stress at which buckling starts is  $\frac{0.3 \times 10^7 \times 0.020}{20} = 3,000 \text{ lb./in.}^2$  so panels A, B, and C would be expected to buckle and carry stresses not to exceed 3,000 lb./in.<sup>2</sup>. Panel A will then be  $\frac{3,000}{9,860} = 0.304$  effective; B,  $\frac{3,000}{8,350} = 0.359$ , and C,  $\frac{3,000}{5,600} = 0.535$ .

A limited experience in computing  $I/y$  of the effective section indicates it to be between 50 and 60 percent of the  $I/y$  for the entire section so the stresses on the stiffeners and panels of skin as computed above will be doubled. It will be assumed that they are doubled in the following evaluation of effective widths and efficiency factors.

Stiffener	Assumed stress, $\sigma_{cr}$	Effective width <sup>1</sup>	Effective area	Stiffener area	Effective stiffener area	Skin panel	Panel width	Efficiency factor	Effective width	Effective area
1.....	20,500	0.75	0.0150	0.0566	0.0716	A	7.08	0.152	1.075	0.0215
2.....	18,900	.78	.0156	.0566	.0722	B	7.02	.180	1.265	.0253
3.....	14,500	.89	.0178	.0566	.0744	C	6.80	.268	1.820	.0364
4.....	7,860	1.21	.0242	.0566	.0808	D	7.25	.765	5.55	.1110
5.....	0									

<sup>1</sup>  $b_s = 1.7t \sqrt{\frac{E}{\sigma_{cr}}}$

The trial neutral axis of the effective section may now be determined:

1.  $0.0716 \times 20.00 = 1.432$
- A.  $2 \times .0215 \times 19.23 = .827$
2.  $.0722 \times 18.45 = 2.665$
- B.  $2 \times .0253 \times 16.30 = .825$
3.  $2 \times .0744 \times 14.15 = 2.105$
- C.  $2 \times .0364 \times 10.91 = .796$
4.  $2 \times .0808 \times 7.66 = 1.239$
- D.  $2 \times .111 \times 3.83 = .851$

$$\Sigma \text{ area} = 0.9148 \quad 10.740$$

$$0.0566 (20 + 36.90 + 28.30 + 15.32) = 5.690$$

$$\pi(0.020) (20) (12.72) = 15.980$$

$$-21.67$$

$$\text{Neutral axis lies } \frac{-21.67 + 10.74}{2.681} = \frac{-10.93}{2.681}$$

$$= 4.08 \text{ inches below diameter 5-13.}$$

$I$  about neutral axis:

1.  $0.0716 \times 24.08^2 = 41.51$
- A.  $.0430 \times 23.31^2 = 23.36$
2.  $.1444 \times 22.53^2 = 73.29$
- B.  $.0506 \times 20.38^2 = 21.01$
3.  $.1488 \times 18.23^2 = 49.40$
- C.  $.0728 \times 14.99^2 = 16.35$
4.  $.1616 \times 11.74^2 = 22.27$
- D.  $.222 \times 7.91^2 = 13.89$
5.  $.1132 \times 4.08^2 = 1.88$
6.  $.1132 \times -3.58^2 = 1.45$
7.  $.1132 \times 10.07^2 = 11.48$
8.  $.1132 \times 14.37^2 = 23.38$
9.  $.0566 \times 15.92^2 = 14.35$

$$\text{Sheet } 1.257 \times 8.64^2 = 93.80$$

$$407.51$$

$$^1 \text{Area} = 0.9148 + 9(0.0566) + 1.2566 = 2.681 \text{ in.}^2$$

$$I = I_o \text{ (of lower skin)} + 407.51 = 47.5 + 407.51 = 455.01$$

$$\text{in.}^4$$

$$f = \frac{350,000 \times 24.08}{455.0} = 18,530 \text{ lb./sq. in. at the extreme fiber.}$$

A second determination of the stresses, neutral axis and moment of inertia of the effective material will now be made on the basis of the above approximation.

Stresses on stringers and sheet areas:

$$f_1 = \frac{350,000 \times 24.08}{455.0} = 18,520$$

$$f_2 = \frac{350,000 \times 22.53}{455.0} = 17,320$$

$$f_3 = \frac{350,000 \times 18.23}{455.0} = 14,020$$

$$f_4 = \frac{350,000 \times 11.74}{455.0} = 9,030$$

$$f_5 = \frac{350,000 \times 4.08}{455.0} = 3,140$$

$$f_A = \frac{350,000 \times 23.31}{455.0} = 17,920$$

$$f_B = \frac{350,000 \times 20.38}{455.0} = 15,670$$

$$f_c = \frac{350,000 \times 14.99}{455.0} = 11,530$$

$$f_d = \frac{350,000 \times 7.91}{455.0} = 6,080$$

$$\text{Buckling stress on panels} = \frac{0.3 \times 10^7 \times 0.020}{20} = 3,000$$

$$\text{lb./in.}^2, \text{ as in the first approximation.}$$

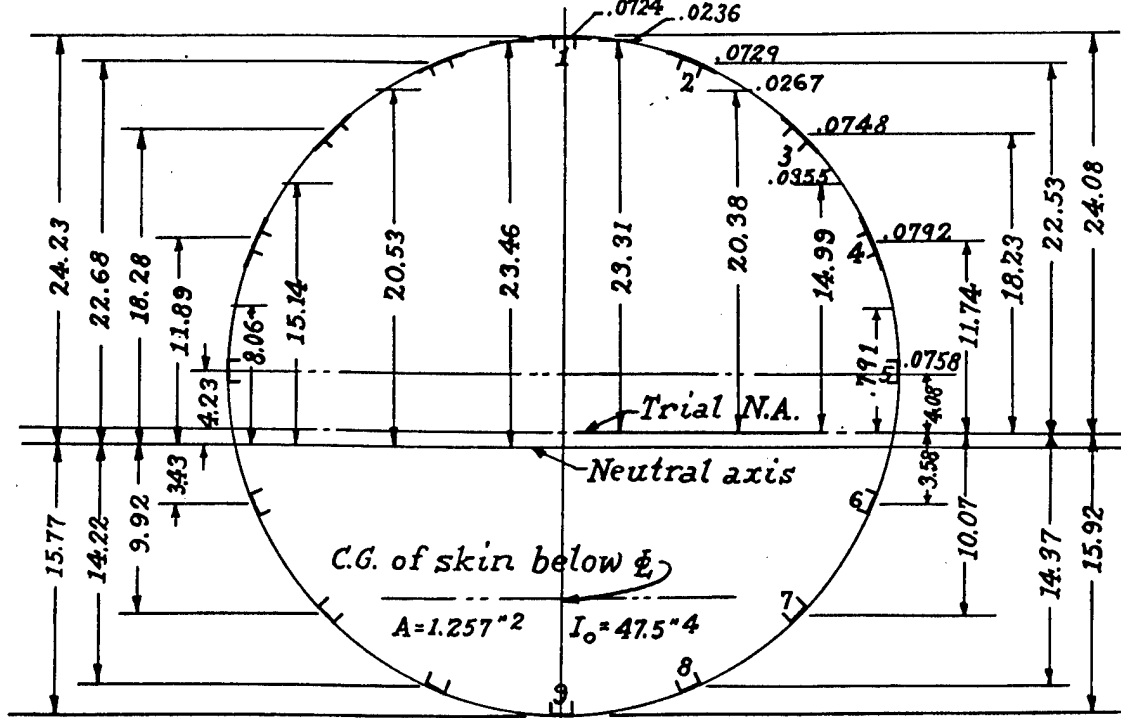


FIGURE 34.

Stiffener	Stress	Effective width	Effective sheet area	Stiffener area	Effective area	Skin panel	Panel width	Efficiency factor	Effective skin width	Effective skin area
1-----	18,520	0.790	0.0158	0.0566	0.0724	A	7.05	0.167	1.178	0.0236
2-----	17,320	.816	.01632	.0566	.0720	B	6.99	.191	1.335	.0267
3-----	14,020	.908	.01818	.0566	.0748	C	6.83	.260	1.775	.0355
4-----	9,030	1.132	.0226	.0566	.0792	D	6.33	.494	3.140	.0628
5-----	3,140	1.192	.0192	.0566	.0758					
		2								

<sup>1</sup> Effective width of skin with stiffener 5 is that above the  $\Phi$  since all skin below  $\Phi$  is included as a unit.

The neutral axis of the effective section is, then,

$$\begin{aligned} 1 \times 0.0724 &= 0.0724 \times 24.08 = 1.744 \\ A. 2 \times .0235 &= .0470 \times 23.31 = 1.096 \\ 2. 2 \times .0729 &= .1458 \times 22.53 = 3.287 \\ B. 2 \times .0267 &= .0534 \times 20.38 = 1.089 \\ 3. 2 \times .0748 &= .1496 \times 18.23 = 2.728 \\ C. 2 \times .0355 &= .0710 \times 14.99 = 1.065 \\ 4. 2 \times .0792 &= .1584 \times 11.74 = 1.860 \\ D. 2 \times .0628 &= .1256 \times 7.91 = .994 \\ 5. 2 \times .0758 &= .1516 \times 4.08 = .620 \\ \text{Area} &= \frac{.9745}{14.483} \end{aligned}$$

$$\begin{aligned} 9. 1 \times 0.0566 &= .0566 \times 15.92 = 0.901 \\ 8. 2 \times .0566 &= .1132 \times 14.37 = 1.628 \\ 7. 2 \times .0566 &= .1132 \times 10.07 = 1.091 \\ 6. 2 \times .0566 &= .1132 \times 3.58 = .405 \\ \pi(0.020)(20) &= 1.257 \times 8.64 = 10.857 \\ \text{Area} &= \frac{1.6532}{14.882}, \text{Mom.} = \frac{14.882}{14.483} \end{aligned}$$

New location of the neutral axis is

$$\frac{-14.882 + 14.483}{0.9745 + 1.6532} = \frac{-0.390}{2.627} = -0.152 \text{ in.}$$

below trial location. The  $I$  about this axis is, then,

$$\begin{aligned} 1. 0.0717 \times 24.23^2 &= 42.50 \\ A. 0.0470 \times 23.46^2 &= 25.85 \\ 2. 0.1458 \times 22.68^2 &= 74.95 \\ B. 0.0534 \times 20.53^2 &= 22.53 \\ 3. 0.1496 \times 18.38^2 &= 50.60 \\ C. 0.0710 \times 15.14^2 &= 16.28 \\ 4. 0.1584 \times 11.89^2 &= 22.41 \\ D. 0.1256 \times 8.06^2 &= 8.17 \\ 5. 0.1516 \times 4.23^2 &= 1.70 \\ 6. 0.1132 \times 3.43^2 &= 1.38 \\ 7. 0.1132 \times 9.92^2 &= 11.13 \\ 8. 0.1132 \times 14.22^2 &= 22.88 \\ 9. 0.0566 \times 15.77^2 &= 14.06 \\ \text{Sheet } 1.257 \times 8.49^2 &= 90.50 \\ &= \frac{404.89}{404.89} \end{aligned}$$

$$I = I_o \text{ (of bottom skin)} + 404.89 = 47.5 + 404.89 = 452.39 \text{ in.}^2$$

$$f = \frac{350,000 \times 24.23}{452.39} = 18,730 \text{ lb./sq. in.}$$

This is in such close accord with the first approximation that no further revision is necessary.

The allowable stress on stiffener 1 with its 0.0790-inch effective width of sheet is found as follows:

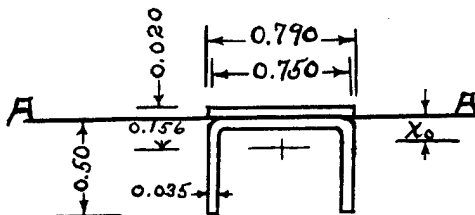


FIGURE 35.

$$\text{Sheet area} = 0.0158 \text{ sq. in.}$$

$$\text{Stiffener area} = 0.0566 \text{ sq. in.}$$

$$I_o \text{ of stiffener} = 0.00145 \text{ in.}^4$$

Distance from A-A to c. g. of sheet and stiffener:

$$\begin{aligned} (0.020 \times 0.790)(-0.010) &= 0.0158(-0.010) = -0.000158 \\ 0.0566 \times 0.156 &= +0.00883 \\ 0.0724 &= 0.008672 \end{aligned}$$

$$X_o = \frac{0.008672}{0.0724} = 0.120 \text{ in.}$$

$I$  of skin and stiffener:

$$\begin{aligned} I_o &= 0.00145 \\ 0.0566 \times 0.036^2 &= 0.000073 \\ 0.0158 \times 0.130^2 &= 0.000267 \\ &= 0.001790 \text{ in.}^4 \\ \rho &= \frac{0.001790}{0.0724} = 0.156 \quad L/\rho = 12/0.156 = 77 \end{aligned}$$

The crushing stress on this stiffener, as obtained on page 23, is 28,000 lb./in.<sup>2</sup> so the column strength for  $L=12$  in.,  $C=1.0$  is

$$\begin{aligned} f &= 28,000 - \frac{28,000^2 \times 77^2}{4 \times 1 \times \pi^2 \times 10^7} = 28,000 - 11,600 \\ &= 16,400 \text{ lb./in.}^2 \end{aligned}$$

Similar computations have been made for the cylinders having bulkheads at 6- and 18-inch intervals, and the allowable stresses have been computed on the basis that  $C=1.0$  and 1.5. For the case of the 18-inch bulkhead spacing the combination of skin and stiffener lies in the Euler column range, so Euler's formula was used in place of Johnson's. The results are compared in table 22.

TABLE 22

Bulk-head spacing	Compressive stress on stiffener 1	Allowable stress for $C=1.0$	Percent of error	Allowable stress for $C=1.5$	Percent of error
6	27,900	25,100	111	26,065	17
12	18,730	16,400	114	20,250	-7½
18	12,400	7,450	166	11,200	111

<sup>1</sup> Represents error which would be conservative in actual design.

It appears from the above that the method leads to conservative results when allowable stresses are based on  $C=1.0$ , the results being extremely conservative for transverse frame spacings giving high values of  $L/\rho$  for the longitudinal stiffeners. An assumption of  $C=1.5$  appears to be justified in the latter case, also in the case where the column is so short that its failing stress approaches its crushing strength, but it is somewhat on the unsafe side for the cylinder with 12-inch frame spacings. It is to be noted that the results in table 22 are based on the cylinder with the plywood bulkheads, the strongest of the four listed in table 21, so the discrepancy between

Computed and allowable stresses for  $C=1.0$  would be lessened by using the weaker sections, the discrepancy for the  $C=1.5$  values would, on the other hand, be made worse. Until further data become available, it is therefore suggested that allowable stresses be based on  $C=1.0$  when using this pseudorational method of design.

The method requires further study, particularly when applied to fuselages which, due to double curvature of the skin, entail stiffening effects not present in the circular cylinders investigated. For such cases it would be expected that values of  $C$  between 1.5 and 2.0 would be justified.

A simplification of the above method, which is less tedious to apply and which appears to lead to conservative results, may be had by neglecting the load carried by the areas of skin between stiffeners and by assuming the effective area of skin acting with each stiffener to depend on some arbitrary width such as 30 times the thickness of the skin itself. As assumed in the more rational procedure described above, the effective width should depend on the intensity of the stress at the stiffener, but an assumed value of 30 or 40 times the skin thickness is reasonable for the aluminum alloys.

Applying this procedure to the three cylinders previously employed results as follows:

Bulk-head spacing	Moment at failure	Computed stress at extreme fiber	Computed allowable stress $C=2.0$	Error (percent)
6	475,000	37,700	26,570	-30
12	350,000	27,800	22,280	-20
18	261,000	20,750	15,130	-27

The above errors are computed from  
 $\frac{\text{Computed allowable stress}}{\text{Stress from test}} - 1$ ,

expressed in percent. From these three sections it would appear that this approximate method is so conservative that it will produce heavier structures than are necessary. In these particular cases, the use of a fixity coefficient greater than 2.0 appears justified for the determination of allowable stresses, but the evidence is not sufficient to warrant its use without further study.

Whatever method of analysis is used, allowances must be made for the maximum stresses occurring at some point other than the extreme fiber and careful consideration must be given to the effects of stress redistribution resulting from cut-outs, inspection holes, and similar discontinuities. Neither theory nor adequate empirical data exist at present for the evaluation of these factors, but they must be provided for by the resourcefulness and judgment of the designer.

One way of looking at the stress distribution problem in bending is to reverse the usual method of visualizing longitudinal shear as running from zero at the most stressed fiber of a symmetrical section to a maximum at the neutral axis and to consider the shear at the neutral axis as having to be transmitted through the various elements of the section so that it is reduced to zero at the extreme fiber. It then becomes apparent that a sheet

buckled by compressive or shear forces will not, due to its lack of rigidity, transmit shear forces across a panel as effectively as an unbuckled sheet so that some redistribution of stress is to be expected in the parts of the structure farthest from the neutral axis, hence, that once panels have buckled the fibers which the beam theory indicates are most heavily stressed will actually be subjected to less than their expected loads. It is not always necessary that a panel buckle to shirk its work in transmitting shear. For instance, the effective rigidity of a quadrilateral panel having curved edges varies when one corner moves out of the plane of the other three, so the amount of shear transmitted across such an element becomes a function of the distortions of the structure in which it is incorporated. Wagner in N. A. C. A. Technical Memo No. 774, "Tension Fields in Originally Curved Thin Sheets Carrying Shearing Stresses," presents methods for evaluating some of these effects, but there are many items not yet rationalized for which the designer must provide by the use of his common sense and experience.

Such experience is best obtained from stress measurements on static test structures and the following suggestions are applicable to wings in particular and are the results of tests conducted by two manufacturers. In one case the wing had two main spars, but was covered by a skin having adequate stiffeners to cause the skin to carry load. The skin, however, was not attached to the center section at the root of the panel but was designed to transmit its load to the spars so that they in turn carried it into the center section. Such a structure did not, of course, utilize the stiffened skin near the root to its full efficiency and a study of the deflections obtained in static test showed that the efficiency was reduced for about 35 percent of the span of the outer panel from the root. It was also found that the ratio of Effective  $I$  of skin and stiffeners to Geometric  $I$  of skin and stiffeners was about 0.80 over an area from 35 percent of the span to 70 percent of the span from the root; that this ratio decreased as a straight line to zero at the root and as smooth curve to zero at the tip. No explanation is given for the drop-off in effectiveness at the tip, but it is believed that this may be a characteristic of this particular wing (Boeing 247, p. 19, Rep. D-1313) rather than a general condition.

Data on another wing test show that the compressive stresses expected on the sheet and stiffeners between the spars are not attained, but that the stress drops off as one approaches the stiffener midway between the spars, and that it is very low on the sheet areas between the stiffeners. Unfortunately, the stresses at the spar sections are not given in the data available, so no definite conclusions may be drawn as to the efficiency of the intermediate stiffeners. On the basis of the stresses given (Boeing XF7B1, p. 25, Rep. D-1313), the stiffener nearest the front spar carried a stress of 5,600 lb./in.<sup>2</sup>, the one halfway between the spars, 4,550 lb./in.<sup>2</sup>, or 81 percent and the stiffener nearest the rear spar 5,100 lb./in.<sup>2</sup> or 91 percent of the stress on the forward stiffener.

Another designer, also on the basis of static tests, recommends the assumption of 100 percent effectiveness for the covering and stiffeners carrying compression at the webs on a two-shear-web, stiffened, metal cov-

ered wing with a parabolic reduction to 60 percent effectiveness for skin and stiffeners halfway between the spars. This designer normally neglects the contribution made to the moment of inertia by the covering ahead of the front and behind the rear shear webs when determining the stresses due to bending and assumes the whole moment to be carried by the box beam composed of the shear webs and the top and bottom covering between them.

An experimental study of the stress distribution around the periphery of a single shear web monocoque wing panel in order to determine the effect of "shear lag" has been started at the Matériel Division. The results of this study will be published at a later date as an addendum to this report. The experimental data were obtained by means of deForest strain gages located on all longitudinal stiffeners at several stations along the span. As a result of this study it is expected that empirical formulas for use in design will be evolved.

### SECTION 13. ISOTROPIC FLAT RECTANGULAR PLATES, UNSTIFFENED—SHEAR IN PLANE OF SHEET

As in previous parts of this report, the question of allowable stress in shear will be divided into two parts, one having to do with the stresses at which buckling starts; the other with stresses causing permanent set of the buckles or rupture of the material.

#### SECTION I.—Conditions to produce buckling.

The general expression for shear stress at start of buckling is

$$\tau_{cr} = \frac{K\pi^2 E}{12(1-\mu^2)} \left(\frac{t}{b}\right)^2$$

$\tau_{cr}$  = intensity of shear stress.

$K$ ,  $E$ ,  $\mu$ ,  $t$ , and  $b$  are as for compression in sheet.

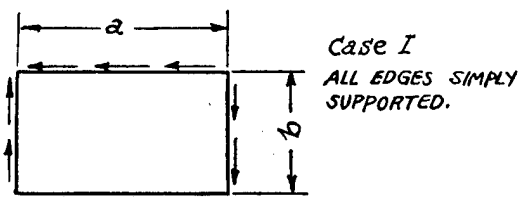


FIGURE 36.

$a/b$	1.0	1.2	1.4	1.5	1.6	1.8	2.0	2.5	3	$\infty$
$K$	9.4	8.0	7.3	7.1	7.0	6.8	6.6	6.3	6.1	5.35

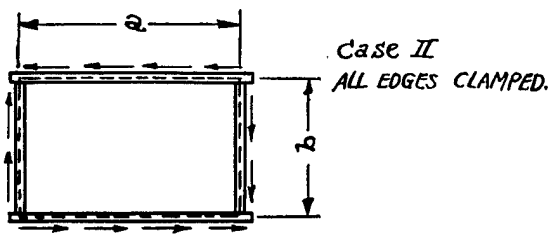


FIGURE 37.

$a/b$	1	2	$\infty$
$K$	15.45	11.55	9.00

For further data on the behavior of sheets in shear see Timoshenko, "Theory of Elastic Stability," page 357; Cox, R. and M. 1553; N. A. C. A. Technical Memo, No. 785.

#### SECTION II.—Conditions of permanent set and rupture.

Since the airplane designer is normally more interested in the stress causing permanent buckling or rupture of the sheet than in the stress producing initial buckling, the following data are given. If it be assumed that once buckling starts in a thin sheet, the resistance of the sheet to compressive forces becomes small and the intensity of tensile stress becomes twice the intensity of the shear, it would be concluded that rupture should occur when the intensity of shear is one-half the tensile strength of the material and that the buckles should take a permanent form when the shear stress exceeds one-half the yield point.

Tests made at M. I. T. by Sauerwein and Gale and by Grahn indicate that unstiffened, flat, aluminum alloy sheets will show ratios approximately as follows:

Shear stress at permanent set of buckles = 0.397, say 40

Tensile stress at yield point of material percent

Shear stress at permanent set of buckles = 0.513, say 50

Shear stress at rupture of specimen percent

Shear stress at permanent set of buckles = 0.256, say 25

Ultimate tensile strength of material percent

Shear stress at rupture of specimen = 0.498, say 50 percent

Ultimate tensile strength of material percent

### SECTION 14. ISOTROPIC FLAT RECTANGULAR PLATES, STIFFENED—SHEAR IN PLANE OF SHEET

The problem of determining the size of stiffener required to prevent the buckles formed in flat sheet subjected to shear from crossing the stiffener and causing it to fail is treated by Timoshenko in "Theory of Elastic Stability" on pages 382 and 383. The problem is treated from two points of view. The first results in an expression for the ratio between the flexural rigidity of the stiffeners and that of the sheet for a stiffener rigid enough to prevent the buckles crossing it when they are first formed. The second provides a means for determining the critical shear stress at which a stiffened plate will buckle.

The first of these methods gives

$$R = \frac{12(1-\mu^2) E_{st} I_{st}}{b E_{sh} t_{sh}^3}$$

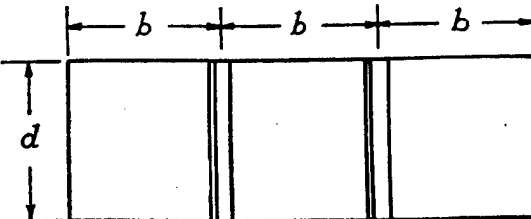


FIGURE 38.

where  $R$  is the flexural rigidity ratio defined above and has the value shown in figure 39 and  $b$  is the distance between stiffeners. The curves given cover the cases of one and two intermediate stiffeners.

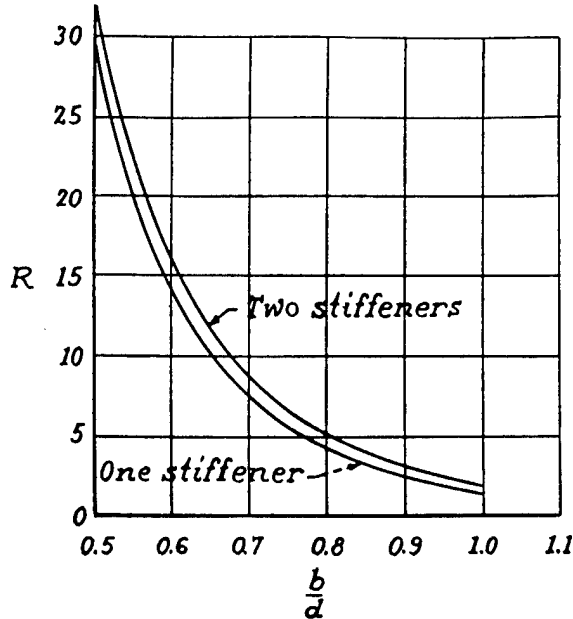


FIGURE 39.

(Fig. 224, p. 418, Timoshenko's "Theory of Elastic Stability.")

Where several stiffeners are used the second method may be applied. It gives the intensity of shear stress at which the panels will start to buckle.

$$\tau_{cr} = K \frac{\pi^2 E l^2}{12(1-\mu^2) d^2}$$

Where  $K$  is a function of  $\gamma$ , and

$$\gamma = \frac{2\pi B \sin^2 \frac{\pi c}{d}}{E t^2 d}$$

$$B = EI \text{ of the stiffener about plane of attachment to sheet.}$$

$c$  = distance of stiffener from edge of sheet.

$d$  = length of sheet parallel to stiffener.

$t$  = thickness of sheets.

The values of  $K$  are given as:

$\gamma$	5	10	20	30	40	50	60	70	80	90	100
$K$	6.98	7.70	8.67	9.36	9.90	10.4	10.8	11.1	11.4	11.7	12.0

As is evident from the following application of these methods to the data obtained by W. H. Gale at M. I. T., the results are limited to applications requiring the determination of the stress at which a shear-resistant panel buckles and resists the shear as a tension field element. The dimensions of Gale's sheets and stiffeners are shown in figure 40.

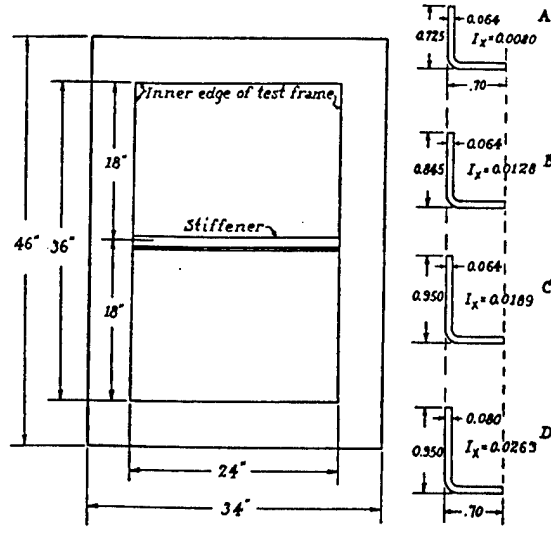


FIGURE 40.  
Applying the first method the ratio between rigidity of stiffener and rigidity of sheet is found as follows:

$$\frac{b/d}{24} = \frac{18}{24} = 0.75$$

From figure 39,  $R=5$ .

$$I_{st} = \frac{R t^3 b}{10.9} = \frac{5 \times 18 \times t^3}{10.9} = 8.25 t^3$$

For various sheet thicknesses the required moments of inertia to prevent the stiffeners buckling with the sheet are as follows:

$t$	$I_{st}$
0.020	$8 \times 10^{-4}$
.031	$29.79 \times 10^{-4}$
.040	$64.0 \times 10^{-4}$
.064	$262.14 \times 10^{-4}$
.081	$614.13 \times 10^{-4}$

A comparison of these required moments of inertia with those used on the sheets shows that the required stiffeners would be totally inadequate for use in wing or fuselage structures. The largest section required is less rigid than the smallest used in the tests. While they might suffice to make the sheet buckle as a series of panels instead of as a single sheet and to prevent the stiffener bending and buckling due to the action of the deformed sheet at low loads, they are obviously inadequate to develop high stress intensities in the sheet since they are so flexible that they would bend with it as the buckles increased in size.

The second method leads to essentially the same results except that it shows the intensity of shear stress at which the panels adjacent to a stiffener start to buckle.

For an 0.064-inch sheet with a size D stiffener, one obtains.

$$I_{st} = 0.0263, B = EI_{st} = 263,000$$

$$c = 18", d = 24", c/d = 0.75$$

$$\sin^2\left(\frac{\pi c}{d}\right) = 0.500$$

$$D = \frac{Et^3}{12(1-\mu^2)} = \frac{10^7 \times 64^3 \times 10^{-9}}{10.9} = 240$$

$$\gamma = \frac{2 \times 263,000 \times 0.5}{240 \times 24"} = 45.6$$

$$K = 10.18$$

$$\tau_{cr} = \frac{10.18 \pi^2 \times 240}{0.064 \times 24^2} = 655 \text{ lb./in.}^2$$

In the test data it is noted that the stiffener itself suffered no permanent set when the stress on the sheet reached 12,980 lb./in.<sup>2</sup>, but that it had a permanent bow after the stress had been increased to 13,700 lb./in.<sup>2</sup>, hence the effective failure of the stiffener, but not its ultimate strength, was shown to occur at a stress about 20 times that which produced buckling of the sheet in the panels to either side of it. It is the ability of the stiffener to resist buckling until the stress in the sheet has reached a point where the buckles take permanent form that is of interest to the designer in most cases, but no satisfactory method, rational or empirical, exists for determining the critical loads in such cases.

See also N. A. C. A. Technical Memorandum 809, page 10, for an expression for buckling of web and stiffeners.

H. Wagner in a paper presented at the Fourth National Aeronautic Meeting of the A. S. M. E. in May 1930, offers the following equation for the required moment of inertia of a stiffener to be used with a shear resistant web.

$$I_{st} = \frac{2.29d}{t} \left( \frac{Vh}{33E} \right)^{\frac{1}{2}}$$

$I_{st}$  = moment of inertia of stiffener.

$d$  = center line distance between stiffeners.

$h$  = depth of web plate, over-all.

$V$  = vertical shear at section.

$t$  = web thickness.

$E$  = modulus of elasticity.

This formula is similar to those given previously in that its intent is to provide a means for determining the moment of inertia of the stiffener required to cause the sheet to buckle into two panels, when buckling starts without having the wrinkles cross the stiffener. Wagner, in the same paper, gives the stress at which a thin sheet starts to wrinkle in shear as  $\tau_{cr} = \frac{5E}{(d/t)^2}$  where  $d$  is the distance between stiffeners. He notes that this expression is in good agreement with test data. It also indicates that little is to be gained by having the ratio of  $d/t$  less than 50, since for duralumin the critical shear stress at this ratio is equal to the yield point of the material in shear.

Grahn's tests on 17ST aluminum alloy specimens, 16 inches square outside by 10 inches square inside the test frame, showed no definite changes in the shear stress at which the buckles became permanent or the shear stress at failure when a single angle, channel or zee stiffener was added to divide the sheet into two 5- by 10-

inch panels. The following table shows the results obtained by Grahn.

#### Shear stress at permanent set

Sheet gage	No stiffeners	Angle	Channel	Zee
0.012	16,200	16,200	16,200	16,200
.018	14,925	14,925	15,760	15,925
.030	17,400	16,925	17,400	16,200
.040	13,440	13,440	13,800	14,525
.050	13,140	14,325	14,325	-----

#### Shear stress at failure

Sheet gage	No stiffeners	Angle	Channel	Zee
0.012	27,350	29,300	28,700	28,800
.018	28,950	29,700	29,600	28,300
.030	29,500	29,450	31,300	30,850
.040	31,700	31,500	31,900	31,700
.050	30,200	31,600	30,150	-----

Gale and Sauerwein, on the other hand, using sheet of the dimensions shown in figure 40 and a size C angle stiffener found some change in shear stress at permanent set with change in stiffener spacing. Figure 41 shows the results from their tests, and is included here as a guide to designers. Attention is called to the lower stresses obtained on the unstiffened 24- by 36-inch panels than on the 10- by 10-inch. Whether this is due to variations in the materials used or to the effect of the greater depths of buckles in the larger sheet is not known.

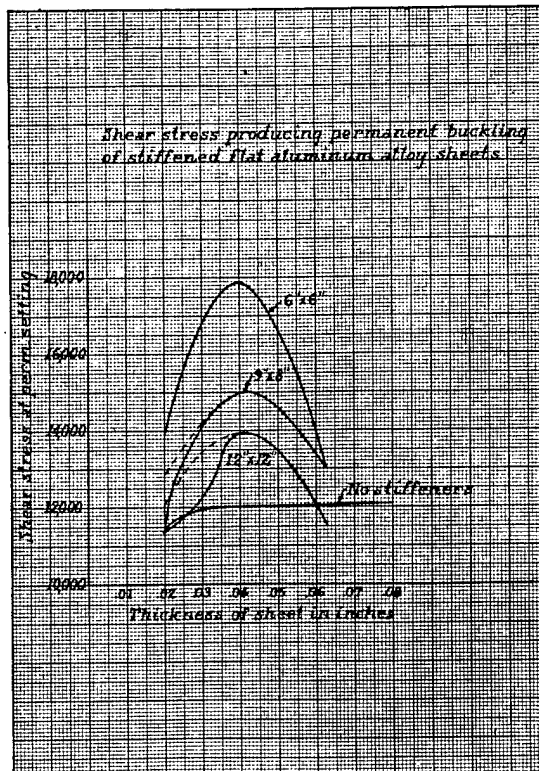


FIGURE 41.

While the formulas given above have not been checked against test data, except as shown, it is believed that they may be useful and satisfactory in determining the stress at which a stiffened shear-resistant web is transformed to a tension field sheet. For the analysis of a majority of stiffeners attached to tension field members, the methods developed by H. Wagner and described in N. A. C. A. Technical Notes 604, 605, and 606 will be found to apply and yield reasonable results. Such stiffeners act as compression members to keep two sides of the panel apart while serving as stiffening members preventing the sheet from buckling. Wagner's method for determining the critical loads on such members, while somewhat conservative for the thicker sheets used in aircraft structures, is the best available as yet and is recommended for the design of stiffeners on tension field webs until something better is evolved.

### SECTION 15. ISOTROPIC CURVED RECTANGULAR PLATES—SHEAR ON STIFFENED SHEET

Few test data exist on curved panels in shear and there are disconcerting discrepancies in the figures available. The effect of boundary conditions on the stability of curved panels is marked, particularly as regards the edges maintaining the curvature of the panel so the results of various investigations differ. Research on this problem is desirable and, when conducted, should include the investigation of the behavior of the shear modulus of elasticity as the panel distorts.

Younger, on page 216 of "Structural Design of Metal Airplanes," gives the critical stress, the stress at which buckling starts, for thin curved sheets in shear as  $\tau_{cr} = 0.06E \frac{t}{R}$ .

Wagner and Ballerstedt, in N. A. C. A. Technical Memo. No. 774, gives the buckling stress for a simply supported curved panel in shear as  $\tau_{cr} = 0.1E \frac{t}{R} + 5.3E \left(\frac{t}{b}\right)^2$  where  $t$  is the thickness of the sheet,  $R$  the radius of curvature and  $b$  the distance, measured along the arc, between longitudinal stiffeners.

Of the two expressions given above it is believed the latter, though less conservative, is the more nearly in accord with test data. The designer is referred to Technical Memo. No. 774 for a discussion of the problems.

### SECTION 16. CORRUGATED SHEET—AXIAL COMPRESSIVE LOAD PARALLEL TO CORRUGATIONS

#### CRUSHING STRESS

The following empirical formulas are offered for the determination of the crushing strength of corrugated aluminum alloy sheets, having a pitch to depth ratio of  $3\frac{1}{2}$  and carrying a compressive load acting parallel to the direction of the corrugations.

$$\text{For } 17\text{ST}, \sigma_{cr} = 34,000 \log \frac{200t}{R}$$

$$24\text{ST Alclad}, \sigma_{cr} = 37,000 \log \frac{200t}{R}$$

$$24\text{ST Alloy and } 24\text{SRT Alclad}, \sigma_{cr} = 41,000 \log \frac{200t}{R}$$

Other materials,  $\sigma_{cr} = K \times (\sigma_{cr} \text{ for } 17\text{ST})$  where

$$K = \sqrt{\frac{E \times \sigma_{vp}}{10^7 \times 36,000}}$$

Figure 42 shows the first and third of these equations plotted against test data available when this study was made. The agreement between tests and formulas is reasonable.

For other pitch and depth ratios and other materials the following modifications are suggested since the data upon which they are based are inadequate to permit the formulation of a more definite procedure. To provide for the effect of pitch to depth variation, multiply the values obtained for  $\sigma_{cr}$  from the above expressions by  $C_1$ , the coefficient plotted versus pitch/depth ratio in figure 43. The method of obtaining this coefficient is described later. It appears to check fairly well for values of  $P/d$  in the vicinity of 6, but there are few data against which to check it for ratios between 2 and  $3\frac{1}{2}$ .

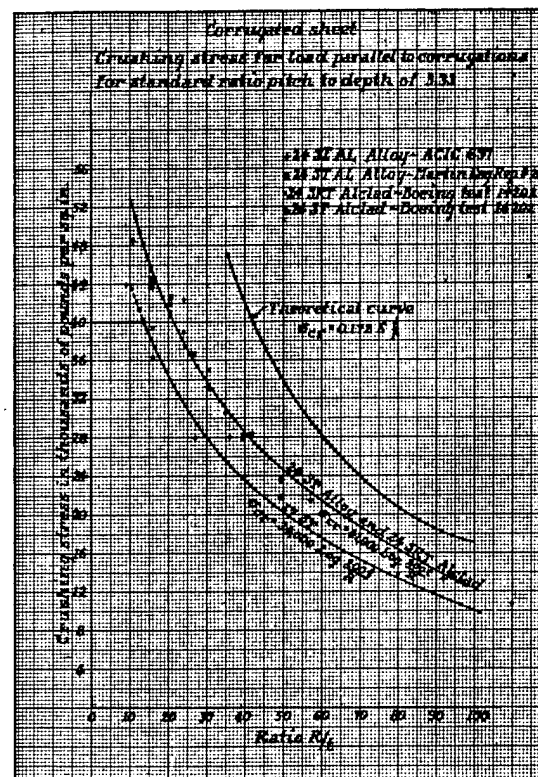


FIGURE 42.

For materials other than those considered in the foregoing, it is suggested that the values of the crushing stress for 17ST be increased in the ratio  $\sqrt{E \times \sigma_{vp}} / 10^7 \times 36,000$  where  $E$  and  $\sigma_{vp}$  are the modulus of elasticity and yield point of the other material respectively.

Pending further test data to vindicate the above, the methods suggested should be looked upon as reasonable indications of what may be expected, but they should be substantiated by suitable tests before use in design.

The coefficient for various pitch/depth ratios is obtained by the theoretical method for treating ortho-

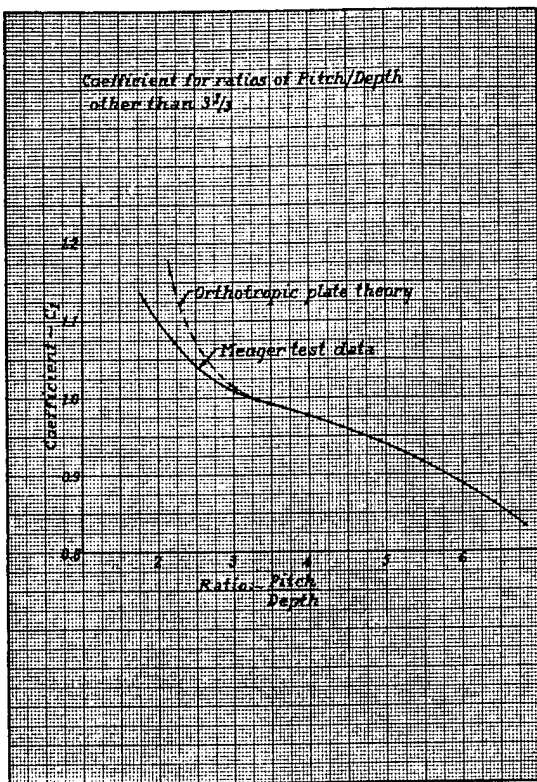


FIGURE 43.

tropic plates described on page 381 of Timoshenko's "Theory of Elastic Stability." The formula for the critical stress,  $\sigma_{cr}$ , is

$$\sigma_{cr} = \frac{2\pi^2}{b^2 t} \left[ \sqrt{D_1 D_2} + D_3 \right]$$

where  $D_1$ ,  $D_2$ , and  $D_3$  have the following general and particular values,

$$D_1 = \frac{(EI)x}{1 - \mu_x \mu_y} = \frac{l E t^3}{s 12}$$

$$D_2 = \frac{(EI)y}{1 - \mu_x \mu_y} = E k_I t d^2$$

$$D_3 = \frac{1}{2} \left[ \mu_x D_2 + \mu_y D_1 \right] + 2(GI)_{xy} = \frac{s G t^3}{l 6}$$

The particular values of  $D_1$ ,  $D_2$ , and  $D_3$  are from Seydel's "Shear-Buckling Tests of Corrugated Metal Sheets", D. V. L. Yearbook 1931, pages 233-245, Wright Field Translation No. 295. It is there stated that  $\mu_x$  and  $\mu_y$  may be taken as zero;  $s$ ,  $l$ , and  $d$  are as shown in figure 44.

From figure 45 (fig. 140 of Army Handbook or fig. 46 of A. C. I. C. 685) the following values are obtained for

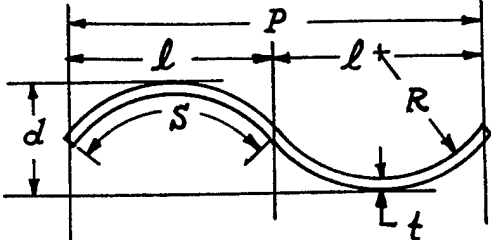
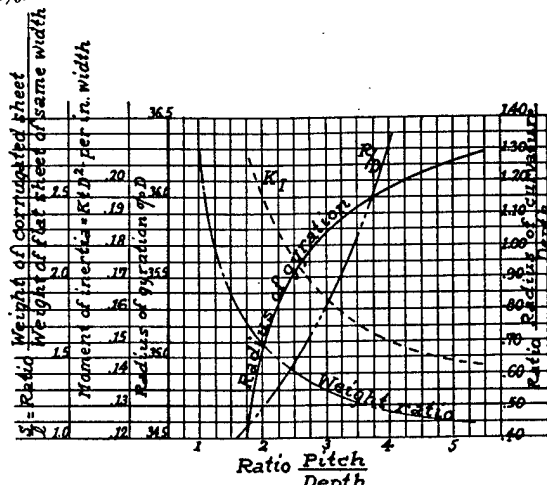


FIGURE 44.

corrugations having standard pitch/depth ratio equal  $3\frac{1}{3}$ .



$$S_{1/2} = 1.23, K_{1/2} = 0.158, R/d = 0.95, P/d = 3.33.$$

FIGURE 45.

Substituting the values for  $D_1$ ,  $D_2$ , and  $D_3$  in the expression for  $\sigma_{cr}$  yields,

$$\sigma_{cr} = \frac{\pi^2 Et}{b^2} \left[ d \sqrt{\frac{IK_1}{3s}} + 0.133 \frac{s}{l} t \right]$$

and on the assumption that  $b$ , the length of half wave parallel to the loaded edge, is equal to the pitch of the corrugations we get, for the pitch/depth ratio  $3\frac{1}{3}$ .

$$\begin{aligned} \sigma_{cr} &= \frac{\pi^2 Et}{(3.51R)^2} \left[ \frac{R}{0.95} \sqrt{\frac{0.158}{3 \times 1.23}} + 0.133 \times 1.23 t \right] \\ &= 0.799 E \left( \frac{t}{R} \right)^2 \left[ 0.216 \frac{R}{t} + 0.164 \right] \end{aligned}$$

For the normal case the second term in the brackets 0.164, is small as compared with the first and may be neglected. Hence,

$$\sigma_{cr} = 0.172 E \frac{t}{R}$$

This curve is plotted on figure 42 and, as may be seen, has approximately the same shape as the empirical curves, but gives higher values. Changing the coefficient from 0.172 to 0.11 gives a fair agreement with the curve for 17ST for the higher values of  $R/t$  but some other coefficient would be required for the 24ST and 24SRT. As is evident from the determination of the coefficient 0.172, it depends essentially on the dimensions of the section and is independent of the properties of the material. By employing the same system for other pitch/depth ratios we get:

TABLE 23

$P/d$	$C$	$C_1 = \frac{C}{C \text{ for } 3\frac{1}{3}}$
2	0.250	1.45
2.5	.206	1.20
3	.179	1.04
3 1/3	.172	1.00
4	.168	.98
4.5	.165	.96
5	.162	.94
5.5	.159	.92
6	.153	.89

Where  $C$  is defined by the equation,  $\sigma_{cr} = CE \frac{t}{R}$

Values of  $C_1$  are plotted in figure 43. Data to check them are limited, there being a few tests with  $P/d$  values of 2, a few of 6. This coefficient should, therefore, be used with caution.

The rational method indicates the critical stress to be a function of  $E$  and the test data show it to vary when  $\sigma_{yp}$  varies. The ratio between  $\sigma_{cr}$  for the 17ST and stainless steel specimens tested is about 1 to 3, so are the ratios between moduli of elasticity and yield point stress of the two materials, hence it appears that  $\sigma_{cr}$  may vary as  $\sigma_{yp}$ , as  $E$  or as  $\sqrt{E} \times \sigma_{yp}$ . By analogy with the flat plate formulas it seems reasonable to assume a variation proportional to  $\sqrt{E} \times \sigma_{yp}$  and it is on that basis that the foregoing recommendations are made.

Such justification as can be found by comparison of the above method with test data is indicated in the following tables, the data being from Wright Field Serial Report No. 3420, "Comparative Column Tests of Some Corrugated Stainless Steel and Aluminum Alloy Sheets," by Lt. P. H. Kemmer and S. R. Carpenter, from A. C. I. C. No. 697, "An Investigation of Compressive Strength Properties of Stainless Steel," and from Fleetwings, Inc., Engineering Report No. 49.

TABLE 24.—17ST aluminum alloy

[Report 3420]

$\frac{P}{d}$	$\frac{R}{t}$	$\sigma_{cr}$ (fig. 42)	$C_1$ (fig. 43)	$C_1 \sigma_{cr}$	Test $\sigma_{cr}$
6.13	49.6	20,400	0.880	17,450	17,390
5.64	55.1	18,800	.910	17,100	18,430
6.04	47.0	21,200	.886	18,800	17,450
6.04	46.0	21,400	.886	19,000	19,050
6.05	49.6	20,400	.885	18,050	14,600
6.05	49.6	20,400	.885	18,050	18,900

The agreement for the aluminum alloy is good enough to indicate the validity of using  $C_1$  for  $P/d$  ratios near 6 in conjunction with the curve of figure 42.

For the stainless steel specimens of Report No. 3420 the average value of  $E$  was 28,200,000 and the average yield point 112,700, where for 17ST aluminum alloy,  $E$  is taken as 10,000,000,  $\sigma_{yp}$  as 36,000, hence, on the basis of a variation proportional to  $\sqrt{E} \sigma_{yp}$ , the coefficient would be

$$K = \sqrt{\frac{28,200,000 \times 112,700}{10,000,000 \times 36,000}} = 2.97$$

TABLE 25.—Stainless steel

[Report 3420]

$\frac{P}{d}$	$\frac{R}{t}$	$\sigma_{cr}$ (17ST fig. 42)	$C_1$	$K$	$C_1 K \sigma_{cr}$	Test $\sigma_{cr}$
6.58	48.1	20,800	0.851	2.97	52,500	50,500
6.43	46.5	21,200	.863	2.97	54,500	56,000
6.23	48.5	20,600	.875	2.97	53,500	48,100
6.27	47.6	21,000	.873	2.97	54,500	51,400

TABLE 26.—Stainless steel

[A. C. I. C. No. 697, table XVI]

$\frac{P}{d}$	$\frac{R}{t}$	$\sigma_{cr}$ (17ST fig. B-1)	$C_1$	$K$	$C_1 K \sigma_{cr}$	Test $\sigma_{cr}$
2	25	31,000	1.10	3.5	118,200	92,000
3	40.5	23,400	1.01	3.5	82,600	89,000
4	66	16,200	.975	3.5	55,400	50,900
2	12.5	41,200	1.10	3.5	158,500	155,400
3	20.3	34,000	1.01	3.5	120,000	119,000
4	33	26,600	.975	3.5	90,800	104,200
2	8.3	45,000	1.10	3.56	176,100	186,100
3	13.5	40,200	1.01	3.56	144,500	154,600
4	22	33,000	.975	3.56	114,600	160,000

In the above tests  $K$  is based on averaged values of  $E$  and  $\sigma_{yp}$ ,  $E$  being taken as  $28 \times 10^6$ ,  $\sigma_{yp}$  as 112,700.  $E$  at 27,500,000 would probably have been better since 3 out of 4 specimens were less than 28,000,000. For the last 3 specimens  $\sigma_{yp}$  = 162,150. In this table the highest stress obtained for any specimen in a group was taken as "test  $\sigma_{cr}$ " since errors in testing will reduce the strength of such panels so the highest is the most nearly correct.

TABLE 27.—Stainless steel

[Fleetwing's Inc., Engineering Report No. 49]

$\frac{P}{d}$	$\frac{R}{t}$	$\sigma_{cr}$ (17ST)	$C_1$	$K_1$	$C_1 K_1 \sigma_{cr}$	Test $\sigma_{cr}$
2.14	25	31,000	1.08	3.05	102,000	108,000
2.20	30.7	28,000	1.07	3.05	91,500	99,500
2.18	34.1	26,200	1.075	3.05	86,000	96,000
2.12	46.9	21,200	1.08	3.05	70,000	77,000

Averaged  $E = 21,300,000$ .  $\sigma_{yp} = 157,500$ .

The above data show that the method gives results of the correct order of magnitude, though it involves errors of about 10 percent, frequently on the unsafe side. It is approximately correct for 24ST Alclad if the  $\sigma_{yp}$  for 17ST be taken as 36,000 lb./sq. in., and that for 24ST Alclad be taken as 38,000, since  $\sqrt{\frac{38,000}{36,000}} \times 36,000 = 37,000$  which checks the value for the two tests available. (Boeing test report 14202 gives the maximum yield point as 40,370, the minimum as 38,083 for the 24ST Alclad specimens tested.)

In the case of the 24SRT Alclad, again using Boeing data,  $\sigma_{yp}$  maximum = 52,830,  $\sigma_{yp}$  minimum = 46,670. Using the lower value,  $\sqrt{\frac{46,670}{36,000}} \times 36,000 = 41,000$  which checks the coefficient for the curve in figure 43 exactly. It would be more reasonable to use 34,000 as the yield point for the 17ST alloy since that is the coefficient for that basic curve, but doing so involves an additional error of some 3 percent, so it is suggested that the ratios used in computing  $K$  be based on 36,000 lb./sq. in. for the yield point of 17ST.

## SECTION 17. COLUMN STRESS (CORRUGATED SHEET)

Once the crushing stress has been determined, it may be substituted for the yield point in the Johnson parabolic column formula and the stress may be determined

for various values of  $L/\rho$ . The curves of figures 22, 23, 24, 25, may be used to facilitate this operation. For the higher values of  $L/\rho$ , the Euler formula is applicable.

The use of the Johnson formula in conjunction with the crushing strength of the sheet is somewhat on the conservative side since tests have shown the crushing stress to be constant over lengths corresponding with a range in  $L/\rho$  from 0 to 10 when  $R/t=10$  and with a range from 0 to 95 when  $R/t=100$ . To substitute a parabolic reduction in stress for the constant value obtained empirically is obviously on the safe side but it is believed to be desirable practice, certain of the manufacturers having found that it gives better agreement with their data than the straight line relations previously recommended.

### SECTION 18. FIXITY COEFFICIENTS (CORRUGATED SHEET)

The crushing stress is essentially independent of the end restraint but as the length of the corrugated sheet column increases, the end conditions become of importance just as they do in the case of tubular members. Curves have been given, figures 22 to 25, inclusive, for fixity coefficients of 1.0, 1.5, 2.0, and 3.0.

When corrugated covering is simply laid over ribs or bulkheads and riveted to them, it is recommended that  $C=1$  be used for design and that the effective length,  $L$ , be taken as the distance between the ribs or bulkheads. If the edges are restrained by attachment to members sufficiently strong to prevent local failure and if the unsupported width is less than  $\frac{3}{4}$  the unsupported length, it is permissible to increase  $C$  to a value not to exceed 1.5.  $C=1.5$  may be used when an uncorrugated sheet is laid over a corrugated, while  $C=3$  is permissible when a second corrugated sheet is laid over the principal stress carrying sheet and so attached to it that column action is prevented. In any case, however, the buckling stress as determined from the  $R/t$  ratio is critical for the shorter lengths of corrugated sheet.

### SECTION 19. EFFECT OF CURVING CORRUGATED SHEET

When a corrugated sheet whose corrugations originally lie in one plane is bent so they form elements of a cylindrical surface, the strength of the sheet under compressive loads parallel to the corrugations appears to be reduced. Data are scarce and somewhat inconclusive. Figure 46, based on a thesis, "An Investigation of Flat and Corrugated Duralumin Sheets at Various Radii of Curvature," W. H. Weeks and C. I. Richardson, M. I. T., 1930, shows the effect of cambering a corrugated sheet. The data upon which the curves are based are few, so the results should be considered as qualitative rather than quantitative.

The reduction of strength following the cambering of the corrugated sheet may be due to the fact that the radius of corrugation is no longer constant when the sheet is bent, the bending having the effect of reducing the radius at the crest of the corrugation, increasing it at the trough and probably tending to increase the "flat" area near the nodes of the corrugations. Since the critical stress decreases as  $R/t$  increases, it is probable that failures start in the regions where  $R/t$  is increased by the cambering of the sheet.

Another explanation for the weakening effect is that when the plate is cambered the material on the concave side of the curve is subjected to compressive stresses acting across the corrugations, thus reducing the ability of the sheet to carry compression parallel to the corrugations. Which of these effects predominate is hard to say but it is probable that both contribute to the weakening effect produced by curving a corrugated sheet.

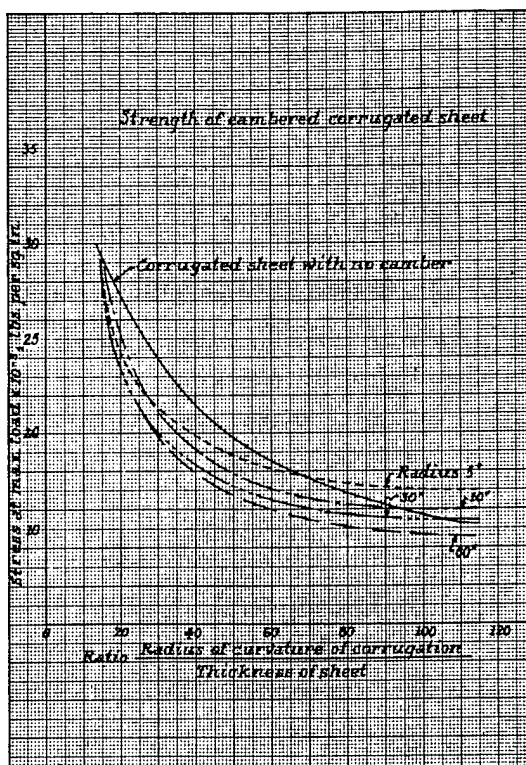


FIGURE 46.

### SECTION 20. COMPRESSION ON COMBINED FLAT AND CORRUGATED PANELS

It seems reasonable to assume that a corrugated sheet, when attached to a flat one, will act as a series of stiffeners for the flat sheet and will cause an effective area of flat sheet equal to  $b_e = 1.7t\sqrt{\frac{E}{\sigma_{cr}}}$  to act at each line of attachment between flat and corrugated sheet. A check of this assumption by comparing predicted loads with test values obtained by the Boeing Aircraft Co., Boeing Test Report No. 14202, indicates it to be somewhat on the conservative side and would lead one to the conclusion that, due to the frequency of the stiffening elements and the fact that they are interconnected, the actual area of flat sheet carrying load is greater than  $b_e$ . The results are in reasonable agreement and somewhat on the conservative side, at least for this series of tests, when the effective area of flat sheet is taken as  $b_e$ ,  $\sigma_{cr}$  being the stress at which the corrugated sheet, if tested alone, would fail as a column.

In table 28 the crushing stress for the corrugated sheet is obtained from figure 42 and reduced for column

TABLE 28

Corru-gated sheet gage	Crushing stress	Column stress	Flat sheet gage $t$	$b_e$	Effective area $b_e \times t$	Load	Number of effective areas	Flat sheet load	Corru-gated sheet load	Loads at failure	
										Predicted	Test
0.016	23,000	22,000	0.016	0.598	0.00963	214	5	1,070	4,795	5,865	15,060
.016	23,000	22,000	.021	.780	.01628	358	5	1,700	4,795	6,585	15,455
.020	29,000	28,000	.016	.526	.00847	237	5	1,185	7,670	8,855	5,825
.020	29,000	28,000	.0205	.675	.01384	388	5	1,940	7,670	9,610	6,075
.020	29,000	28,000	.0235	.774	.01819	510	5	2,550	7,670	10,220	8,500
.025	33,000	31,500	.021	.652	.01370	432	5	2,160	10,740	12,900	9,150
.025	33,000	31,500	.033	1.023	.0338	1,065	5	5,325	10,740	16,065	9,950
.033	38,000	36,500	.0235	.664	.0156	570	5	2,850	16,420	19,270	12,120
.033	38,000	36,500	.033	.952	.0314	1,145	5	5,725	16,420	22,145	11,330
.033	38,000	36,500	.040	1.155	.0464	1,695	5	8,470	16,420	24,860	15,810
.039	41,000	39,500	.033	.914	.0302	1,189	5	5,950	21,050	27,000	15,395
.039	41,000	39,500	.039	1.080	.0421	1,663	5	8,320	21,050	29,370	17,335
											16,610
											23,225
											24,375
											25,005
											25,060
											26,260
											24,095
											29,825
											30,375
											1 27,020
											30,340

<sup>1</sup> Rivet failure.

action,  $L/\rho = 28.5$  and  $C=2$ , by use of figure 24. It is assumed that the flat sheet develops this same intensity of stress, and the effective width is determined on that basis. The panels tested were 11½ inches wide, 8 inches long, and were of 24SRT Alclad except those of 0.016 gage which were 24ST Alclad. In the width of the specimen, there were four corrugations averaging 2.69 by 0.79 inches, so there were five rows of rivets with sufficient material between the outer rows and the edges of the sheet that the flat sheet had five effective areas carrying stress.  $E$  was 10,500,000 lb./in.<sup>2</sup> and  $\rho$  approximately 0.28, so  $L/\rho$  was taken as 28.5 throughout. This is an averaged value, but the column stress developed is so near the crushing strength of the corrugated sheet that the exact determination of  $L/\rho$  is unnecessary.

Except for the panels having the 0.016-inch corrugated sheet, the above procedure gives conservative results as indicated by these data. A closer agreement between predicted and test values might have been obtained by taking a fixity coefficient of 3 instead of 2 in determining the column stress for the corrugated sheet, but it is believed that this practice cannot be justified on the basis of the data available since the lengths of specimens tested are so short that the column stress and crushing stress are practically the same.

If a variable coefficient,  $C_f$ , as recommended by Sechler and determined from the curve of figure 5 is used in determining the effective width of flat sheet from the formula  $b_e = C_f t \sqrt{\frac{E}{\sigma_{cr}}}$ , smaller widths of effective sheet and smaller predicted loads are obtained in each case. Thus a closer agreement between predicted and test loads is obtained for the 0.016-inch corrugations, while the discrepancy is increased for all other corrugation gages. In general the use of the constant coefficient of 1.7 gives better results for this limited

series of tests than does Sechler's variable coefficient

On the basis of the above data it is concluded that the method proposed for obtaining the strength of combinations of flat and corrugated sheet carrying compression parallel to the corrugations is satisfactory. Further comparisons with test data may show that modifications or refinements are needed to provide for the varying degrees of elastic support offered the flat sheet by various shapes of corrugated sheet.

## SECTION 21. SHEAR LOADS PARALLEL AND PERPENDICULAR TO THE CORRUGATIONS

### BUCKLING STRESSES

Formulas for the critical loads on corrugated sheet in shear are given on page 384 of "Theory of Elastic Stability," by Timoshenko, the sheet being treated as orthotropic. The formulas given below are similar to those for compression parallel to the corrugation. They give the critical average shearing force per unit length of plate edge, assuming the plate edge to be simply supported.

$$(Nxy)_c = \frac{4k^4 \sqrt{D_1 D_2}}{b^2} \text{ for } \theta > 1$$

and

$$(Nxy)_c = \frac{4k \sqrt{D_2 D_3}}{b^2} \text{ for } \theta < 1$$

$$\theta = \frac{\sqrt{D_1 D_2}}{D_3}, \beta = \frac{b}{a} \sqrt{\frac{D_1}{D_2}}$$

$k$  is a coefficient, dependent on  $\theta$  and  $\beta$ , taken from figure 47.

$a$  is the length of side transverse to the corrugations  
 $b$  the length parallel to them.

$D_1 = \frac{lEt^3}{s12}, D_2 = Ek_1 t d^2, D_3 = \frac{SGt^3}{16}$ , as in the case of compression.

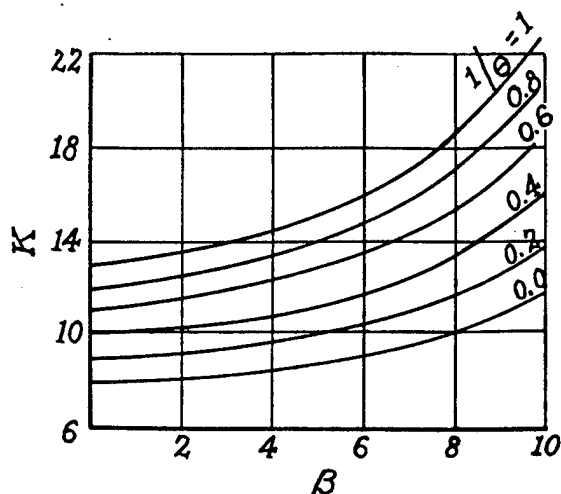


FIGURE 47.

The above formulas are based on the assumption of simply supported edges and normal dimensions of sheet. Similar expressions are available for the case of clamped edges. Both simply supported and clamped edges are provided for in the case of rectangular plates having high ratios of  $\frac{a}{b}$  strictly speaking,  $\frac{a}{b} = \infty$ . For cases where  $\theta$  lies between 1 and  $\infty$  the following values of  $K$  apply:

	$\theta$	1	2	3	5	10	20	40	$\infty$
Simple support.....	$K =$	13.17	10.8	9.95	9.25	8.7	8.4	8.25	8.125
Clamped edge.....	$K =$	22.15	18.75	17.55	16.6	15.85	15.45	15.25	15.07

For the values of  $\theta$  between 0 and 1.

	$\theta$	0	0.2	0.5	1.0
Simple support.....	$K =$	11.71	11.8	12.2	13.17
Clamped edge.....	$K =$	18.59	18.85	19.9	22.15

In all of the above cases the load is assumed to act in a direction parallel to the corrugations.

Figures 48 and 49 show theoretical and experimental curves for 17ST aluminum alloy sheets, the test data being from Wright Field Serial Report No. 3682.

The agreement between theory and test data as evidenced by figures 48 and 49 is not close enough to warrant the use of theory for design. The disagreement may be due to the edges being restrained instead of simply supported or the fact that the theory is based on buckling instead of stress at maximum load. Dependence must be placed on empirical data such as that given in figures 50, 51, and 52. The stress at maximum load as plotted on these curves is for the stress on the edge parallel to the corrugations. The data were taken from Serial Report 3682, but were modified so all allowable stresses are figured on the basis of the area of the edge parallel to the corrugations regardless of whether the load acts parallel or perpendicular to them.

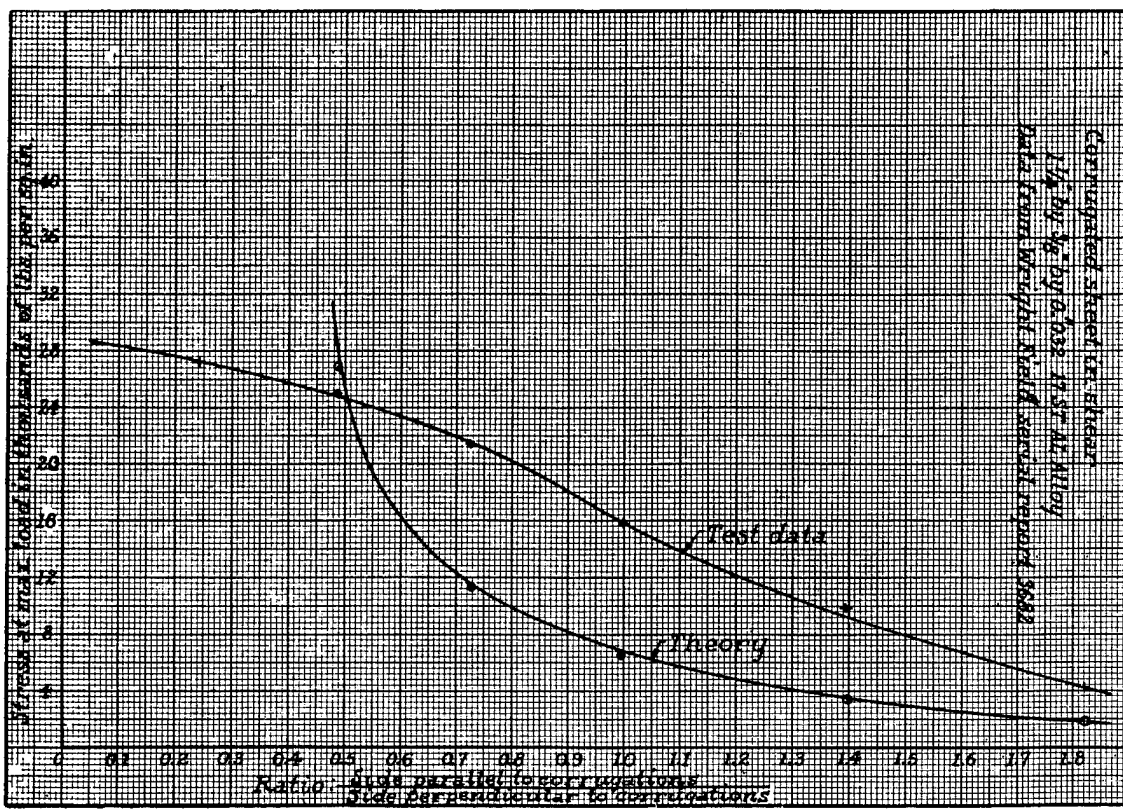


FIGURE 48.

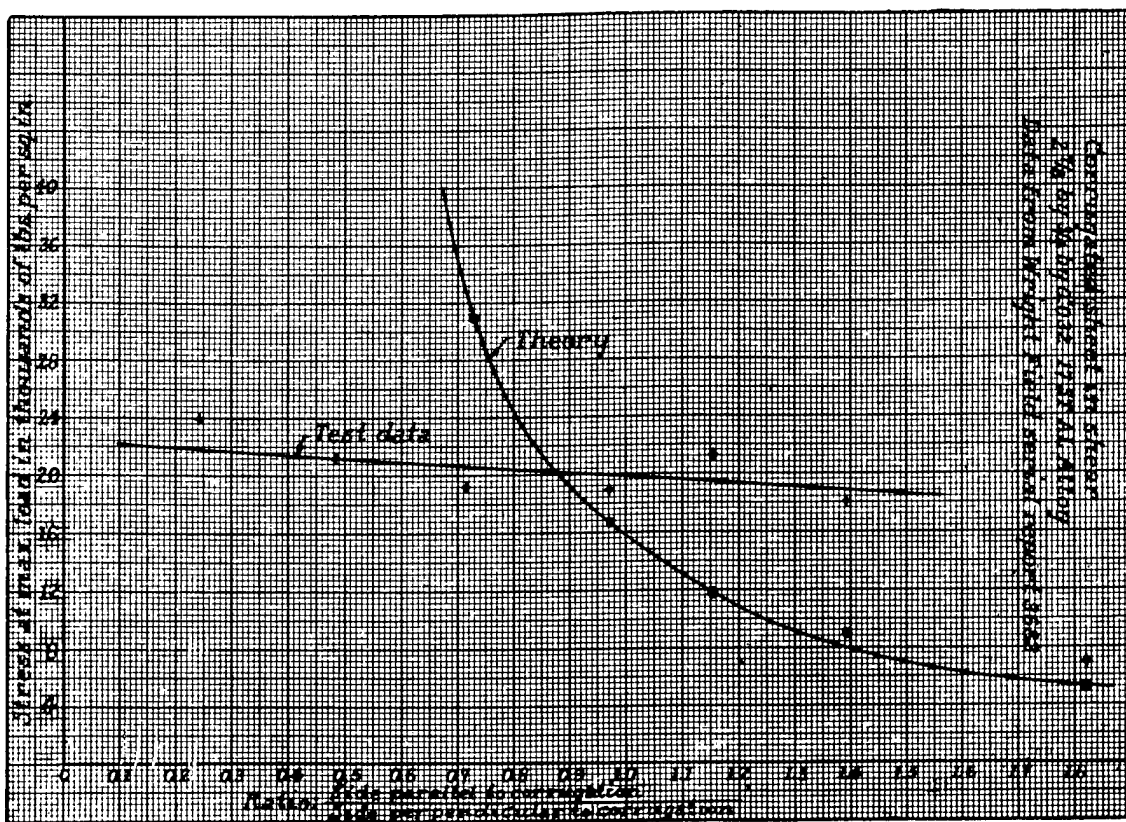


FIGURE 49.

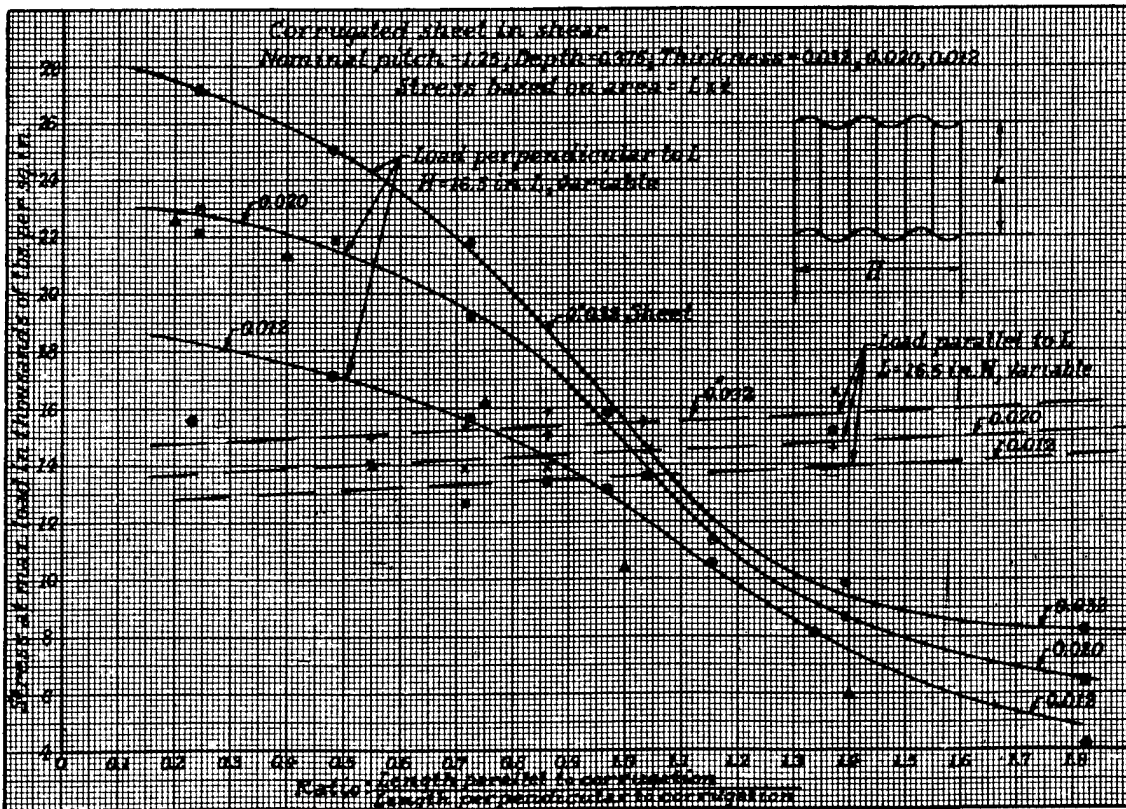


FIGURE 50.

Attention is called to the fact that when the length parallel to the corrugations,  $L_1$  is fixed the critical stress is essentially independent of the number of corrugations in the test specimen as indicated by the width  $H$ . There is a slight increase for the narrower panels, as shown in figure 50, but it is not great. When  $H$  is constant and  $L$  variable the allowable stress changes along a curve similar in shape to a Johnson-Euler column curve. This is shown in figures 50 and 51 and even more definitely in figure 52 which is drawn for a single thickness, 0.020", but with three values of  $H$  and several of  $L$ . The three curves of figure 52 tend to converge at a single point for  $\frac{L}{H} = 0$ , a point representing a stress of 23,400 lb./sq. in. as the curves are drawn.

It is believed that this point corresponds with a critical stress representing crushing or collapse of the corrugation due to shear and that this stress is a function of  $E$ ,  $\sigma_{vp}$ , and  $R/t$ . Lack of data preclude establishing an empirical basis for obtaining the value of this stress for 17ST alloy or for any other material and it is recommended that extensive tests be made on a series of corrugated sheets of different sizes, gages, lengths, widths, and materials. The data available appear to show that the stress variation due to  $L$  is not in accord with theory since the curves of stress plotted against  $L/H$  do not vary as  $L^2$  when  $H$  is constant. They are in fair accord with theory in indicating that for a constant value of  $L$ , the critical shear stress is essentially independent of the width  $H$ , such

variation as occurs being capable of representation as a straight line. The data needed are, then, those necessary for the construction of a series of curves similar to figure 52 for various gages of sheet and various materials. From such curves it is believed that an empirical relation can be established for determining the critical stresses for collapse of the corrugations, in terms of  $R/t$ ,  $E$ , and  $\sigma_{vp}$  of the materials involved and that satisfactory empirical equations can be developed to show the variation from that stress for different values of  $L$  and  $L/H$ .

In future plotting of data on corrugated panels, it is suggested that shear stresses be given in terms of the area of an edge parallel to the corrugations rather than an edge transverse, since the former does not depend on a coefficient introduced to provide for the difference between actual and projected lengths of corrugations.

Until further data are available for the development of empirical criteria, it is felt that little can be done but use those of serial report No. 3682.

## SECTION 22. SHEAR IN COMBINED SMOOTH AND CORRUGATED PANELS

There are few data available on the shear strength of combinations of smooth and corrugated sheet. Messrs. Bicknell and Bennet in their thesis, "The Shear Properties of Riveted Combinations of Flat and Corrugated Duralumin Sheets," M. I. T. 1934, present data on nine specimens, 34 by 46 inches, having the

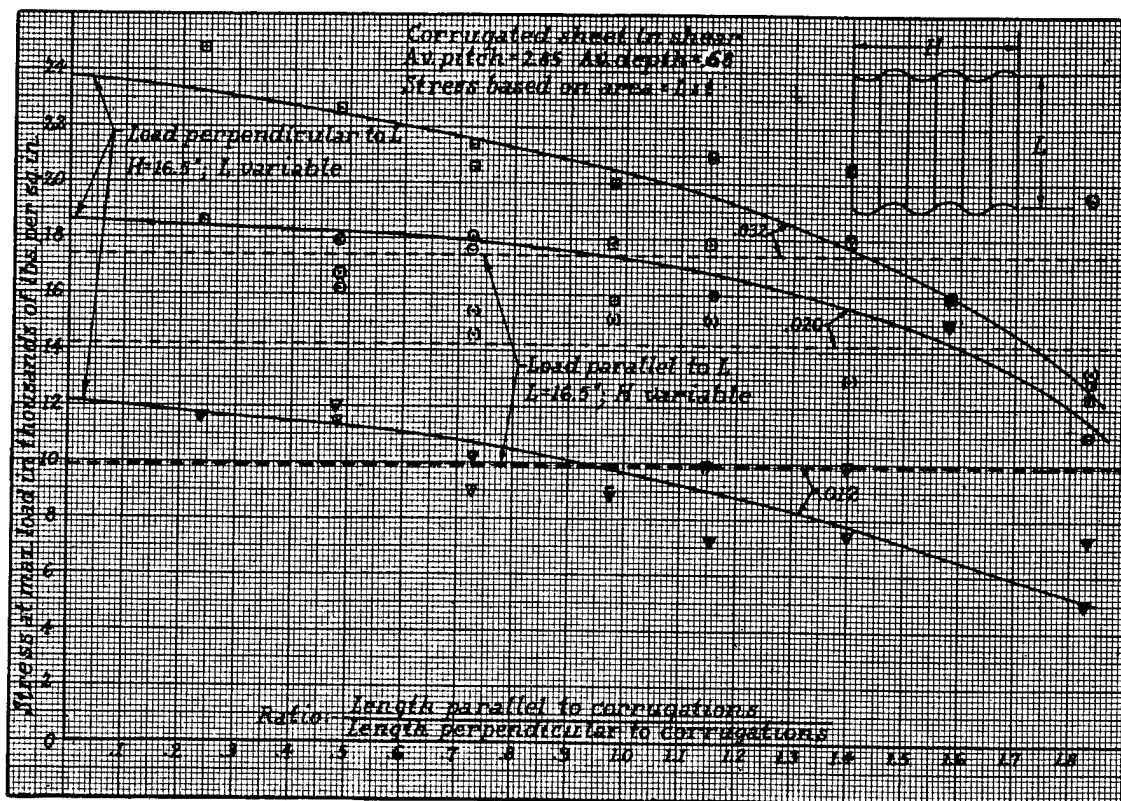


FIGURE 51.

TABLE 29

Specimen No.	1	2	3	4	5	6	7	8	9
Thickness of smooth sheet.....	0.0207	0.0197	0.0208	0.0208	0.0311	0.0195	0.0208	0.0294	0.0300
Thickness of corrugated sheet.....	0.0425	0.0411	0.0166	0.0166	0.0400	0.0611	0.0152	0.0424	0.0615
Rivet pitch.....	2.5	5.0	5.0	2.5	5.0	5.0	5.0	5.0	5.0
Shear stress at permanent set <sup>1</sup> .....	14,800	14,100	10,600	10,300	13,300	10,200	10,000	13,400	9,050
Shear stress at failure <sup>1</sup> .....	21,400	21,300	11,000	10,700	20,200	21,500	10,600	20,700	21,300
Shear stress at permanent set <sup>2</sup> .....	9,700	10,400	8,600	6,400	14,000	9,500	10,500	12,700	8,200
Shear stress at failure <sup>2</sup> .....	14,000	16,000	9,000	6,600	19,500	16,000	10,900	10,700	18,400
Approximate proportion of load <sup>3</sup> carried by flat sheet in percent.....	21-22	21-22	39-43	38-32	58-38	31-20	90-66	38-35	23-28

<sup>1</sup> Based on load divided by area of combination, both on edge perpendicular to corrugations.<sup>2</sup> Based on stress in flat sheet as determined from strain gage readings along tensile direction on flat sheet. Shear stress assumed to be  $\frac{1}{2}$  measured tensile stress.<sup>3</sup> Proportion of loads obtained from strain gage data. First figure is for low stresses, second for stress near maximum load. Variations are, roughly, straight lines.

corrugations parallel with the shorter side and having various ratios of smooth to corrugated sheet thicknesses as well as two rivet pitches, 2.5 and 5.0 inches. The following conclusions were drawn from the results of the test:

Little effect in strength is noted due to changing rivet pitch from 2.5 to 5.0 inches. With the increased pitch the shear stress in the smooth sheet increases slightly. The tendency is for the smooth sheet to take a disproportionate part of the shear, probably due to its greater shear modulus, but close riveting tends to relieve it somewhat by transferring stress to the corrugated sheet.

The most economical combination of sheet thicknesses requires that the corrugated sheet be  $1\frac{1}{2}$  or 2 times the thickness of the smooth sheet in which case shear

stresses slightly greater than 20,000 lb./in.<sup>2</sup> may be attained. The areas used in computing the above values are those across the corrugation. The corrugations were nominally  $2\frac{1}{4}$  by  $\frac{1}{4}$  inch.

The more interesting results of these tests are shown in table 29.

The data in table 29 confirm the conclusions reached by Bicknell and Bennett, but are not sufficient to generalize upon. Further research on this problem is necessary if structures involving combinations of smooth and corrugated sheets are to be used extensively.

### SECTION 23. SHEAR ON CYLINDERS—COMBINED SMOOTH AND CORRUGATED SHEET

Boeing Test Report No. 14267, "Shear Tests on Combined Flat and Corrugated Sheet," presents data on 24SRT Alclad cylinders composed of corrugated sheet

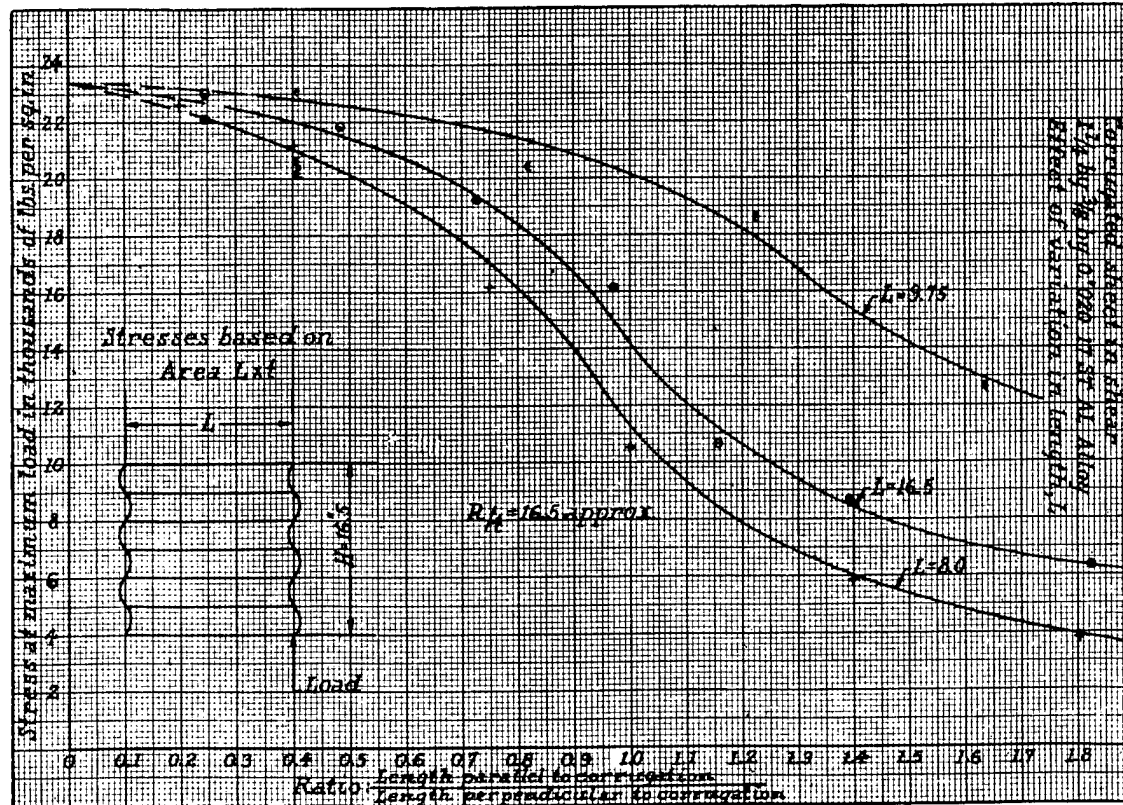


FIGURE 52.

with a smooth skin outside. The corrugations were of a  $2\frac{1}{2}$ -inch pitch  $\frac{1}{4}$ -inch depth, nominally, and the cylinders were  $38\frac{1}{16}$  inches in diameter, by 54 inches in length. The tests were made in torsion.

Assuming the smooth skin at 19.09-inch radius, the corrugated skin at 18.72 inches from the center of the cylinder, the corrugated skin being converted into equivalent smooth skin by multiplying the thickness by 1.23, the cylinders had the following properties:

TABLE 30

Cylinder	Smooth skin		Corrugated sheet			Cylinder $I_p$
	$t_s$	$I_{ps}$	$t_s$	$1.23t_s$	$I_{ps}$	
9-1107	0.016	700	0.032	0.0394	1,625	2,325
9-1107-1	.025	1,000	.025	.0308	1,270	2,360
9-1107-2	.032	1,400	.016	.0197	815	2,215
9-1107-3	.016	700	.051	.0627	2,590	3,290
9-1107-4	.016	700	.016	.0197	815	1,515
9-1107-5	.025	1,000	.025	.0308	1,270	2,360

The following table shows the variation in effective shear modulus,  $G$ , as the torsional load produces increasing shear stresses:

$$G = \frac{TL}{iI_p} = \frac{54T}{iI_p}. \quad \text{Stress} = \frac{TR}{I_p} = \frac{19.1T}{I_p}$$

TABLE 31

T	i	$I_p$	$G_{eff}$	Stress
Cylinder 9-1107				
145,600	0.00108	2,325	3,100,000	1,195.
529,600	.00483	2,325	2,540,000	4,350.
1,042,000	.01125	2,325	2,160,000	8,560. Skin $t=$ $\frac{1}{2}$ corrugated $t$ .
1,362,000	.01633	2,325	1,935,000	11,200.
1,618,000	.02200	2,325	1,710,000	13,300.
Cylinder 9-1107-1				
145,600	.00108	2,360	3,080,000	1,180.
529,600	.00458	2,360	2,640,000	4,280.
1,042,000	.01058	2,360	2,280,000	8,450. Skin $t=$ corrugated $t$ .
1,362,000	.01650	2,360	1,980,000	11,030.
Cylinder 9-1107-2				
145,600	.00092	2,215	3,860,000	1,255.
529,600	.00408	2,215	3,180,000	4,560. Skin $t=$ 2 corrugated $t$ .
785,600	.00692	2,215	2,770,000	6,770 (failure).
Cylinder 9-1107-3				
172,800	.00092	3,290	3,080,000	1,005.
556,800	.00392	3,290	2,335,000	3,300.
1,069,000	.00883	3,290	1,935,000	6,200.
1,325,000	.01175	3,290	1,850,000	7,700. Skin $t$ approximately $\frac{3}{4}$ corrugated $t$ .
1,645,000	.01658	3,290	1,630,000	9,550.
1,773,000	.01867	3,290	1,560,000	10,300.
Cylinder 9-1107-4				
108,800	.00067	1,515	5,790,000	1,370.
172,800	.00150	1,515	4,100,000	2,175. Skin $t=$ corrugated $t$ .
300,800	.00400	1,515	2,680,000	3,790.
428,800	.00675	1,515	2,260,000	5,400.
Cylinder 9-1107-5				
108,800	.00058	2,360	4,300,000	800.
556,800	.00500	2,360	2,550,000	4,510. Spot welded.
1,069,000	.01383	2,360	1,760,000	8,650. Skin $t=$ corrugated $t$ .

Since the shear modulus normally runs about 4,000,000 for the aluminum alloys, the high values obtained for cylinders 9-1107-4 and 9-1107-5 are difficult to explain unless the gage of sheet used exceeded the nominal dimensions, so the actual  $I_p$  was greater than the computed.

The reduction in effective shear modulus with increase in stress is to be expected since the value of  $G$  of the smooth sheet varies with the wrinkling of the sheet (see Wagner's article on "Tension Fields in Originally Curved Thin Sheets," N. A. C. A. Technical Memo. No. 774) and the stiffness of the curved corrugated sheet in shear is undoubtedly a function of the stress also. It is interesting to note that cylinders 9-1107 and 9-1107-1 have essentially the same stiffness and essentially the same polar moment of inertia, although the ratio of skin thickness to corrugation thickness is  $\frac{1}{2}$  to 1 in one case, 1 to 1 in the other. Attention is called to the fact, however, that the same amount of material is used in both, the equivalent thickness of one being  $0.016 + 0.0394 = 0.0554$  and of the other  $0.025 + 0.0308 = 0.0558$  inch.

For cylinder 9-1107-2 the skin is twice as thick as the corrugation with a material gain in  $G$ , while the 9-1107-3 cylinder has a skin  $\frac{1}{2}$  as thick as the corrugation with some loss of stiffness at the higher stresses even though the  $I_p$  is approximately 50 percent greater.

Cylinder 9-1107-4 had the same corrugated sheet as 9-1107-2, but the outer sheet was only half as thick. The  $I_p$  is about two-thirds that of cylinder 9-1107-2 but the torsion required to produce a given angular rotation is only about 60 percent as great, indicating that the greater the thickness of the outer skin in proportion to that of the corrugation, the greater is the stiffness of the cylinder.

Cylinder 9-1107-5 was the same as 9-1107-1, except that the smooth sheet was spot welded instead of riveted to the corrugated. The initial stiffness is noticeably greater, but due to failure in the welds the ultimate strength is very much less.

It was found that the deflections of the cylinders could be predicted with reasonable accuracy by assuming the material in the corrugated sheet 50 percent as effective as that in the skin. To resist shear it was concluded that the most effective place to put material was in the smooth skin. However, if the skin shear stress is assumed twice as great as that in the corrugation, the material being twice as effective, care should be exercised in proportioning the two so that the stress in the skin will not cause failure of the skin before the corrugations are heavily stressed. Assuming the tensile stress in the skin to be twice the shear stress, as is approximately true when the skin wrinkles and forms tension fields, it is evident that the skin may be very highly stressed while the corrugated sheet is relatively lightly loaded.